Investigations on the Kitaev Model and some of its generalisations.

By
SAPTARSHI MANDAL
The Institute of Mathematical Sciences, Chennai

A thesis submitted to the
Board of Studies in Physical Sciences

In partial fulfillment of requirements
For the Degree of
DOCTOR OF PHILOSOPHY
of
HOMI BHABHA NATIONAL INSTITUTE

February, 2011

Homi Bhabha National Institute

Recommendations of the Viva Voce Board

As members of the Viva Voce Board, we recommend that the dissertation prepared by Saptarshi Mandal, *Investigations on the Kitaev Model and some of its generalisations,* may be accepted as fulfilling the dissertation requirement for the Degree of Doctor of Philosophy.

_____ **Date :**

Chairman -

_____ **Date :**

Convenor -

_____ **Date :**

Member 1 -

_____ **Date :**

Member 2 -

_____ **Date :**

Member 3 -

Final approval and acceptance of this dissertation is contingent upon the candidate's submission of the final copies of the dissertation to HBNI.

I hereby certify that I have read this dissertation prepared under my direction and recommend that it may be accepted as fulfilling the dissertation requirement.

_____ **Date :**

R Shankar -

Certificate

I certify that the thesis entitled *Investigations on the Kitaev Model and some of its generalisations,* submitted for the degree of Doctor of Philosophy by *Saptarshi Mandal* is the record of research carried out by him during *March, 2004* to *August, 2008* under my guidance and supervision, and that this work has not formed the basis for the award of any degree, diploma, associateship, fellowship or other titles in this Institution or any other University or Institution of higher learning.

R. Shankar
Professor, Physics
The Institute of Mathematical Sciences
C. I. T. Campus, Taramani
Chennai 600 113, India

Declaration

I, hereby declare that the investigation presented in this thesis has been carried out by me. The work is original and has not been submitted earlier as a whole or in part of a degree/diploma at this or any other Institution/University.

Saptarshi Mandal.

To my parents, brother and sisters to whom I owe much of my happyness, comfort and wellbeings.

Acknowledgement

My heartfelt gratitude to my Ph. D. supervisor Prof. R Shankar with whom any kind of discussions, academic or non academic, was a pleasure to take part. Every time whenever I was at the receiving ends of understanding the research problem or mental impatience as a result of repeated failure on my part, his fatherly guidance and encouragement brought in me the right spirit to carry out the research problem.

My sincere gratitude also to Prof G Baskaran who had introduced me to my research problem. It was always a pleasure to listen the intricacies of physics from him. I learnt how to think all the details of a problem and give importance to every possible physics involved.

Here I also express my thanks to Prof M V N Murthy for many academic discussions especially about the generalised exclusion statistics and generalised Pauli principles.

My thanks also to Dr Naveen Surendran. I have learnt many basics from him and also the need to be organised and clear when addressing ones research problem to others. Many times it was hard to appreciate his emphasis with every details(sometimes what seems to be insignificant) but later it would bring in a sense of completeness and gratification.

I also wish to thank Prof Krishnendu Sengupta, Prof Julien Vidal and Dr Sebastien Dussel for their suggestion and insightful explanation regarding my research problems.

I thank all my fellow colleagues which are too many to mention. They always stood by my side asking over and over again.

I am grateful to the library and the computer staffs for their help. I wish to acknowledge all the non-academic staffs for their work. I must thank the institute and its academic and administrative members for ensuring an excellent academic atmosphere and facilities for research work.

Synopsis

We study a frustrated quantum spin 1/2 model on a hexagonal lattice [A] which was originally proposed and analysed by A. Kitaev. This model was introduced for possible implementation in the field of topological quantum computation. It has anisotropic type nearest neighbour spin spin interaction which depends on the direction of the bonds which can be written as follows,

$$H = -\sum_{x-\text{link}} J_x \sigma_i^x \sigma_j^x - \sum_{y-\text{link}} J_y \sigma_i^y \sigma_j^y - \sum_{z-\text{link}} J_z \sigma_i^z \sigma_j^z \qquad (1)$$

Here x, y and z link are three different bonds in the hexagonal lattice which are related by 120^o rotation and i,j denotes nearest neighbour sites. The model has conserved quantities associated with each hexagonal plaquette and all closed loops. The energy eigenvalues of the ground state energy and a set of low lying excited states have been calculated exactly. The original spin model has been fermionised with four Majorana fermions to fermionise the local spin 1/2 operator. This fermionisation process enlarges the local Hilbert space of the spin 1/2 operator and maps the original spin 1/2 Hamiltonian into a tight binding Hamiltonian of Majorana fermion hopping problem where hopping matrix element is coupled with local static Z_2 gauge fields. It has been shown that ground state sector belongs to the case where all Z_2 gauge fields take value 1. It has been shown that for this particular gauge configuration the spectrum has two distinct phases. For certain values of parameter the spectrum is gapless otherwise it is gapped. While the gapped phase contains abelian anyonic excitations, the gapless mode contains non-abelian excitations. In Chapter 1 and 2 of this thesis , we give a brief introduction of the Kitaev model and review the relevant research done on it.

Though it was proposed with the view of application in quantum computation, we are interested in many-body aspect of the Kitaev Model. To this end, an alternative method of the exact solution of this model using Jordan-Wigner fermionization has been studied. The ground state degeneracy of the system on a torus has been shown to be four all over the parameter space. These have been presented in Chapter 3. In Chapter 4, spin-spin correlation function has been calculated exactly. A spin operator is shown to be fractionalised into two static π fluxes and a dynamical Majorana fermion. Multi-spin correlations are also computed. The entanglement aspect of this model has been investigated in Chapter 5. In Chapter 6, the toric code limit ($J_z \gg J_x, J_y$) of the Kitaev model has been studied in terms of gauge

invariant Jordan-Wigner fermions. The stability of this spin model has been studied against Ising perturbation in Chapter 7. In Chapter 8 and 9, an extension of the 2D Kitaev model to 3 spatial dimensions has been presented and solved exactly. Various many body aspects and the low energy excitations of this 3D spin model have also been studied .

Exact solution by Jordan-Wigner fermionisation :

To solve this spin model exactly we have used Jordan-Wigner fermionisation (JWF) to map the spin problem into a fermionic problem. This JWF is exact and it does not enlarge the local Hilbert space of spin 1/2 operators. We have formulated a generalised JWF which can be used in open boundary as well as in periodic boundary condition. It has been shown that JWF also maps the spin problem into a tight binding Majorana fermion hopping problem. It is quite clear in our formalism that it can be thought of as a Z_2 gauge fixing procedure. We showed that this transformation simplifies the conserved quantities in terms of the gauge invariant Jordan-Wigner fermions. Also JWF enables to construct the eigenstates of conserved quantities explicitly. We have reproduced the phase diagram of Kitaev model exactly. Moreover it has been shown that in the thermodynamic limit the ground state is four-fold degenerate on a torus and it is true for both the gapless and gapped regime [4]. This four fold degeneracy corresponds to topologically different gauge field configurations corresponding to uniform flux free configuration. We have analytically showed that these can be taken care of by suitably defining fourier transformation with various boundary conditions in the reciprocal(momentum) space.

Spin correlation and fractionalisation :

Extending Kitaev's fermionisation we have formulated a canonical transformation introducing the concept of bond fermion. This clarifies the dynamics of the spin explicitly and shows that a spin can be thought of a composite of a Majorana fermion and two static adjacent Z_2 fluxes [1]. Using this method we have shown that two-spin correlation function is zero beyond nearest neighbour separation. This is true for not only ground state but also for every eigenstate. We have also shown the bond dependency of the two spin correlation functions. Existence of such spin-spin correlations is a consequence of flux conservations. We have analysed multispin correlations. We have shown that particular dimer-dimer correlation can be long range with power law behaviour in gapless phase of the spectrum. We

have also shown the presence of multi-spin correlation function which is a string like operator. This short range nature of spin-spin correlation prevails over the entire parameter space irrespective of gapless or gapped phase.

Entanglement study :

We have calculated concurrence and entanglement entropy for this model. While the concurrence is zero the entanglement entropy is finite throughout the parameter space and never diverges. This is expected given the short range nature of the correlation and absence of any long range correlation between the spins.

Abelian anyons :

In the toric code limit($J_z \gg J_x, J_y$) [B] of the 2D Kitaev model we have derived an effective Hamiltonian in terms of the gauge invariant Jordan-Wigner fermions and showed that the effective Hamiltonian takes very simple form. The four degenerate ground states have been explicitly constructed. The excitations over the ground state have been discussed and it has been shown that if one takes one excitation across the torus and brings it back to its original position the original state goes to a different state. This shows that wave function behaves like a multicomponent object. Moreover we are able to show that winding of an excitation over the torus in two orthonormal directions commutes. This is in conformity with the abelian nature of the quasiparticle excitation in the toric code limit.

Stability of Kitaev model :

We have analysed the stability of Kitaev model against an Ising perturbations [3]. The Jordan Wigner fermionisation still yields a local Hamiltonian though it contains four Majorana fermion terms. The gauge fields are no longer static and turn out to be dynamic. Using appropriate mean field expansion we have decomposed each four fermionic term in the Hamiltonian. The resulting Hamiltonian now consists of three different parts. The first one refers to the Majorana fermions which appear in pure Kitaev model and the second corresponds to the fermions which form the gauge fields. The Hamiltonian also contains a coupling between these two species of fermions. We solve this mean field ansatz numerically and it is found that for ferromagnetic Ising Hamiltonian there is a first order phase transition at $\lambda = 0.07$, where λ is the strength of Ising interaction. This first order

phase transition is marked by the vanishing of conserved gauge field from 1 to 0 and simultaneous onset of non zero spin-order parameter. The energy density also shows a discontinuity in its derivative. For anti ferromagnetic Ising perturbations, Kitaev model is seen to be stable up to $\lambda = 0.08$ and after this the system undergoes a first order transition with similar characteristics as seen in Ferromagnetic case.

Exactly solved 3-Dimensional Kitaev model :

We introduce a spin 1/2 model [2] in three dimensions which is a generalisation of the 2D Kitaev model on a honeycomb lattice. Here we also notice the presence of large number of conserved quantities each associated with every closed loop in the lattice. We have solved this spin model exactly by mapping it to a theory of noninteracting fermions in the background of static Z_2 gauge fields. The ground state lies in the vortex free sector like 2D Kitaev model. We have numerically verified this. For the vortex free sector the phase diagram consists of a gapped phase and a gapless one, similar to the 2D case. Low energy excitations are the fermionic excitations in the gapless phase. We notice that unlike in the two dimensional model, in the gapless phase the gap vanishes on a contour in the **k**-space. Again here we see that two spin correlation function is short range providing an example of 3 dimensional quantum spin liquid. We also see the presence of string type and brane type correlations which are nothing but various multispin correlations. We also notice, like in the 2D Kitaev model, there is no obvious symmetry breaking associated with the gapless to gapped transition of the spectrum. Furthermore, we show that the flux excitations of the gauge fields, due to some local constraints, form loop like structures; such loops exist on a lattice formed by the elementary loops of the original lattice and is topologically equivalent to the pyrochlore lattice.

Effective Hamiltonian of 3d Kitaev model in $J_z \gg J_x, J_y$ limit.

In analogy to 2D Kitaev model toric code limit, we have derived an effective Hamiltonian in the limit $J_z \gg J_x, J_y$ for our 3D Kitaev model. The analysis shows that the low energy excitations in this limit are the flux like excitations (which exist in the form of closed loop) rather than point like excitations. These flux excitations are nothing but the conserved loop operators expressed in this limit. Again the ground state belongs to the vortex free sector. This corroborates the numerical finding that the vortex free sector is the ground state sector for the the case of arbitrary value of

J_x, J_y, J_z. We have classified the basic excitations over the ground state. The ground state is an example of condensation of closed string operators. We have shown the existence of string operators which create loop like excitations at the end of the string. We have also demonstrated the existence of membrane operators which are able to detect these loop excitations.

List References

A. A. Yu. Kitaev, Anyons in an exactly solved model and beyond. Ann. Phys. **321**, 2-30 (2006) .

B. A. Yu. Kitaev, Fault-tolerant quantum computation by anyons. Ann. Phys. **303**, 2-111 (2003) .

List of papers

1. G Baskaran , Saptarshi Mandal, and R. Shankar, Exact results for spin dynamics and fractionalisation in the Kitaev model. Phys. Rev. Lett, **98**, 247201 (2007).

2. Saptarshi Mandal and Naveen Surendran, An exactly solvable Kitaev model in three dimensions, Phys. Rev. B **79**, 024426 (2009).

3. Saptarshi Mandal, Subhro Bhattacharjee, Krishnendu Sengupta, R Shankar , Confinement-deconfinement transition in a generalized Kitaev model, arXiv:0903.3785.

4. G Baskaran, Saptarshi Mandal, R Shankar. "RVB physics, gauge fixing and the Jordan-Wigner transformations in the Kitaev model".*

***** In preparation.

Contents

List of Figures

List of Tables

The woods of Arcade are dead
And over is their antique joy
Of old the world on dreaming fed
Grey Truth is now her painted toy
The song of the happy shepherd- W B Yeats

Chapter 1

Introduction

The traditional condensed matter physics based on Landau's theory of phase transition and symmetry breaking mechanism [1, 2] is quite successful in explaining a variety of phenomenon. The essence of this theory is that different phases of matters correspond to different orders among the constituent atoms or molecules. It is the order or the symmetry among the constituent particles which determines the phases. When a material changes from one order to another order (i.e, as the material undergoes a phase transition), what happens is that the symmetry of the organisation of the constituent particles changes. The simplest examples is liquid to solid transition. We see that the continuous translation symmetry is present in the liquid phases and absent in the solid phase and this difference characterises the phase transition completely. The successful implementation of Landau's theory of phase transitions based on symmetry breaking mechanism can be found in explaining different phases of magnetism, super-fluid phases of He^4 and He^3, the superconductivity in metals, etc.

But in recent theoretical speculations as well as experimental systems, it has been observed that the symmetry alone can not characterise the phase transitions [3, 9–12]. Moreover the phase transitions associated with such phenomena are not associated with any long range orders. In fact, for the case of quantum Hall liquid (QHL) [3–8], the different phases correspond to the same symmetry. It could also be mentioned that a theoretical model to explain high temperature superconductivity(Kalmeyer and Laughlin, 1987) also assumed no symmetry breaking [9]. The new order which goes beyond the Landau theory (based on local order parameters and long range correlations) which distinguishes the phase transition associated with these novel phases is called topological order [14–18]. Topological order is a new type of

order distributed over many particles. Local measurements may not specify it. One might try to think of this as a result of long range quantum entanglement distributed over many particles which can not be quantified by local order parameters or long range correlations of local operators. For this reason when in a phase transition the topological order changes from one to another, local order parameters would not be able to detect it. However topological orders can be described by a new set of quantum numbers, such as ground state degeneracy, quasi particle fractional statistics, edge states, [4, 14, 15] topological entropy etc.

Systems with topological orders predict existence of exotic phases which must be explained with new theory. These systems are important for many other reasons also, for example, its possible application in quantum computations. As mentioned before, in the system with topological order, the excitations are topological defects which are distributed over many particles. For this reason they do not undergo decoherence easily. These topological defects may be created, moved and manipulated for the effective implementations in quantum computations [23–35]. These topological defects may show exotic exchange statistics depending on the dimensions of the systems. While in three and higher dimensions, they can only obey Bose or Fermi statistics, in two dimensions such topological excitations may show exchange statistics which are in between fermions and bosons. In two dimension when such two particles are exchanged, the wave function in general gets multiplied by a phase $e^{i\theta}$ other than +1 or -1. It is the braid group and not the permutation group which determines the effect of exchange of such quasi particles [41, 42]. These special objects are termed as Anyons. Anyons are important not only for theoretical interests but also for other reasons. Recently it has been proposed to use certain classes of topological anyonic excitations [37–39] (which are quite stable) as q-bits which will be able to store and manipulate informations [20, 23, 34, 35]. The braiding property of anyons would govern the manipulation of q-bits. These form the basics of topological quantum computations. A quantum computer is a device which makes use of distinctively quantum mechanical phenomena such as superposition and entanglement to perform operations on data. The data is stored in qubits which is abbreviation of **qu**antum **bi**nary digi**ts**. But basic problems with qubits are that they very easily interact with external world and decohere instantly. In this perspective the anyons which are stable due to their topological character, hold a promise to be good candidates for quantum bits. The motivation for quantum computer arises as it can provide fast solutions for certain computational problems(e.g factoring and

discrete logarithm) which require exponential time on an ordinary computer.

With the view of quantum computations, Kitaev proposed a topologically ordered state which can serve as a simple physical realization of such anyons [32]. This particular model which is often referred as "toric code model" realizes abelian anyons as excitations. Let us imagine a spin 1/2 objects residing on the links of a torus of square lattice. Then this model is defined by the following Hamiltonian,

$$\begin{aligned} H &= -\sum_{plaquette} A_p - \sum_{stars} B_s \qquad (1.1) \\ A_p &= \prod \sigma_i^z \quad ; \qquad B_s = \prod \sigma_j^x \end{aligned}$$

Here the product over 'i' runs over the four bonds of a plaquette and the product over 'j' runs over the four bonds emanating from each vertices. The ground state($|G\rangle$) is given by the condition $A_p(B_s)|G\rangle = |G\rangle$. It has been shown that in this model there exists two distinctively basic excitations corresponding to negative eigenvalues (-1) of the operator 'A_p' and 'B_p'. We can call these excitations as 'A' particles and 'B' particles for simplicity. It was shown that when a 'A' particle moves around another 'A' particle the wave function does not pick up any phase. Same is true for two 'B' particles. But taking one 'A' particle around another 'B' particle yields a phase factor $e^{i\pi}$ to the wave function. It was also shown that a composite object of 'A' and 'B' particle behaves as fermions. Going beyond this toric code model he discussed the non abelian anyons which might be useful in quantum computation. The braiding group of such anyons which are fundamental in view of executing and manipulation of such qubits has been discussed at length.

Recently he proposed an exactly solvable spin 1/2 model [33] on the 2-dimensional hexagonal lattice which drew a considerable attention from the condensed matter community. The toric code Hamiltonian (1.1) mentioned before can be realized in this model at some special limit. This particular spin model contains anisotropic nearest neighbour spin-spin interaction. One may identify three different kind of bonds in hexagonal lattice which are related by 120^o rotations. Let us call them x-bonds, y-bonds and z-bonds. The Hamiltonian contains bond dependent nearest neighbour interactions. If the two spins are joined by a x-bonds they only interact with their x-component of spin operator. So we can write the Hamiltonian as,

$$H = -\sum_{x-\text{link}} J_x \sigma_i^x \sigma_j^x - \sum_{y-\text{link}} J_y \sigma_i^y \sigma_j^y - \sum_{z-\text{link}} J_z \sigma_i^z \sigma_j^z \qquad (1.2)$$

Here J_x, J_y, and J_z are the strength of interactions along three different directions. It is noteworthy to mention that in reference [39], a similar model in a square lattice was proposed in the context of quantum computations. Besides the novelty of this interaction which causes a frustration to the spins at each site, this model contains local conserved quantities associated with every plaquette. This conserved quantities also commute mutually. It was shown that this model shows the emergence of both abelian as well as non abelian anyons depending on the relative magnitude of J_x, J_y, J_z. Kitaev showed that this model can be solved exactly by suitably fermionising the spin operators in terms of Majorana fermions. The effective Hamiltonian reduces to Majorana fermions hopping problem coupled with local static Z_2 gauge field. The ground state belongs to the gauge sector where all Z_2 gauge fields are 1. The spectrum thus obtained is gapless in the region $|J_x - J_y| \leq J_z \leq J_x + J_y$, otherwise it is gapless. The toric code limit which corresponds to $J_z \gg J_x, J_y$ contains the abelian anyons. It was shown that the gapless phase opens up a gap in the presence of small magnetic field and Chern number calculation demonstrated that it is ± 1 for the gapless phase and zero for the gapped phases. This proves that theses two phases are topologically distinct . While in the gapless phase the excitations are non abelian anyons, the gapped phase contains abelian anyons as the low energy excitations. The braiding property of these anyonic excitations which are fundamental in defining the basic operations in the context of quantum computations, was discussed at length. On the other hand the perturbative study of toric code Hamiltonian (1.1) in the presence of magnetic field was shown to give rise a nontrivial phase diagram which displays first-order and second-order transition lines merging in a topological multi critical point located at the confluent of topological and ordered states [90]. It is important to note that though the excitations of the toric code limit Hamiltonian is dispersion less, perturbative study in the presence of magnetic field showed that these excitations acquires a dispersion [46].

Though this novel spin model has been proposed with the view of quantum computation, it is a very interesting many body quantum system in its own right. There is reason why researchers have extensively explored different aspects of this model [46, 74, 76–78, 80, 82, 83, 85–88, 91]. Exactly solvable models [92–95] in condensed matter physics are very rare. In comparison to other quantum spin liquid systems Kitaev model is quite distinct and has unusual properties. It is an example of a frustrated quantum spin system but unlike other frustrated spin model (eg. Heisenberg model defined on Pyrochlore lattice) frustration does not arise due the geometry

of lattice. The frustration is due to the competing anisotropic interactions along three different directions. The ground state does not have any symmetry breaking. Thus the four fold degeneracy found for the ground state is of topological origin. It was already mentioned that the mapping of the spins in terms of Majorana fermion makes this spin model into a Majorana fermion hopping problem coupled to static Z_2 gauge field. These gauge fields reside on the links. It very closely resembles the situation for a RVB state which was proposed in the context of high temperature superconductivity [50–56]. A valence bond state is a singlet state, $\frac{1}{\sqrt{(2)}}(|\uparrow_i\rangle|\downarrow_j\rangle - |\downarrow_i\rangle|\uparrow_j\rangle)$ associated with two site. For nearest neighbour sites this state lives on a bond. The Z_2 gauge structure in the Kitaev model shows that it is in the same universality class of RVB state.

An important investigation [82] studied quench dynamics and defect production in Kitaev model. It showed contrasting results compared to known behaviour . Quantum phase transition is accompanied by diverging length scales [102] leading to the adiabaticity for the system sufficiently close to the quantum critical points. Thus a quantum system fails to follow its instantaneous ground state when some parameter in its Hamiltonian is varied in time at a finite rate $1/\tau$ which takes the system across the critical point. This study [82] carried the quenching of the Kitaev model by varying J_z from $-\infty$ to ∞ at a rate $1/\tau$, keeping J_x, J_y fixed. It showed that density of defect production scales as $1/\sqrt{\tau}$ instead of expected scaling $1/\tau$ [103].

Recently a general spin-S Kitaev model [83, 84] has been studied and unlike spin 1/2 Kitaev model it is not exactly solvable. But surprisingly the Z_2 gauge structure of the spin 1/2 Kitaev model survives along with a set of commuting plaquette operators. This makes the spin-spin correlation to be of same nature as spin 1/2 Kitaev model. This study also shows that ground state of the classical spin-S model has a correspondence with dimer coverings and with self avoiding walks on honeycomb lattice.

The novel of the nature of interaction of the Hamiltonian (1.2) makes it challenging to find a real systems to have such kind of interaction. But there has been proposal to experimentally realize this spin 1/2 model using cold atoms as well as using polar molecules [96–98]. Recently it has been proposed to realize Kitaev model in a real system [99, 100]. Also many schemes have been developed how to create and manipulate the abelian anions (in the toric code limit) and hence making way of successful implementations of braiding effect of anyons [104–108].

The inherent novel exact solubility with the possibility of anyonic excitation has resulted in proposing many other models in two as well as in three dimensions which has Kitaev like interaction [85–88]. It has been shown that a Kitaev like Hamiltonian can be defined if one replaces a single site of the hexagon lattice by three sites. The resultant lattice is called decorated triangle [86]. The Kitaev model extended in this lattice is shown to break time reversal symmetry spontaneously signifying the presence of chiral spin liquid. Very recently many 3 dimensional model with Kitaev like Hamiltonian have been investigated and it is observed that all this is exactly soluble and one can construct chiral spin liquid in three dimensions [85, 87]. The study of 3 dimensional topological model [19, 109] is also important from the point of quasi-particle excitations. We know that 2 dimensional Kitaev model supports abelian and non abelian anyon in different parameter regime and they exhibit nontrivial statistics. But anyons are special and they exist only in two dimensions. However in three dimensions the topologically ordered state is shown to include (deconfined) gauge bosons as well as fermions.

A large class of 3dimensional models with topological order has been discussed in the references [21]. It was shown that topological phases of such system can be characterised by string-net and membrane net condensation. At low energy the microscopic degrees of freedom can organise themselves in extended objects which are called strings [19, 21, 22]. A string-net is a object which is made of strings that meet at branching point or nodes. Ends of open strings are particle like objects which can have a nontrivial statistics. When in a two-dimensional system such a quasi particle winds around another quasi particle of a different kind, its wave function picks up a phase. This phenomena corresponds to the fact that the ends of an open string can be detected by a closed string of another type that encloses its ends. On a three dimensional lattice , the end of an open string can be detected by a closed surface. This motivates an enquiry about the meaning of the condensation of closed membranes. A microscopic picture of topological phase transition of certain systems has been investigated in terms of string-net and membrane-net condensation [19, 21, 22]. The Landau's phase transition can be understood as particle condensation. For a topological phases the notion of particles are generalised to notion of strings and membrane. Dynamics of these string-nets governs the dynamics of low energy dynamics. If this strings extend over the system size it condenses (very much like particles condensations) and one gets topologically ordered states. Similar to closed-string condensation , closed-membrane condensation is a

superposition of closed membranes of arbitrary sizes , shapes and numbers. Just like closed-string condensations, closed-membrane condensations also implies topological order as a big closed membrane can explore the topology of the lattice. Many 3D model with topological order have been analysed with condensation of either membrane-net or string-net or both [22].

In the present work we present some theoretical investigations regarding many body aspects of 2D Kitaev model and some of its generalisations. In the next chapter, we introduce the Kitaev model very briefly and present its formal solution as obtained by Kitaev himself [33]. In chapter 3, we shall solve the Kitaev model using Jordan-Wigner Fermionisation(JWF). Kitaev model is one of the very few 2 dimensional model where the one dimensional Jordan-Wigner transformation produces a local Hamiltonian [77, 78, 80]. This is quite significant in the sense that this reaffirms the exact solubility of Kitaev model. Because in the JWF we do not introduce any extra degrees of freedom. The Hilbert space dimension of the spin space and the fermionic space is equal. We give a complete mapping of all the conserved quantities in terms of gauge invariant Jordan-Wigner fermions and calculate the eigenstates of the conserved quantities and the fermionic Hamiltonian explicitly. We also derive the four field degeneracy explicitly in the thermodynamic limit.

In chapter 4, we derive the spin-spin correlations by using Kitaev's fermionisation. We show that two spin correlation function vanishes beyond nearest neighbour separation. This proves that Kitaev model is an example of quantum spin liquid. Two spin correlation is shown to depend on the directions of bonds. We explicitly show that a spin undergoes fractionalisaton into a dynamic Majorana fermion and two static Z_2 fluxes. This is very similar to what has been observed in other quantum spin liquids where fractionalisation occurs [60–67]. The spin-spin correlation shows absence of long range order in both the gapless and gapped phases. Thus it proves no obvious symmetry breaking at the phase transition which is a good indicator of topological order. Though the two spin correlation functions is short range, certain many spin correlation could be long range. Our derivation of spin-spin correlation functions in the Kitaev model can be easily generalised to other Kitaev like model which have been proposed recently [85–88].

In chapter 5, some results regarding quantum entanglement measure for the Kitaev model are presented. The entanglement studies captures the signature of quantum phase transition across the gapless to gapped phase.

Recently varius aspects of entanglements and fidelity have been investigated in [129–134]. In references [130, 131], a quantity called 'topological entropy' is shown to capture the topological order of the Kitaev model. In [132, 133], fidelity susceptibility(FS) has been investigated and it has been shown that it scales differently in gapless and gapped region of the Kitaev model. While in gapless region FS scales as $L^2 lnL$, in gapped region it scales as L^2.

Next, in chapter 6, we discuss the toric code limit of the Kitaev model in terms of gauge invariant Jordan-Wigner fermions. We derive the effective Hamiltonian corresponding to toric code limit in terms of the gauge invariants Jordan-Wigner fermions. We explicitly calculate the four degenerate ground states and showed that a particular ground state get mapped to another ground state when quasi particles are exchanged over these ground states. It is noteworthy to mention references [45–48] which studied toric code limit in great detail bringing many important revelations.

In chapter 7, we study Kitaev model with an Ising interactions added to it. Ising interactions destroys the exact solubility of Kitaev model. The Z_2 gauge fields which were static in Kitaev model become dynamic. We present a mean field studies of these Z_2 gauge field dynamics. We show, within mean field, that there is a small region of stability around Kitaev model where it retains its quantum spin liquid behaviour and Z_2 gauge fields are essentially static. Beyond this limit the system undergoes a quantum phase transition to a magnetically ordered state and Z_2 gauge fields on the links vanishes identically. Our results may be relevant in the experimental realisation of Kitaev model [100, 101]

We have already mentioned that following Kitaev model [33], a large number of exactly solvable model with Kitaev like Hamiltonian have been proposed and solved exactly [85–88]. We introduce an exactly solvable 3D Kitaev model in chapter 8. It bears all the key features of the 2D Kitaev model and it is an example of a 3D quantum spin liquid. We solve this model exactly and finds it phase diagram. It contains both gapless and gapped phase depending on the relative strength of the interaction parameter. However unlike 2D Kitaev model, in our model dispersion is gapless on a contour in $\mathbf{k}$ space, not on isolated points. We also classify the possible excitations of this 3D model

In the chapter 9, we study the toric code limit of this 3D Kitaev model. We show that the low energy excitation are loop excitations. Statistics of the

elementary loop excitations have been studied. Both fermionic and bosonic loop excitations are shown to exist. We also discuss the the existence of more complex loop excitations and membrane excitations of this model.

We complete this thesis by summarising all our results in chapter 10.

She was a phantom of delight
When first she gleamed upon my sight;
A lovely Apparition, sent
To be a moment's ornament;
She was a phantom of delight- Wordsworth

Chapter 2

The Kitaev Model

In this Chapter we briefly introduce the Kitaev model and discuss it's formal solution as obtained by Kitaev himself [33]. This spin 1/2 model has been defined on a honeycomb lattice with a spin 1/2 at every site.

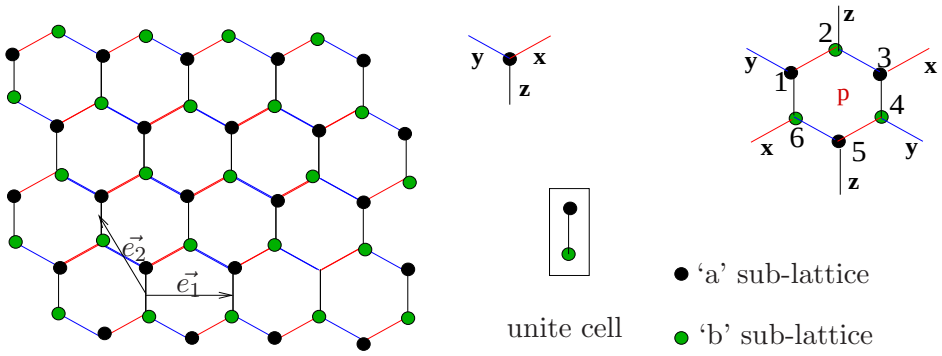

Quantum Spin 1/2 at each site

Figure 2.1: In this figure we pictorially describe the Kitaev model. The Kitaev model describes an anisotropic spin-spin interactions which depend on the orientations of the bonds. Bonds are labelled with x, y or z to indicate the bond-dependent nature of the interactions.

In honeycomb lattice one can identify three kind of bonds which are related by 120^o of rotation. The Hamiltonian describes a nearest neighbour spin-spin interactions which is anisotropic, i.e, depends on the directions of the bonds or links. For this reason the links are divided into three types, "x-links","y-links" and"z-links" as shown in Fig. (2.1). Two nearest neighbour spins joined by x ($\alpha = x, y, z$) link interact with x component of their spins

yielding a term $\sigma_i^x \sigma_j^y$ to the Hamiltonian. Here the subscript 'i' and 'j' stand for site indices. The same is true for interactions along "y-links" and"z-links". Thus we can write down the Hamiltonian as,

$$H = -J_x \sum_{x-\text{links}} \sigma_j^x \sigma_k^x - J_y \sum_{y-\text{links}} \sigma_j^y \sigma_k^y - J_z \sum_{z-\text{links}} \sigma_j^z \sigma_k^z \tag{2.1}$$

where J_x, J_y and J_z, are model parameters. 'j' and 'k' denote generic nearest neighbour sites. From this anisotropic interactions it is clear that this spin model is an frustrated spin system because a spin on a given site could not satisfy all the three different kind of interactions along the three different links simultaneously. Another key feature of this model is the presence of large number conserved quantities. For each plaquette we can define an operator which commutes with the Hamiltonian. We call this plaquette operator as B_p where the subscript 'p' stands for the plaquette index. Plaquette operators defined on different plaquettes commute among themselves. With reference to the Fig. (2.1) B_p is defined as,

$$B_p = \sigma_1^y \sigma_2^z \sigma_x^x \sigma_4^y \sigma_5^z \sigma_6^x. \tag{2.2}$$

Thus for each plaquette 'p' we can define a B_p. It can be easily checked that,

$$[B_p, H] = 0\,, \quad [B_p, B_q] = 0,\ p \neq q, p, q \text{ indicate to different plaquette indices.} \tag{2.3}$$

This implies that B_p's are conserved quantities for this model. It is easy to verify that $B_p^2 = 1$ which implies that eigenvalues of B_p are ± 1.

We now present the formal solution of this spin model as obtained by Kitaev himself [33]. He showed that this spin model can be solved exactly using a fermionisation procedure which expresses the spin 1/2 operators in terms of Majorana fermion operators. In the next section we elaborate on this.

2.1 Fermionisation of spin 1/2 operators

Let us assume that every lattice sites have two fermions labelled by '1' and '2'. Thus we have following creation and annihilation operators associated with these two fermions, $c_1, c_2, c_1^\dagger, c_2^\dagger$. This means we are dealing with a four dimensional fock space with the states $|0,0\rangle, |1,0\rangle, |0,1\rangle, |1,1\rangle$ where '0' and '1' denotes the occupation number of the fermions, the first number and the

second number in the kets signify the occupation number of the first and the second fermion respectively. For a given site we construct four Majorana fermions out of this two complex fermions in the following way,

$$c = (c_1 + c_1^\dagger) \tag{2.4}$$
$$c^x = \frac{1}{i}(c_1 - c_1^\dagger) \tag{2.5}$$
$$c^y = (c_2 + c_2^\dagger) \tag{2.6}$$
$$c^z = \frac{1}{i}(c_2 - c_2^\dagger). \tag{2.7}$$

In the above expressions we have not displayed the site index explicitly. We can easily verify the following commutation relation among these Majorana fermion operators,

$$\{c^\alpha, c^\beta\} = 2\delta_{\alpha,\beta}; \quad c^\alpha = c^{\alpha\dagger}, \quad \alpha, \beta = x, y, z \tag{2.8}$$

Original spin 1/2 operators which are present in the spin Hamiltonian are expressed in terms of this Majorana fermion operators in the following way.

$$\sigma^x = ic^x c \tag{2.9}$$
$$\sigma^y = ic^y c \tag{2.10}$$
$$\sigma^z = ic^z c \tag{2.11}$$

It can be checked that any two operators, $\sigma^\alpha, \sigma^\beta$, anti-commutes for $\alpha \neq \beta$, here α and β stands for any one of the component x, y, z. However this does not complete the Pauli spin algebra. The condition $\sigma^x\sigma^y\sigma^z = i$ implies the constraint, $c_x c_y c_z c = 1$. Let us call $c^x c^y c^z c = D$. D can be written as $D = (2c_1^\dagger c_1 - 1)(2c_2^\dagger c_2 - 1)$. Now D is 1 only in the subspace spanned by the states $|0,0\rangle$ and $|1,1\rangle$. For the other two states, $|0,1\rangle$ and $|1,0\rangle$, D is -1. For this reason the subspace involving only the states $|0,0\rangle$ and $|1,1\rangle$ is called physical subspace as the definitions of spins in terms of Majorana fermions are exact only in this subspace. It can be seen that the operator D acts as a generator of a local Z_2 gauge group. The above definition implies that we must apply the projection operator 'P' which will project out the unphysical states. The projection operator P_i at site 'i' is given by,

$$P_i = (1 + D_i)/2 \tag{2.12}$$

2.2 Quadratic Hamiltonian

Now we write the Hamiltonian in terms of fermionic operators. After inserting the relations given by equations (2.9,2.10,2.11) in Eq. (2.1), the original spin Hamiltonian reduces to

$$\begin{aligned} H &= \sum_{x-\text{link}} J_x (ic^a_{x,i} c^b_{x,j}) ic^a_i c^b_j + \sum_{y-\text{link}} J_y (ic^a_{y,i} c^b_{y,j}) ic^a_i c^b_j \\ &+ \sum_{z-\text{link}} J_z (ic^a_{z,i} c^b_{z,j}) ic^a_i c^b_j \end{aligned} \tag{2.13}$$

We observe that each term in the above Hamiltonian is quatric in Majorana fermion operators. However it can be easily noted that operators in the parenthesis of each term of the above Hamiltonian commute with the Hamiltonian and commute among themselves. It means that they are conserved quantities as far as this fermionised Hamiltonian is concerned. This fact makes Eq. (2.13) to be effectively quadratic in Majorana fermions. Let us call, $ic^a_{x,i} c^b_{x,j} = u^x_{i,j}$ for the x-link. Similarly we define $u^y_{i,j}$ and $u^z_{i,j}$ on y and z links respectively. It is obvious that, $u_{i,j} = -u_{j,i}$ and its eigenvalues can take value ± 1. Here we follow the convention of keeping the indices of the site belonging to the 'a' sub lattice first and then for 'b' sub lattice in the expression of $u_{i,j}$. Then the Hamiltonian takes the following form,

$$H = \sum_{x-\text{link}} J_x u^x_{i,j} ic^a_i c^b_j + \sum_{y-\text{link}} J_y u^y_{i,j} ic^a_i c^b_j + \sum_{z-\text{link}} J_z u^z_{i,j} ic^a_i c^b_j \tag{2.14}$$

Now we see that above Hamiltonian describes a tight binding Majorana fermion hopping interactions but the hopping matrix elements are coupled with gauge fields $u^\alpha_{i,j}$ on each bonds. The conserved quantity B_p can be expressed in terms of the Majorana fermions and it turns out to be,

$$B_p = \prod_{(j,k)\epsilon \text{boundary(p)}} u_{j,k} \tag{2.15}$$

It is to be noted that the new conserved quantities, $u_{i,j}$, were absent in the original spin Hamiltonian and they are not gauge invariants (i.e, it does not commute with the projection operator P). But their product over a plaquette yielding B_p according to equation (2.15) is a gauge invariant object.

The meaning of the Hamiltonian given in Eq. (2.14) is following. It describes free Majorana fermion hopping interactions with a Z_2 gauge potential in the background. Here we call $u_{i,j}$ as the Z_2 gauge potential. For

each configuration of $u_{i,j}$ along every link we realize a distinct free Majorana fermion hopping Hamiltonian on a honeycomb lattice. Let us call this Hamiltonian as $H_{\{u\}}$ corresponding to a certain distribution of $u_{i,j}$ along every links. This $H_{\{u\}}$ can formally be diagonalised and one would then get the spectrum leading to ground state energy for such distribution of $u_{i,j}$. A natural question arises for what configurations of $\{u\}$ the spectrum contains global minima. A theorem by Lieb [110] states that the minimum energy configuration is achieved by taking $B_p = 1$ for each plaquette and this is obtained by fixing $u_{i,j} = 1$ for every link. This has also been confirmed by Kitaev numerically [33]. It is to be noticed that all configurations of $u_{i,j}$ which produces a certain realizations of B_p for each plaquette are equivalents as B_ps are the only gauge invariant objects. For the uniform choices of $u_{i,j}$(which corresponds to global minima) we can easily diagonalise the Hamiltonian and get the ground state $|\psi\rangle_{ext}$ in the extended space. To get the true ground state belonging to the physical subspace we must project out the unphysical state which is done in the following way.

$$|\psi\rangle_{\rm w} = \hat{P}|\psi\rangle_{\rm ext} \tag{2.16}$$

Where $\hat{P}$ is the global projection operator and is defined as,

$$\hat{P} = \prod_{i\epsilon {\rm all\ \ sites}} \frac{(1+D_i)}{2} \tag{2.17}$$

Here $|\psi\rangle_{\rm w}$ is the ground state belonging to the physical subspace. The configuration 'w' denotes the equivalent class of 'u' under the gauge transformation D_i. However the spectrum obtained in the extended subspace remains valid as Hamiltonian commutes with the global projection operator. Next we proceed to calculate the spectrum for Kitaev model.

2.3 The ground state

We have already argued that it is the uniform configuration of $B_p = 1$ which contains the global minima of the spectrum. Here we consider the choice u_{ij} =1 for each link which is one of the realizations of $B_p = 1$ for each plaquette. After doing so we notice that Majorana fermion hopping Hamiltonian reduces to a translational invariant Hamiltonian facilitating easy solution using Fourier transformations. The translational invariant Hamiltonian is given by,

$$H \ = \ \sum_{x-{\rm link}} J_x i c_i^a c_j^b + \sum_{y-{\rm link}} J_y i c_i^a c_j^b \sum_{z-{\rm link}} J_z i c_i^a c_j^b \tag{2.18}$$

To solve the above Hamiltonian we define the Fourier transformations for the Majorana fermion operators as ,

$$c_i^{a,b} = \sum_k \frac{1}{\sqrt{MN}} e^{i\vec{k}.\vec{r}} c_k^{a,b}. \tag{2.19}$$

Here we have taken a lattice with M and N unit cells in the directions of $\vec{e_1}$ and $\vec{e_2}$ respectively(Fig. (2.1)). Here $\vec{r} = m\vec{e_1} + n\vec{e_2}$ and $\vec{k} = \frac{p}{M}\vec{G_1} + \frac{q}{N}\vec{G}_2$, where $\vec{G}_{1,2}$ are the reciprocal lattice vectors and are given by,

$$\vec{G_1} = \frac{4\pi}{\sqrt{3}}(\frac{\sqrt{3}}{2}\mathbf{e}_x + \frac{1}{2}\mathbf{e}_y) \; ; \; \vec{G_2} = \frac{4\pi}{\sqrt{3}}\mathbf{e}_y \tag{2.20}$$

Here 'p' and 'q' varies from $-M/2$ to $M/2$ and $-N/2$ to $N/2$ respectively. The above discussion fully describes the Brillouin zone. We notice that the property $c_i^\dagger = c_i$ implies $c_k = c_{-k}^\dagger$. After performing the Fourier transformation, we get the Hamiltonian in k-space as follows,

$$H = \sum_{k\epsilon \mathrm{HBZ}} (c_{k,a}^\dagger c_{k,b}^\dagger) \begin{pmatrix} 0 & if_k^* \\ -if_k & 0 \end{pmatrix} \begin{pmatrix} c_{k,a} \\ c_{k,b} \end{pmatrix} \tag{2.21}$$

In the above equation 'HBZ' stands for half Brillouin zone. The spectral function f_k is given by,

$$f_k = J_z + J_x e^{-ik_1} + J_y e^{-ik_2} \tag{2.22}$$

In above expression 'k_1' and 'k_2' are the components of $\vec{k}$ along x bond and y bond respectively. They are given by,

$$k_1 = \vec{k}.\hat{n}_1 \; ; \; k_2 = \vec{k}.\hat{n}_2 \tag{2.23}$$

$$\hat{n}_1 = \frac{1}{2}\hat{e}_x + \frac{\sqrt{3}}{2}\hat{e}_y \; ; \; \hat{n}_2 = \frac{-1}{2}\hat{e}_x + \frac{\sqrt{3}}{2}\hat{e}_y \tag{2.24}$$

Here $\hat{n}_1$ and $\hat{n}_2$ are the unit vector along the x and y bond respectively. The Hamiltonian given in Eq. (2.21) can be diagonalised easily with the following unitary transformation given below,

$$\begin{pmatrix} c_{k,a} \\ c_{k,b} \end{pmatrix} = \frac{1}{\sqrt{2}} \begin{pmatrix} v_k & -v_k \\ 1 & 1 \end{pmatrix} \begin{pmatrix} \alpha_k \\ \beta_k \end{pmatrix}, \tag{2.25}$$

with $v_k = if_k^*/|f_k|$. The diagonalised Hamiltonian is given by,

$$H = \sum_k E_k(\alpha_k^\dagger \alpha_k - \beta_k^\dagger \beta_k) \tag{2.26}$$

Where $E_k = |f_k|$ is the quasi particle energy associated with new field operators α_k and β_k. The ground state is obtained by filling up all the negative energy states of β_k quasi particles and can be written as,

$$|G\rangle = \Pi_{k,\mathrm{HBZ}} \beta_k^\dagger |0\rangle \tag{2.27}$$

Where $|0\rangle$ represents the quasi particle vacuum such that $\alpha_k|0\rangle = \beta_k|0\rangle = 0$. Here the summation is over the half Brillouin zone. To find whether the spectrum is gapless or not we solve for $f_k = 0$. It turns out that the, $f_k = 0$, has solutions if and only if $|J_x|, |J_y|, |J_z|$ satisfy the following triangle inequalities:

$$|J_x| \leq |J_y| + |J_z|, \;\; |J_y| \leq |J_x| + |J_z|, \;\; |J_z| \leq |J_x| + |J_y| \tag{2.28}$$

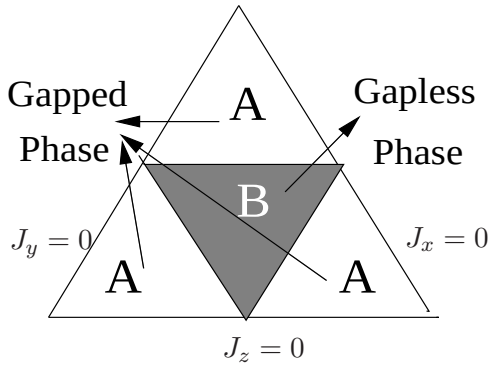

Figure 2.2: Phase diagram for Kitaev model in the parameter space. A point in the above triangle describes relative magnitudes of J_x, J_y, J_z. Three sides of the triangle describe $J_x = 0, J_y = 0$ and $J_z = 0$ as given in the figure. The region 'A' is gapped and the region 'B' is gapless. The gapless region acquires a gap in the presence of Magnetic field.

If the inequalities are strict, there are exactly 2 solutions: $\mathbf{k} = \pm\mathbf{q}_*$, one in each HBZ . The region defined by inequalities in Eq. (2.28) is the shaded region B in Fig. (2.2); this phase is gapless. The region marked by A is gapped. The low energy excitations are different in these two phases. In

the gapless phase the low energy excitations are the Majorana fermions but in the gapped phases the low energy excitations corresponds to the vertex excitations which corresponds to the excitations of B_p. In the presence of magnetic field the phase B acquires a gap. These two regions are topologically distinct as indicated by spectral Chern number which is zero for phase A and 1 for the phase B [33]. We have argued that as the projection operator $\hat{P}$ commutes with the Hamiltonian, the solution obtained in the extended Hilbert space is exact. One can indeed show that there exists a non zero projections (in chapter four we elaborate more on this). But this method of solving does not give exact eigenstates of the Hamiltonian as well as the eigenstates states of the conserved quantities in an easy way. In the next chapter, we will solve the Kitaev model with the help of Jordan-Wigner transformations and apart from recovering the exact eigenvalues obtained in this chapter, we construct explicit eigenstates of the Hamiltonian and the conserved quantities.

I came upon a little town
That slumbered in the harvest moon,
And passed a-tiptoe up and down,
Murmuring, to a fitful tune,
The madness of king Goll-W B Yeats

Chapter 3

Exact eigenstates:J-W transformations

Jordan-Wigner transformation is quite well known for its successful application to one dimensional spin 1/2 models which involve local interactions [135, 136]. We know that in this particular procedure spin operators are re-expressed in terms of new fermionic operators which are non-local in general but in one dimension if the Hamiltonian involves local spin-spin interactions it often yields local fermionic Hamiltonian which is easy to solve. Recently a generalisation of Jordan-Wigner transformation to higher dimensions has been suggested in [136]. In this chapter we show that the novelty of Kitaev model enables us to apply the one dimensional Jordan-Wigner transformation(JWT) to solve this two dimensional spin 1/2 model. In the previous chapter we have used four Majorana fermions(or equivalently two complex fermions) to fermionise the spin operators at a given site. It implies local fock space dimensions at each site to be four though the original spin 1/2 was defined with a fock space dimensions two at every sites. The importance of Jordan Wigner transformation is that it does not enlarge the Hilbert space dimensions of a given site as it deals with one spin-less complex fermion at a given site. Moreover we are able to construct explicit eigenstates of the conserved quantities and Hamiltonian. We also confirm that the solution for spectrum obtained in previous chapter is exact [77, 78]. We note that though Jordan-Wigner transformation has been applied previously to solve Kitaev model in [78, 79], our method has some advantage as it can be applied for any kind of boundary conditions. Moreover our construction can be generalised to higher dimensional Kitaev model also.

We can define the Jordan-Wigner transformation(JWT) for Kitaev model

with open and periodic boundary conditions. In this chapter, we apply JWT for periodic boundary conditions, i.e on a torus. In the appendix A, we have given the details of JWT for open boundary condition.

Before coming to the JWT, we discuss in more detail about the conserved quantities of this model for a lattice with periodic boundary condition. This would explain the degeneracies associated this model.

3.1 Conserved quantities

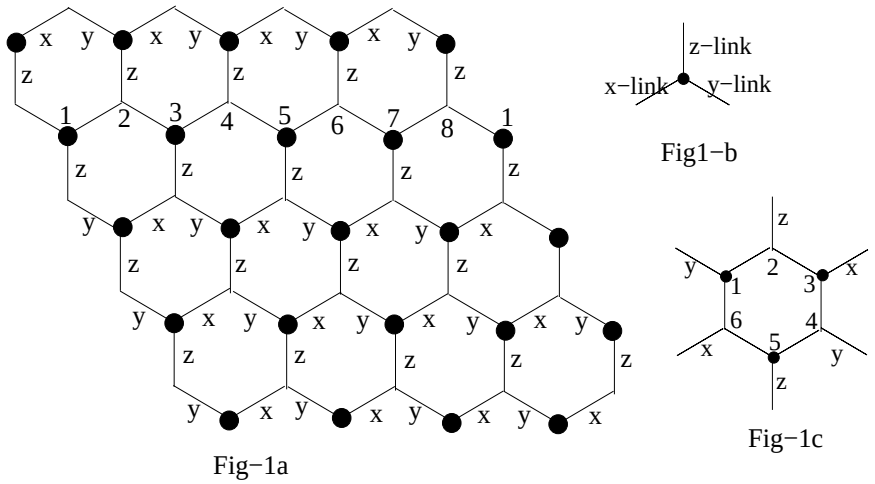

Figure 3.1: In figure 1a, we have shown a part of honeycomb lattice. Links are marked with x,y and z to indicate the bond dependent nature of spin-spin interactions. There exists a non trivial loop operator for each 1D chain of this two dimensional model. We have indicated such a chain by the index 1 to 8. In figure 1c, we have presented a single hexagon to explain B_p. See text for more explanation.

We mentioned before that there is a conserved quantity associated with every plaquette of the lattice. If the plaquette is denoted by 'p' and its vertices are labelled as shown in Fig. (3.1, 1c) then, following Kitaev's notation, the conserved quantity is,

$$B_p = \sigma_1^y \sigma_2^z \sigma_3^x \sigma_4^y \sigma_5^z \sigma_6^x \tag{3.1}$$

We have $B_p^2 = 1$, implying that the eigenvalues of B_p can take values ± 1. It is clear that a product of any number of B_p commutes with the Hamiltonian.

In fact there is a conserved quantity associated with every closed self avoiding loop, C, on the lattice which can be defined in the following way. If the sites of C are $i_1, i_2, ...i_N$, then the conserved quantity associated with it is,

$$B_c = \prod_{n=1}^{N} \sigma_{i_n}^{\alpha_n} \tag{3.2}$$

where α_n denotes the outgoing bond at the site i_n . It can be verified that,

$$[B_c, H] = 0, \qquad B_c^2 = 1 \tag{3.3}$$

We call C topologically trivial if it can be written as a product of only B_ps. On the torus, we have two loop operators which wind around the torus in two orthogonal directions and which cannot be expressed as a product of B_ps. These two topologically non-trivial loops are denoted by B_{c_1} and B_{c_2}. From the Fig. (3.1, 1a) we find for horizontal winding along a complete $x-y$ chain, the following conserved operator, B_{c1} ,

$$B_{c1} = \sigma_1^z \sigma_2^z \sigma_3^z \sigma_4^z \sigma_5^z \sigma_6^z \sigma_7^z \sigma_8^z. \tag{3.4}$$

For each $x-y$ chain we can find one conserved operator like above. However only one among these is independent. Same is true for winding along $x-z$ chain which gives the other non-trivial loop conserved operator B_{c2}. However winding along $y-z$ chain does not result into another independent conserved loop operator as it can be constructed out of B_{c1}, B_{c2} and suitable combinations of B_ps. We note that all the B_ps are not independent due to the following constraint on a torus,

$$\prod_p B_p = 1 \tag{3.5}$$

Thus there are $N_p - 1$ independent B_p, where $N_p = MN$ is the number of plaquettes. Together with B_{c_1} and B_{c_2}, we have a total of $N_p + 1$ conserved quantities on the torus. Let us count the number of independent ways we can choose a certain configuration of B_p(i.e a distribution of eigenvalues of B_p for each plaquette) and we obtain,

$$\frac{2^{N_p+1}}{2^{N_p-1}} = 2^2 = 4 \tag{3.6}$$

The above counting shows that there are four different states having same configuration of B_p . Thus if the ground state sector belongs to the

uniform configuration of B_p, we should obtain four degenerate states having same ground state energy as the spectrum depends only on B_p and not on B_{c_1} and B_{c_2}. Indeed, later we will show that this is the case. Now we are in a position to discuss JWT transformation for Kitaev model.

3.2 J-W TRANSFORMATION FOR PERIODIC BOUNDARY CONDITION

To define the Jordan-Wigner transformation, we need a path defined on the lattice which we call Hamilton path. This Hamilton path should contain all the sites of the lattice and it should be self avoiding. Hexagonal lattice has connectivity three which means a site is connected to three neighbouring sites. If we consider a particular site we find that Hamilton path contains two of the bonds coming out from this site. We call these two bonds 'tangent bonds'. The remaining bond which go out from the Hamilton path is called 'normal bond'. In Fig. (3.2), we explain our notion of normal bonds and tangential bonds. When we find such Hamilton path we observe that the normal bonds form a dimer covering of the lattice as shown in Fig 3.3. We associate two tangential vectors for the two tangent bonds, $\hat{\mathbf{t}}_{1i}$ and $\hat{\mathbf{t}}_{2i}$ which are either $\hat{\mathbf{x}}$, $\hat{\mathbf{y}}$ or $\hat{\mathbf{z}}$ according to the direction of the incoming bond and the outgoing bond respectively. The subscript 'i' refers a particular site on the Hamiltonian path. We then define a normal vector $\hat{\mathbf{n}}_i$ as ,

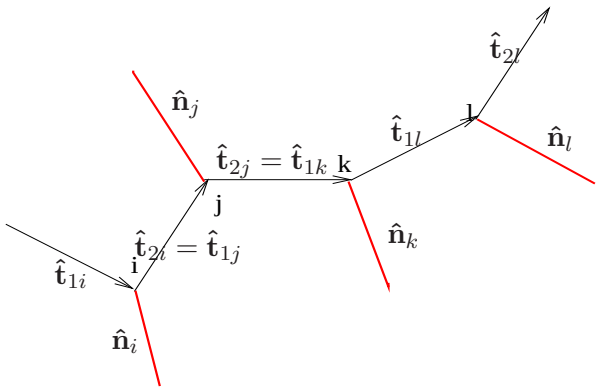

Figure 3.2: A part of the Jordan-Wigner path. The red links constitute the normal bonds and the black links constitute the tangential bonds. The Jordan-Wigner path is shown by the direction of arrows.

$$\hat{\mathbf{n}}_i \equiv \hat{\mathbf{t}}_{1i} \times \hat{\mathbf{t}}_{2i} \tag{3.7}$$

We now explicitly define the periodic boundary condition which is being used in this thesis. The honeycomb lattice is a triangular lattice with a basis of two sites. The sites of the triangular lattice are given by,

$$\mathbf{R}_I = I_1\mathbf{e}_1 + I_2\mathbf{e}_2 \tag{3.8}$$

where $I_1,\ I_2$ are integers and $\mathbf{e}_1 \cdot \mathbf{e}_2 = -\frac{1}{2},\ \mathbf{e}_1 \cdot \mathbf{e}_1 = 1 = \mathbf{e}_2 \cdot \mathbf{e}_2$. The label '$i$' which is used to denote a site for the honeycomb lattice therefore stands for (I_1, I_2, r) where $r = 1, 2$ is the sub lattice indices. The periodic boundary conditions are then defined by,

$$\sigma^a_{I_1,I_2,r} = \sigma^a_{I_1+M,I_2+N,r} \tag{3.9}$$

3.2.1 The 'Disorder' Variable for JWT

We define the Jordan-Wigner transformation as follows. We take a Hamilton path on the lattice defined by a sequence of sites $i_n,\ n = 1, \ldots, N_S$, where N_S is the number of sites in the lattice. Next we introduce the disorder variables which are useful to define the JWT in an easy way.

$$\mu_{i_n} = \prod_{m=1}^{n-1} (\hat{\mathbf{n}}_{i_m} \cdot \boldsymbol{\sigma}_{i_m}) \tag{3.10}$$

we note that while we are using the standard Jordan-Wigner nomenclature in calling these the disorder variables, there is no order-disorder transition in this model. The disorder variables have the following properties,

$$\begin{aligned}
\mu_{i_n}^2 &= 1 && && (3.11)\\
[\mu_{i_n}, \mu_{i_m}] &= 0 && && (3.12)\\
[\hat{\mathbf{t}}_{ai_n} \cdot \boldsymbol{\sigma}_{i_n}, \mu_{i_m}] &= 0 && a = 1,2 \quad m \leq n && (3.13)\\
\{\hat{\mathbf{t}}_{ai_n} \cdot \boldsymbol{\sigma}_{i_n}, \mu_{i_m}\} &= 0 && a = 1,2 \quad m > n && (3.14)
\end{aligned}$$

It is instructive to express μ_{i_n} in terms of the Majorana fermions. Using the identities,

$$\begin{aligned}
\hat{\mathbf{t}}_{1i_n} &= \hat{\mathbf{t}}_{2i_{n-1}} && (3.15)\\
\mathbf{c}_{i_n} \cdot \hat{\mathbf{n}}_{i_n} &= \pm\, (\hat{\mathbf{t}}_{1i_n} \cdot \mathbf{c}_{i_n})\, (\hat{\mathbf{t}}_{2i_n} \cdot \mathbf{c}_{i_n}) && (3.16)
\end{aligned}$$

we get,

$$\mu_{i_n} = \pm\, \hat{\mathbf{t}}_{2i_{n-1}} . \mathbf{c}_{i_{n-1}}\ \left(u_{i_{n-1}i_{n-2}} \ldots u_{i_2 i_1}\right)\ \hat{\mathbf{t}}_{1i_1} \cdot \mathbf{c}_{i_1} \tag{3.17}$$

μ_{i_n} is therefore an open Wilson line with two Majorana fermions attached at the ends. The operator which corresponds to a closed Wilson loop along the Hamilton path is a conserved quantity which we call $\mathcal{S}$.

$$\mathcal{S} \equiv \prod_{n=1}^{N_S} (\hat{\mathbf{n}}_{i_m} \cdot \boldsymbol{\sigma}_{i_m}) \tag{3.18}$$

$$= \left(u_{i_1 i_{N_S}} u_{i_{N_S} i_{N_S-1}} \dots u_{i_3 i_2} u_{i_2 i_1}\right) \tag{3.19}$$

$\mathcal{S}$ is a well known conserved quantity in the one-dimensional applications where it corresponds to the total number of fermions modulo 2 and determines the boundary conditions on the fermions. Here we will see that it also gives a constraint on the total number of fermions. Also the conserved quantity $\mathcal{S}$ can be interpreted as the generator of suitable rotation at every sites of the lattice which keeps the spin Hamiltonian invariant. To elucidate this we first notice that a global rotation of $n\pi$ around z-axis makes every σ_i^x and σ_i^y to be $\pm\sigma_i^x$ and $\pm\sigma_i^y$ respectively. Kitaev Hamiltonian is invariant under such global rotation with open boundary conditions. This rotational operator can be written as,

$$\mathcal{S} = e^{in\pi \sum_i \sigma_i^\alpha} \tag{3.20}$$

In above equation α denotes that component of spin which is associated with the normal bond coming put from the site 'i'. The significance of the operator $\mathcal{S}$ is that it generates a local rotation at every site of the lattice so that the Kitaev Hamiltonian remains invariants under periodic boundary condition. Thus for a given Jordan-Wigner path the operator $\mathcal{S}$ generates such a unitary transformations which keeps the Hamiltonian invariant.

3.2.2 Gauge invariant Jordan-Wigner fermions

The Jordan-Wigner fermions are defined as usual as the product of the spin variables with the disorder variables,

$$\xi_{i_n} = (\hat{\mathbf{t}}_{1 i_n} \cdot \boldsymbol{\sigma}_{i_n})\, \mu_{i_n} \tag{3.21}$$

$$\eta_{i_n} = (\hat{\mathbf{t}}_{2 i_n} \cdot \boldsymbol{\sigma}_{i_n})\, \mu_{i_n} \tag{3.22}$$

The anti-commutation relations of the fermions follows from equations (3.11-3.22),

$$\begin{aligned} \{\xi_i, \xi_j\} &= 2\delta_{ij} \\ \{\eta_i, \eta_j\} &= 2\delta_{ij} \\ \{\xi_i, \eta_j\} &= 0 \end{aligned} \tag{3.23}$$

Since the Jordan-Wigner fermions are constructed entirely from the spin operators, they are manifestly gauge invariant. It is also instructive to rewrite equations (3.21) and (3.22) in terms of the original Majorana fermions and gauge fields,

$$\xi_{i_n} = ic_{i_n} \left(u_{i_{n-1}i_{n-2}} \dots u_{i_2 i_1}\right) \hat{\mathbf{t}}_{1i_1} \cdot \mathbf{c}_{i_1} \tag{3.24}$$

$$\eta_{i_n} = i\mathbf{c}_{i_n} \cdot \hat{\mathbf{n}}_{i_n} \left(u_{i_{n-1}i_{n-2}} \dots u_{i_2 i_1}\right) \hat{\mathbf{t}}_{1i_1} \cdot \mathbf{c}_{i_1} \tag{3.25}$$

Above transformations can be inverted to write the spins in terms of the fermions as written below,

$$\hat{\mathbf{n}}_{i_n} \cdot \boldsymbol{\sigma}_{i_n} = i\xi_{i_n}\eta_{i_n} \tag{3.26}$$

$$\hat{\mathbf{t}}_{1i_n} \cdot \boldsymbol{\sigma}_{i_n} = \xi_{i_n}\mu_{i_n} \tag{3.27}$$

$$\hat{\mathbf{t}}_{2i_n} \cdot \boldsymbol{\sigma}_{i_n} = \eta_{i_n}\mu_{i_n} \tag{3.28}$$

3.2.3 The gauge fixed Hamiltonian

After implementing Jordan-Wigner transformations (as discussed in the previous subsection), original spin Hamittonian takes the following form,

$$\tilde{H} = J_x \sum_{\langle ij\rangle_x} i\xi_i \tilde{u}_{ij} \xi_j + J_y \sum_{\langle ij\rangle_y} i\xi_i \tilde{u}_{ij} \xi_j + J_z \sum_{\langle ij\rangle_z} i\xi_i \tilde{u}_{ij} \xi_j \tag{3.29}$$

where the gauge fixed Z_2 fields, $\tilde{u}_{ij}$ are,

$$\tilde{u}_{ij} = i\eta_i\eta_j, \quad \text{for normal bonds} \tag{3.30}$$

$$= 1 \quad \text{for tangential bonds except } (ij) = (i_1 i_{N_S}) \tag{3.31}$$

$$\tilde{u}_{i_1 i_{N_S}} = \mathcal{S}, \quad \text{for end bonds} \tag{3.32}$$

Here it is instructive to compare the above Hamiltonian with that of Eq. (2.14). While in Eq. (2.14) Z_2 gauge fields appear on every bonds, in Eq. (3.29) they appear selectively, namely on normal bonds. Thus the Jordan-Wigner transformation is equivalent to a gauge fixing procedure where all the gauge fields on the tangential bonds (except on the end bonds) are set

equal to 1. The choice of the Hamilton path amounts to a gauge choice since it defines which of the bonds are tangential and which are not. It also defines the sign in the definition of u_{ij} for the normal bonds uniquely. In equations (3.30,3.31,3.32), the sign corresponds to a Hamilton path which winds regularly in the $\hat{\mathbf{e}}_1$ direction as shown in Fig. (3.3). Here after all explicit computations will be done with respect to this Hamilton path. A general algorithm to go to this gauge from any arbitrary gauge, which we refer to as the Jordan-Wigner gauge, is discussed in appendix A.

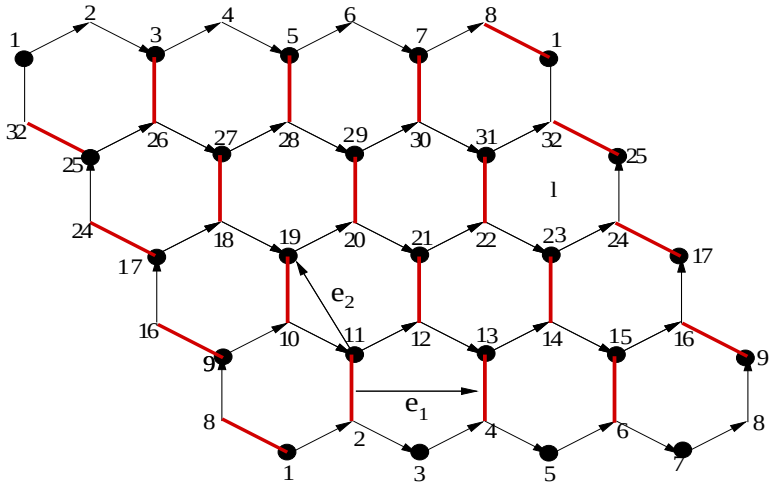

Figure 3.3: Jordan-Wigner path for PBC. The red links constitute the normal bonds. The Jordan-Wigner Path is shown by the direction of arrays.

3.2.4 The fermionic conserved quantities

We note that all the gauge invariant Z_2 fields are conserved quantities. We re-express them in terms of the gauge fixed bond fermions, χ_{ij}, defined on the normal bonds connecting sites 'i' and 'j',

$$\chi_{ij} \equiv \frac{\eta_i + i\eta_j}{2} \quad \chi_{ij}^\dagger \equiv \frac{\eta_i - i\eta_j}{2} \tag{3.33}$$

The conserved quantities are then reduced to occupation number operators of the bond fermions defined on every normal bonds,

$$\tilde{u}_{ij} = 2\ \chi_{ij}^\dagger \chi_{ij} - 1 \tag{3.34}$$

As there are N_p normal bonds, the bond fermion occupation numbers form a set of N_p conserved quantities. Thus along with $\mathcal{S}$, we have N_p+1 conserved

quantities consistent with total number of conserve quantities derived before in section (3.1). This gives a complete account for conserved quantities in terms of fermions and spin variables. To see the meaning of $\mathcal{S}$, it is convenient to define complex fermions out of the two ξ fermions on every normal bond as given below,

$$\psi_{ij} \equiv \frac{\xi_i + i\xi_j}{2} \quad \psi^\dagger_{ij} \equiv \frac{\xi_i - i\xi_j}{2} \tag{3.35}$$

It can then be shown that,

$$\mathcal{S} = (-1)^{\left(N_\psi + N_\chi + N_S + 1\right)} \tag{3.36}$$

$$N_\psi \equiv \sum_{\substack{\text{normal}\\ \text{bonds}}} \psi^\dagger_{ij}\psi_{ij} \tag{3.37}$$

$$N_\chi \equiv \sum_{\substack{\text{tangential}\\ \text{bonds}}} \chi^\dagger_{ij}\chi_{ij} \tag{3.38}$$

Thus the operator $\mathcal{S}$ fixes total number of ψ and χ fermions of the system. We can easily express the operator B_p in terms of this gauge invariant fermions. We see that every plaquette contains two normal bonds. B_p for any plaquette is just the product of the conserved Z_2 fields associated with these two normal bonds.

$$B_p = \hat{u}_{ij}\hat{u}_{kl} \tag{3.39}$$

$$\tag{3.40}$$

In the above equations 'ij' and 'kl' denote pairs of sites of z-bonds shared by the plaquette 'p'. Though the above representation is true for all the plaquettes, it is different for the plaquette where the Jordan-Wigner ends points meet. We need to multiply the above expressions with $-\mathcal{S}$ to get the expressions for B_p. Now we express the topologically nontrivial loop operators B_{c1} and B_{c2} in terms of the Jordan-Wigner fermions. We know that B_{c1} is nothing but the product of σ^z for all sites which reside in a given horizontal $x-y$ chain. With reference to Fig. (3.3), we notice that any horizontal zig-zag $x-y$ chain contains a slanted normal y-bond. Then we find that B_{c1} for this $x-y$ chain is given by the conserved gauge field $\hat{u}_{ij}$ present on the slanted normal y-bond for this $x-y$ chain. We see that all the sites of a given $x-y$ chain can be denoted by the lattice indices (m,n) where 'm' runs from 1 to 'N' and 'n' is fixed. We take this 'n' to label the $x-y$ chain. Then the conserved quantity for this chain is given by,

$$B^n_{c1} = \hat{u}_{\substack{0,n \\ 0,n+1}} \tag{3.41}$$

Similarly we can label zig-zag $y-z$ chain by the index 'm' where 'm' corresponds to lattice translation along $\mathbf{e_1}$ direction. Now we see that it contains a number of normal bonds, each one having a conserved gauge field associated with it. Then B_{c2} is just the product of all these conserved gauge fields living on these normal bonds. Thus we can write,

$$B^m_{c2} = \prod_{n=1,N} \hat{u}_{m,n}. \tag{3.42}$$

3.3 Four fold degeneracy for ground state

We have shown before that there are four different states having identical configuration of B_ps. This is also true for ground state configuration of of B_p implying four fold ground state degeneracy. This is due to the presence of B_{c1} and B_{c2} which can take four possible different values for a given configuration of B_p. We will show that when we fix this four possible choices for the eigenvalues of B_{c1} and B_{c2}, it imposes constraints on the values of Z_2 gauge fields. But in thermodynamic limit the fermionic ground state energies obtained in different gauge choices are identical. Now we examine each of these four flux free configurations and compute the corresponding fermionic ground state energy in each case and show that in thermodynamic limit they lead to identical ground state energy.

All the calculations are done following the Jordan-Wigner gauge which has been explained in detail in the appendix B and corresponds to the Jordan-Wigner path given in Fig. (3.3). The normal bonds are the ones that form the basis of the triangular lattice except for the (O, I_2, r) line. On this line normal bonds are the ones between $(0, I_2, 1)$ and $(0, I_2+1, 2)$). We choose the first site of the path to be $i_1 = (0, 0, 2)$. We group the terms of the Hamiltonian in three parts, H_{int}, H_{slant} and H_{end}. H_{int} includes interactions for all the internal bonds and H_{slant} includes interactions for all the boundary bonds except one where the Jordan-Wigner end points meets.(Here by boundary bonds we refer slanted red bonds as shown in Fig. 3.3). H_{end} includes the interaction for the bond where the Jordan-Wigner end points meet each other. Similarly all the B_ps are grouped in the above three different ways. The three parts of the Hamiltonian are given by,

$$\begin{aligned} H_{int} &= \sum_{m,n} iJ_x\eta^a_{m,n}\eta^b_{m+1,n+1} + \sum_{m,n} iJ_y\eta^a_{m,n}\eta^b_{m,n+1} \\ &\quad + \sum_{m,n} iJ_zU_{m,n}\eta^a_{m,n}\eta^b_{m,n} \end{aligned} \tag{3.43}$$

Where $U_{m,n}$ is defined on each internal z-bond and represents the eigenvalue of the corresponding gauge field $\hat{u}_{m,n}$.

$$H_{slant} = \sum_{m,n} iJ_yU_{(m,n),(m,n+1)}i\eta^a_{m,n}\eta^b_{m,n+1} + J_zi\eta^a_{m,n}\eta^b_{m,n} \tag{3.44}$$

Where $U_{(m,n),(m,n+1)}$ is defined on each boundary y-bond. The Hamiltonian for the end bond is given by,

$$H_{end} = -\mathcal{S}i\eta^a_{M,N}\eta^b_{M,N} \tag{3.45}$$

Now with the definition of ψ fermion and χ fermion we get the Eq. (3.43) as,

$$\begin{aligned} H_{int} &= J_x(\psi^\dagger_{m,n} + \psi_{m,n})(\psi^\dagger_{m+1,n+1} - \psi_{m+1,n+1}) \\ &\quad + J_y(\psi^\dagger_{m,n} + \psi_{m,n})(\psi^\dagger_{m,n+1} - \psi_{m,n+1}) \\ &\quad + J_zU_{m,n}(2\psi^\dagger_{m,n}\psi_{m,n} - 1) \end{aligned} \tag{3.46}$$

Similarly the Hamiltonian for the slanting bonds is given by ,

$$\begin{aligned} H_{slant} &= \sum_{m,n} J_yU_{\substack{m,n \\ m,n+1}}(\psi^\dagger_{m,n} + \psi_{m,n})(\psi^\dagger_{m,n+1} - \psi_{m,n+1}) \\ &\quad + J_z(2\psi^\dagger_{m,n}\psi_{m,n} - 1) \end{aligned} \tag{3.47}$$

Lastly the Hamiltonian term for the end bond where end points of Jordan-Wigner path meets is given by,

$$H_{end} = -\mathcal{S}J_z(2\psi^\dagger_{m,n}\psi_{m,n} - 1) \tag{3.48}$$

$U_{m,n}$ is the eigenvalue of the conserved quantity $\hat{u}_{m,n}$ defined on each internal z-bond which is given by,

$$U_{m,n} = (2\langle\chi^\dagger_{m,n}\chi_{m,n}\rangle - 1), \tag{3.49}$$

In the above equation angular bracket denotes the eigenvalue of corresponding operator inside the angular bracket. Similarly the conserved quantity defined on each slanting y-bond which is labelled by the z-bonds it is joined with (i,e $u_{\substack{m,n\\m,n+1}}$) is given by,

$$U_{\substack{m,n\\m,n+1}} = (2\langle \chi^{\dagger}_{\substack{m,n\\m,n+1}} \chi_{\substack{m,n\\m,n+1}} \rangle - 1) \tag{3.50}$$

And $\mathcal{S}$, for the Jordan-Wigner gauge, is given by,

$$\mathcal{S} = -(-1)^{MN+N_{\psi}+N_{\chi}}. \tag{3.51}$$

Here MN denotes total number of lattice site and N_{ψ} and N_{χ} denote total number of ψ and χ fermions. Below we discuss in detail the spectrum for four choices of gauge field configurations corresponding to $B_p = 1$ for all plaquettes. Now we proceed to discuss the four field ground state degeneracy. We explicitly describe the gauge field configurations for each case.

3.3.1 Choice 1

Here the flux free configuration is obtained by making all the $U_{m,n}$s to be 1 and $\mathcal{S}$ to be -1. Topologically non-trivial loop conserve quantities B_{c1} and B_{c2} are also set to 1. The above choices make Hamiltonian completely translational invariant(refer to equations (3.46, 3.47, 3.48)) and usual periodic boundary condition in both the directions can be used to define the Fourier transformations. From now on we will explicitly write the Hamiltonian in terms of complex fermion ψ. However one can equivalently work in terms of η, Majorana fermion representation. To keep this in mind we continue to mention appropriate gauge transformations for η fermions as well as for ψ fermions. The translational invariant Hamiltonian is given by,

$$\begin{aligned} H &= J_x(\psi^{\dagger}_{m,n} + \psi_{m,n})(\psi^{\dagger}_{m+1,n+1} - \psi_{m+1,n+1}) \\ &\quad + J_y((\psi^{\dagger}_{m,n} + \psi_{m,n}))(\psi^{\dagger}_{m,n+1} - \psi_{m,n+1}) \\ &\quad + J_z(2\psi^{\dagger}_{m,n}\psi_{m,n} - 1) \end{aligned} \tag{3.52}$$

We see that the above Hamiltonian is equivalent to that of the Kitaev's Hamiltonian after fermionisations. Thus it reaffirms that the solution obtained by Kitaev is exact. This Hamiltonian also signifies a p-wave super conducting Hamiltonian and can easily be diagonalised in going to the momentum space. The boundary condition on $\eta_{m,n}$ is, $\eta_{M+1,n} = \eta_{1,n}$ and

$\eta_{m,N+1} = \eta_{m,1}$, or alternatively, $\psi_{M+1,n} = \psi_{1,n}$ and $\psi_{m,N+1} = \psi_{m,1}$. However we prefer to work in the representation of ψ where implementing the boundary condition on fermion occupation number is easy. We define the Fourier transformation for the $\psi_{m,n}$ as,

$$\psi_{\vec{R}} = \frac{1}{\sqrt{MN}} \sum_{\vec{k}} e^{i\vec{k}.\vec{R}} \psi_{\vec{k}} \tag{3.53}$$

$$\text{or} \quad \psi_{m,n} = \frac{1}{\sqrt{MN}} \sum_{p,q} e^{i(k_1 m + k_2 n)} \psi_{\vec{k}} \tag{3.54}$$

Where $k_1 = 2\pi\frac{p}{M}$ and $k_2 = 2\pi\frac{q}{N}$ and $\vec{R} = m\vec{e_1} + n\vec{e_2}$. This is obtained by noticing the fact that we can write $\vec{k} = \frac{p}{M}\vec{G_1} + \frac{q}{N}\vec{G_2}$ where $\vec{G}_{1,2}$ are the reciprocal lattice vectors and are given by,

$$\vec{G_1} = \frac{4\pi}{\sqrt{3}}(\frac{\sqrt{3}}{2}\mathbf{e}_x + \frac{1}{2}\mathbf{e}_y) \; ; \; \vec{G_2} = \frac{4\pi}{\sqrt{3}}\mathbf{e}_y \tag{3.55}$$

The Eq. (3.53) and the Eq. (3.54) are same. In the former we have used position vector where as in the later we have used the lattice site indices to represent a given site. Substituting Eq. (3.54) in Eq. (3.52) we get,

$$H = \sum_{k\in bz} (\epsilon_k \psi^\dagger_{\vec{k}} \psi_{\vec{k}} + i\frac{\delta_k}{2}\psi^\dagger_{\vec{k}}\psi^\dagger_{\vec{G}-\vec{k}} - i\frac{\delta_k}{2}\psi_{\vec{G}-\vec{k}}\psi_{\vec{k}}) \tag{3.56}$$

Where, $\epsilon_k = 2(J_x \cos k_x + J_y \cos k_y + J_z)$ and $\delta_k = 2(J_x \sin k_x + J_y \sin k_y)$. $k_x = \vec{k}.\vec{n}_x$, $k_y = \vec{k}.\vec{n}_y$ and $\vec{n}_{x,y} = \frac{1}{2}\vec{e}_x \pm \frac{\sqrt{3}}{2}\vec{e}_y$ are unit vectors along x and y-bonds respectively.

Now we rewrite the Hamiltonian in the following way,

$$\begin{aligned} H = & \sum_{k\in hbz} (\epsilon_k \psi^\dagger_k \psi_k - \epsilon_k \psi_{-k}\psi^\dagger_{-k} + i\delta_k \psi^\dagger_k \psi^\dagger_{-k} - i\delta_k \psi_{-k}\psi_k) \\ & + \epsilon_{0,0}\psi^\dagger_{0,0}\psi_{0,0} + \epsilon_{\pi,0}\psi^\dagger_{\pi,0}\psi_{\pi,0} + \epsilon_{0,\pi}\psi^\dagger_{0,\pi}\psi_{0,\pi} + \epsilon_{\pi,\pi}\psi^\dagger_{\pi,\pi}\psi_{\pi,\pi} \\ & + \sum_{k\in hbz} \epsilon_k - MNJ_z \end{aligned} \tag{3.57}$$

In the above equation we have omitted the vector notation for momentum variable. Here the sum over 'k' runs over first half of the Brillouin zone and does not includes the point $(\pi, 0), (0, \pi), (0, 0), (\pi, \pi)$. The first line of the Hamiltonian is diagonalised by the following orthonormal transformations,

$$\begin{pmatrix} \alpha_k \\ \beta_k \end{pmatrix} = \begin{pmatrix} \cos\theta_k & -i\sin\theta_k \\ -i\,sin\theta_k & \cos\theta_k \end{pmatrix} \begin{pmatrix} \psi_k \\ \psi^\dagger_{-k} \end{pmatrix} \tag{3.58}$$

Where $\cos 2\theta_k = \epsilon_k/E_k$ and α_k and β_k denotes new fermionic quasi particles which diagonalizes the Hamiltonian. Rewriting the Hamiltonian we get,

$$\begin{aligned} H &= \sum_{k\in \mathrm{HBZ}} E_k(\alpha^\dagger_k\alpha_k - \beta^\dagger_k\beta_k) \\ &\quad +\epsilon_{0,0}\psi^\dagger_{0,0}\psi_{0,0} + \epsilon_{\pi,0}\psi^\dagger_{\pi,0}\psi_{\pi,0} + \epsilon_{0,\pi}\psi^\dagger_{0,\pi}\psi_{0,\pi} \\ &\quad -\frac{1}{2}(\epsilon_{0,0}+\epsilon_{0,\pi}+\epsilon_{\pi,0}+\epsilon_{\pi,\pi}) + (\sum_{k'}\frac{1}{2}\epsilon_{k'} - N_zJ_z) \end{aligned} \tag{3.59}$$

Here sum over 'k'' runs over full Brillouin zone. The last term in the parenthesis is always zero for a Torus. E_k is defined as,

$$E_k = \sqrt{(\epsilon_k^2 + \Delta_k^2)} \tag{3.60}$$

where $\epsilon_k = 2(J_x\cos k_x + J_y\cos k_y - J_z)$ and $\Delta_k = 2(J_x\sin k_x + J_y\sin k_y)$.

3.3.2 Choice 2

Here the flux free configuration is obtained by making all U to be -1 and $\mathcal{S}$ to be -1. B_{c1} and B_{c2} are also set to -1. We make following gauge transformations to facilitate Fourier transformation. $\eta^b_{M,n} = -\eta^b_{M,n}$ for all 'n'. In terms of ψ fermion the necessary gauge transformation is, $\psi_{M,n} = -\psi^\dagger_{M,n}$ for all 'n'. Then the Hamiltonian demands $\eta_{M+1,n} = -\eta_{1,n}$ and $\eta_{m,N+1} = \eta_{m,1}$(or alternatively $\psi_{M+1,n} = -\psi_{1,n}$ and $\psi_{m,N+1} = \psi_{m,1}$). This constraint amounts to an anti-periodic boundary condition in $\vec{e_1}$ direction and periodic boundary condition in $\vec{e_2}$ direction. To implement this boundary condition we define Fourier transform in the following way,

$$\psi_{m,n} = \frac{1}{\sqrt{MN}}\sum_{p,q} e^{i(k_1m+k_2n)} \tag{3.61}$$

with $k_1 = \frac{2\pi}{M}(m+\frac{1}{2})$; $k_2 = 2\pi\frac{n}{N}$. Substituting this in the Hamiltonian and subsequently diagonalising we get,

$$H = \sum_{k\in \mathrm{HBZ}} E_k(\alpha^\dagger_k\alpha_k - \beta^\dagger_k\beta_k) + (\sum_{k'}\frac{1}{2}\epsilon_{k'} - N_zJ_z) \tag{3.62}$$

Here also 'k' varies over first half of the Brillouin zone and the 'k'' goes over the full Brillouin zone. We note the absence of $(0,\pi),(\pi,0)\,(0,0)$ mode. They do not appear for this anti-periodic boundary condition. Here E_k is defined as,

$$\begin{aligned} E_k &= \sqrt{(\epsilon_k^2+\Delta_k^2)} && (3.63)\\ \epsilon_k &= 2(J_x\cos k_x + J_y\cos k_y - J_z) && (3.64)\\ \Delta_k &= 2(J_x\sin k_x + J_y\sin k_y) && (3.65) \end{aligned}$$

3.3.3 Choice 3

The required values for gauge fields are, $U_{M,n}=-1$ for all 'n' from 1 to N-1. All other Us are 1 and $\mathcal{S}$ is also 1. The loop conserve quantity B_{c1} takes value 1 and and B_{c2} takes value -1. Here the necessary gauge transformation is $\eta^b_{m,N}=-\eta^b_{m,N}$ for all m. In terms of ψ fermion the necessary gauge transformation is $\psi_{m,N}=-\psi^\dagger_{m,N}$ for all 'm'. This gauge transformations implies $\eta_{m,N+1}=-\eta_{m,1}$ and $\eta_{M+1,n}=\eta_{1,n}$(or alternatively $\psi_{m,N+1}=-\psi_{m,1}$ and $\psi_{M+1,n}=\psi_{1,n}$). To meet this constraint we impose ant-periodic boundary condition in $\vec{e}_2$ direction and periodic boundary condition in $\vec{e}_1$ direction. This is obtained by expressing,

$$k_1=2\pi\frac{m}{M};\quad k_2=\frac{2\pi}{N}(n+\frac{1}{2}) \tag{3.66}$$

Next we perform Fourier transformations and subsequently diagonalise the Hamiltonian. The resulting diagonalised Hamiltonian is identical with Eq. (3.62). However here one obtains for ϵ_k,

$$\epsilon_k = 2(J_x\cos k_x + J_y\cos k_y + J_z) \tag{3.67}$$

3.3.4 Choice 4

Here the necessary values of conserved quantity is given by, $U_{M,n}=1$ for all 'n' from 1 to $N-1$. All other Us are -1 and $\mathcal{S}$ is 1. We have for this case, $B_{c1}=-1$ and $B_{c2}=1$. Here we need combined gauge transformations implemented for the choices 2 and 3 i.e we need anti-periodic boundary condition in both the directions which is done by the following way,

$$k_1=\frac{2\pi}{M}(m+\frac{1}{2});\quad k_2=\frac{2\pi}{N}(n+\frac{1}{2}) \tag{3.68}$$

Proceeding as before we get exactly Eq. (3.62) with similar expression for ϵ_k as obtained in Eq. (3.67).

3.3.5 Ground State Energy in the Thermodynamic limit

To get the ground state energy for the choice 2, 3 and 4, we are to fill up the negative quasi particle states β_k consistent with the boundary condition (i, to satisfy the constraint on $\mathcal{S}$ which fixes the number of particle (odd or even number)to be taken). It is given in the Appendix B for every possible cases of M and N whether M and N can be odd or even. For the choice 1, we need to fill up all the β_k states. But for $(0,0),(0,\pi)$ etc mode, we need to check whether $\epsilon_{0,0}$, etc are positive. In any case it is clear after taking into consideration of the constant terms that it only contributes as $\frac{1}{2}|\epsilon_{0,0}|$, $\frac{1}{2}|\epsilon_{0,\pi}|$ etc. Thus for the ground state energy we can write for the choice 1,

$$\mathcal{E}_{g1} = \sum_{k\in \mathrm{HBZ}} -E_k - \frac{1}{2}(\epsilon_{0,0}+\epsilon_{0,\pi}+\epsilon_{\pi,0}+\epsilon_{\pi,\pi}) + (\sum_{k'\in \mathrm{FBZ}} \frac{1}{2}\epsilon_{k'} - N_z J_z) \quad (3.69)$$

In the above sum the four points are excluded. Now we can convert the above sum over the full Brillouin zone (FBZ) as follows,

$$\mathcal{E}_{g1} = \sum_{k\in \mathrm{FBZ}} -\frac{1}{2}E_k + (\sum_{k'} \frac{1}{2}\epsilon_{k'} - N_z J_z) \quad (3.70)$$

with $E_k = \sqrt{\epsilon_k^2 + \delta_k^2}$ where ϵ_k^2 and δ_k^2 is defined after equation (3.56). For the choice 2,3 and 4 , we can write for the ground state energy,

$$\mathcal{E}_{g2} = \sum_{k\in \mathrm{FBZ}} -\frac{1}{2}E_k + (\sum_{k'} \frac{1}{2}\epsilon_{k'} - N_z J_z) \quad (3.71)$$

$$\mathcal{E}_{g3} = \sum_{k\in \mathrm{FBZ}} -\frac{1}{2}E_k + (\sum_{k'} \frac{1}{2}\epsilon_{k'} - N_z J_z) \quad (3.72)$$

$$\mathcal{E}_{g4} = \sum_{k\in \mathrm{FBZ}} -\frac{1}{2}E_k + (\sum_{k'} \frac{1}{2}\epsilon_{k'} - N_z J_z). \quad (3.73)$$

In the above equations, the subscript 2, 3 and 4 refers to the ground state energy corresponding to choice 2, 3 and 4 respectively. The expressions for E_k are not necessarily same since the values of ks are different and they are explicitly defined before. Now for $M, N \to \infty$ the sum over the 'k' points corresponds to same Brillouin zone and the terms in the parenthesis becomes zero. Moreover we notice that appearance of a '$-$' sign in the expression of ϵ_k for choices 2 and 4 can be accounted for by shifting the k_1 integral to

$\pi - k_1$. Thus in the thermodynamic limit ($M, N \to \infty$), we can write for the ground state energy as (for all the above four cases),

$$\mathcal{E}_G = -\frac{\sqrt{3}}{16\pi^2} \int_{\mathrm{BZ}} E(k_x, k_y) dk_1 dk_2 \tag{3.74}$$

With $E(k_x, k_y)$ defined in choice 1. Thus it is clear that in Thermodynamic limit ground state has four fold degeneracy.

To summarise in this chapter we have shown that the Jordan-Wigner transformation in the Kitaev model can be interpreted as a Z_2 gauge fixing procedure resulting in gauge invariant [77–79] (gauge fixed) Majorana and bond fermions . The choice of the Jordan-Wigner path amounts to a choice of the Z_2 gauge. We have also explicitly expressed all the conserved spin variables in terms of JW fermions. We have explicitly derived four degenerate ground states on the torus *in both phases*. This is true for gapless as well as in gapped phase. Our JWT can be implemented for every Kitaev like model [85, 86]. Later we will show that this method can also be implemented in 3D lattice also, in fact in any dimensions provided lattice connectivity three is being maintained.

3.4 The '8' site problem

To examine the correctness of our Jordan-Wigner transformation and subsequent definitions of spin operators in terms of complex fermions we have taken a small system, i.e, 2×2 hexagonal system and compared the results obtained from numerical exact diagonalisation of spin Hamiltonian and the results obtained by solving analytically the fermionic Hamiltonian obtained after Jordan-Wigner transformations. These two results obtained from two different ways match to each other which validate our definition of spin operators in terms of complex fermion. The correlation function obtained numerically is of the same nature as argued before. Energy eigenvalues also match.

The exact diagonalisation of this spin systems revealed many important aspects of Kitaev model. It is observed that ground state of this 8-site system has a large singlet component and a small triplet component as far as the nearest neighbour sites are considered. This signifies its closeness to RVB gauge theory. The average value of the square of the total spin operator S^2 comes about 2.5358 whereas the maximum possible value of S^2 is 20. The value of the nearest neighbour $x - x, y - y$, and $z - z$ correlations along the x, y and z bond respectively is -0.57. Any other nearest neighbour spin

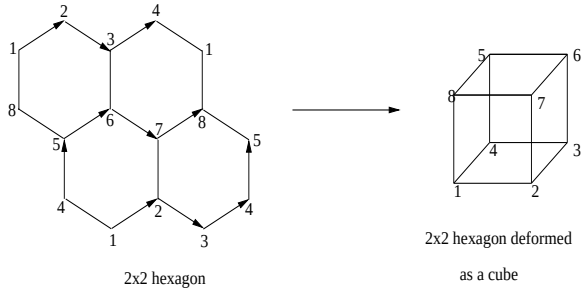

Figure 3.4: 2×2 hexagon and J-W path for periodic boundary condition for this. The numerics in the figure describe the sequences of Jordan-Wigner path

correlations are zero. We have found that the state which is a superposition of the singlet states taken along the x-bond, y-bond and z-bond has about 80 percent overlap with the ground state.

$$\begin{aligned} |Z\rangle &= [1,8][2,7][4,5][3,6] \\ |X\rangle &= [1,4][8,5][7,6][2,3] \\ |Y\rangle &= [1,2][3,4][5,6][7,8] \\ |\Omega\rangle &= \frac{1}{\sqrt{4.5}}(|Z\rangle + |Y\rangle + |X\rangle) \end{aligned} \tag{3.75}$$

In the above $[i,j]$ denotes the singlet on the bond joining site 'i' and site 'j'. We got, $\langle\Omega|G\rangle = 0.8$, where $|G\rangle$ is the ground state wave function. It shows that ground state is primarily a valence bond state. The nearest neighbhour spin-spin correlation obtained with respect to this state is -0.444 which shows that this state is very much near to the actual ground state.

It has been found that ground state for this small system corresponds to uniform $B_p = -1$. From Ref. [110] we note that for a hexagonal lattice the Z_2 flux over a hexagonal plaquette must be 1 for the ground state. For a square lattice the Z_2 flux should be -1. If we look at this small system carefully, we notice that the smallest plaquette for this system is not a hexagonal but a square one, as shown in the Fig. (3.4). Thus if we apply Lieb theorem on the face 1278,2763 and 1234 and add them together we get B_p to be -1 for the path 123658. The same is true for other plaquettes as well. Thus the numerical finding, $B_p = -1$, agrees with the Lieb's result as discussed in [110].

The spin-spin correlation functions for this small system have also been computed. In the next chapter we will be discussing about the spin-spin correlation function in detail. The results we got for this small system conforms with the results shown in next chapter. To mention it is found that two spin correlation are non vanishing only for nearest neighbour sites. The bond dependent nature of correlation function is also checked. It proves that the nature of correlation function does not depend on the size of the lattice as proved in the chapter 4.

This is my delight,
thus to wait and watch at the wayside
where shadow chases light
and the rain comes in the wake of the summer
Where Shadow Chases Light-Tagore

Chapter 4

Spin-Spin correlations

In this chapter we present our study of spin-spin correlation functions in the Kitaev model. We show that for this model we can formally calculate all spin-spin correlation functions exactly for all eigenstates. The method we follow to deduce spin-spin correlation functions is an extension of the fermionisation procedure implemented in [33] . We have already seen that the fermionisation procedure taken in [33] enlarges local Hilbert space dimensions but because of the presence of local conserved quantities in the Kitaev model, Hilbert space enlargement only produces 'gauge copies', without altering the energy spectrum. This helps us to determine the spin-spin correlation function exactly within this formalism. This remarkable feature is absent for standard 2D Heisenberg models when studied using enlarged fermionic Hilbert space [55, 68].

4.1 Bond fermion formalism

We have seen in chapter 2 that two complex fermions yield four Majorana fermions. Basically each complex fermion can be rewritten into two Majorana fermions. Now to facilitate the easy computation of spin-spin correlations we invert the above procedure by regrouping two different Majorana fermions to define a complex fermion. We have seen that at every link there has been one conserve quantity named $u^{\alpha}_{i,j}$ made out of the Majorana fermion $b^{\alpha}_{a,i}$ and $b^{\alpha}_{b,j}$. Here 'i' and 'j' denotes the two sites of a bond, 'a' and 'a' denotes sub-lattice indices and 'α' denotes a specific bond($\alpha = x, y, z$). We regroup these two Majorana fermions to describe a complex fermion named $\chi_{\langle ij\rangle_{\alpha}}$ which lives on the bond joining sites 'i' and 'j'. We call this procedure as bond fermion formalism.

From now on we follow the convention that the site 'i' in the bond $\langle ij\rangle_\alpha$ belongs to a sub-lattice and the' j' belongs to b sub-lattice. Also from now on we do not mention the sub-lattice index 'a' and 'b' explicitly. We define complex fermions on each bond as,

$$\chi_{\langle ij\rangle_\alpha} = \frac{1}{2}\left(c_i^\alpha + ic_j^\alpha\right) \tag{4.1}$$

$$\chi^\dagger_{\langle ij\rangle_\alpha} = \frac{1}{2}\left(c_i^\alpha - ic_j^\alpha\right) \tag{4.2}$$

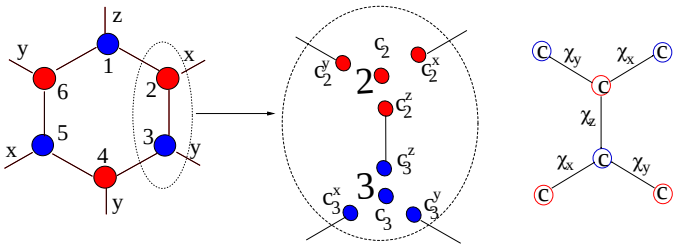

Figure 4.1: Elementary hexagon and 'bond fermion' construction. A spin is replaced with four Majorana fermions (c, c^x, c^y, c^z). Bond fermion $\chi_{\langle 23\rangle}$ for the bond joining site 2 and site 3 is shown . Spin operators are also defined.

For example with reference to the Fig. (4.1), for the z-bond joining site 2 and site 3, and for the y-bond joining site 1 and site 2, we define,

$$\chi_{\langle 23\rangle_z} = (c_2^z + ic_3^z) \;; \chi_{\langle 12\rangle_y} = (c_1^y + ic_2^y) \tag{4.3}$$

Then it follows that for the site '2' and '3' the σ^z operator becomes,

$$\sigma_2^z = ic_2(\chi_{\langle 23\rangle_z} + \chi^\dagger_{\langle 23\rangle_z}) \;\; ; \;\; \sigma_3^z = c_2(\chi_{\langle 23\rangle_z} - \chi^\dagger_{\langle 23\rangle_z}) \tag{4.4}$$

Below we write the result of this re-fermionisation for a bond of type 'α' joining site 'i' and 'j',

$$\chi_{\langle ij\rangle_\alpha} = \frac{1}{2}\left(c_i^\alpha + ic_j^\alpha\right) \;\; ; \;\; \chi^\dagger_{\langle ij\rangle_\alpha} = \frac{1}{2}\left(c_i^\alpha - ic_j^\alpha\right) \tag{4.5}$$

$$\sigma_i^\alpha = ic_i\left(\chi_{\langle ij\rangle_\alpha} + \chi^\dagger_{\langle ij\rangle_\alpha}\right) \;\; ; \;\; \sigma_j^\alpha = c_j\left(\chi_{\langle ij\rangle_\alpha} - \chi^\dagger_{\langle ij\rangle_\alpha}\right) \tag{4.6}$$

It is clear that three components of a spin operator at a site gets connected to three different χ fermions defined on the three different bonds emanating from it. The bond variables are related to the number operators of these

fermions, $\hat{u}_{\langle ij\rangle_\alpha} \equiv ic_i^\alpha c_j^\alpha = 2\chi^\dagger_{\langle ij\rangle_\alpha}\chi_{\langle ij\rangle_\alpha} - 1$. Thus the effective picture is understood easily from the Fig. 4.1. We identify a χ fermion on every bond whose occupation number can be 0 or 1. This occupation number determines the value of $u_{\langle ij\rangle}$ on that bond. But these fermions are conserved and serve as an effective Z_2 gauge potential for hopping 'c' fermions. As χ fermions are conserved, all eigenstates can therefore be chosen to have a definite χ fermion occupation number. The Hamiltonian is then block diagonal in occupation number configurations, each block corresponding to a distinct set of χ fermion occupation numbers for every bonds. Thus all eigenstates in the extended Hilbert space take the following factorised form,

$$|\tilde{\Psi}\rangle = |\mathcal{M}_\mathcal{G}; \mathcal{G}\rangle \equiv |\mathcal{M}_\mathcal{G}\rangle|\mathcal{G}\rangle \tag{4.7}$$

$$\text{with } \chi^\dagger_{\langle ij\rangle_\alpha}\chi_{\langle ij\rangle_\alpha}|\mathcal{G}\rangle = n_{\langle ij\rangle_\alpha}|\mathcal{G}\rangle \tag{4.8}$$

where $n_{\langle ij\rangle_\alpha} = (u_{\langle ij\rangle_\alpha} + 1)/2$ and $|\mathcal{M}_\mathcal{G}\rangle$ is a many body eigen-state in the matter sector determined by 'c' fermions, corresponding to a given Z_2 field configuration determined by $|\mathcal{G}\rangle$.

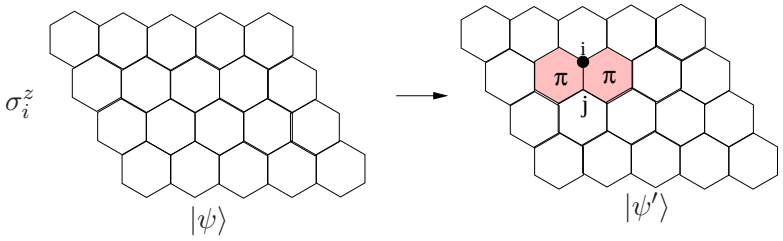

Figure 4.2: How a spin fractionalises into two static π fluxes and a dynamic Majorana fermion is shown. $|\psi\rangle$ is a state with zero flux. We apply σ_i^z where site 'i' is connected with site 'j'. As a result we get a state $|\psi'\rangle$ with two static π fluxes at the plaquette sharing bond $\langle ij\rangle$ and a dynamic Majorana fermion represented by black circle.

Now we discuss the advantage of the above canonical transformations in detail. Written in the above form (refer to Eq. 4.5), the effect of σ_i^α on any eigen-state becomes simple. In addition to adding a Majorana fermion at site 'i', it changes the bond fermion number from 0 to 1 and vice versa (equivalently, $u_{\langle ij\rangle_\alpha} \rightarrow -\, u_{\langle ij\rangle_\alpha}$), at the bond $\langle ij\rangle_\alpha$. The end result is that one π flux is added to each of the two plaquettes that are shared by the bond $\langle ij\rangle a$ (Fig 4.2). We denote this symbolically as

$$\sigma_i^\alpha = ic_i\left(\chi_{\langle ij\rangle_\alpha} + \chi^\dagger_{\langle ij\rangle_\alpha}\right) \quad \rightarrow \quad ic_i\ \hat{\pi}_{1\langle ij\rangle_\alpha}\ \hat{\pi}_{2\langle ij\rangle_\alpha} \tag{4.9}$$

with $\hat{\pi}_{1\langle ij\rangle_\alpha}$ and $\hat{\pi}_{2\langle ij\rangle_\alpha}$ defined as operators that add π fluxes to two adjacent plaquettes shared by the bond $\langle ij\rangle_\alpha$ (Fig (4.2)). Further $\hat{\pi}^2_{1\langle ij\rangle_\alpha} = 1$, since adding two π fluxes is equivalent to adding (modulo 2π) zero flux. It is completely clear that two states with different flux configurations has vanishing overlap as they belong to different distribution of χ fermion occupation numbers. This observation is the key ingredient to compute spin-spin correlations exactly. First we present the calculation of two spin correlations functions. Other multi spin correlation can be calculated with straight forward generalisations of this procedure.

4.2 Two-spin correlations

Here we calculate spin-spin correlation functions in extended Hilbert space. We note this result can be extended exactly in physical Hilbert space for the following reason. *Since the spin operators are gauge invariant, we can compute the correlation in any gauge fixed sector and the answer will be the same as in the physical gauge invariant subspace.* (We have confirmed this by a calculation in the projected physical subspace. For details please look at appendix C). First we consider the two spin dynamical correlation functions, in an arbitrary eigen-state of the Kitaev Hamiltonian in some fixed gauge field configuration $\mathcal{G}$,

$$S^{\alpha\beta}_{ij}(t) = \langle \mathcal{M}_\mathcal{G}|\langle \mathcal{G}|\sigma^{\alpha(t)}_i \sigma^{\beta(0)}_j|\mathcal{G}\rangle|\mathcal{M}_\mathcal{G}\rangle \tag{4.10}$$

Here $A(t) \equiv e^{iHt}Ae^{-iHt}$ is the Heisenberg representation of an operator A, keeping $\hbar = 1$. As discussed before we write the action of spin operator on any eigenstate as,

$$\sigma^{\beta(0)}_j|\mathcal{G}\rangle|\mathcal{M}_\mathcal{G}\rangle = c_i(0)|\mathcal{G}^{i\beta}\rangle|\mathcal{M}_\mathcal{G}\rangle \tag{4.11}$$

$$\sigma^{\alpha(t)}_i|\mathcal{G}\rangle|\mathcal{M}_\mathcal{G}\rangle = e^{i(H-E)t}c_j(0)|\mathcal{G}^{j\alpha}\rangle|\mathcal{M}_\mathcal{G}\rangle \tag{4.12}$$

where, $|\mathcal{G}^{i\alpha(j\beta)}\rangle$ denote the states with extra π fluxes added to $\mathcal{G}$ on the two plaquette adjoining the bond $\langle ik\rangle_\alpha\rangle(\langle lj\rangle_\beta\rangle)$ and E is the energy eigenvalue of the eigenstate $|\mathcal{G}\rangle|\mathcal{M}_\mathcal{G}\rangle$. Since the Z_2 fluxes on each plaquette is a conserved quantity, it is clear that the correlation function in Eq. (4.10) which is the overlap of the two states in equations (4.11, 4.12) is zero unless the spins are on neighbouring sites. Namely, we have proved that the dynamical spin-spin correlation has the form,

$$\begin{aligned} S^{\alpha\beta}_{ij}(t) &= g_{\langle ij\rangle_\alpha}(t)\delta_{\alpha,\beta}\ , \quad \text{for } i,j \text{ nearest neighbours} \\ &= 0 \qquad\qquad\qquad\quad \text{otherwise.} \end{aligned} \tag{4.13}$$

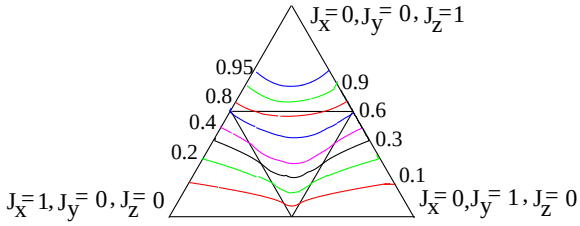

Figure 4.3: Contour plot of nearest-neighbour $z-z$ correlation.

Computation of $g_{ij}(0)$ is straight forward in any eigen-state $|\mathcal{M}_{\mathcal{G}}\rangle$. For the ground state where conserved Z_2 charges are unity at all plaquette, the equal time 2-spin correlation function for the bond $\langle ij\rangle_\alpha$ is given by the analytic expression:

$$\langle \sigma_i^\alpha \sigma_j^\alpha \rangle \equiv S^{\alpha\alpha}_{\langle ij\rangle_\alpha}(0) = \frac{\sqrt{3}}{16\pi^2}\int_{BZ} \cos\theta(k_1,k_2)dk_1dk_2$$

Where $\cos\theta(k_1,k_2) = \frac{\epsilon_k}{E_k}$, $E_k = \sqrt{(\epsilon_k^2+\Delta_k^2)}$, in the Brillouin zone. $\epsilon_k = 2(J_x\cos k_1 + J_y\cos k_2 + J_z)$, $\Delta_k = 2(J_x\sin k_1 + J_y\sin k_2)$, $k_1 = \mathbf{k}.\mathbf{n}_1$, $k_2 = \mathbf{k}.\mathbf{n}_2$ and $\mathbf{n}_{1,2} = \frac{1}{2}\mathbf{e}_x \pm \frac{\sqrt{3}}{2}\mathbf{e}_y$ are unit vectors along x and y bonds. At the point, $J_x = J_y = J_z$, we get $S^{\alpha\alpha}_{\langle ij\rangle_\alpha}(0) = -0.52$. The figure (4.3) shows how the nearest neighbour $z-z$ correlations varies in the parameter (J_x, J_y, J_z) space. To compute $g_{\langle ij\rangle_\alpha}(t)$ we substitute for the σ's from equation (4.1) and (4.2). We choose a gauge where $u_{\langle ij\rangle_\alpha} = -1$ implying $\chi^\dagger_{\langle lj\rangle_\beta}\ |\mathcal{G}\rangle = \chi^\dagger_{\langle ik\rangle_\beta}\ |\mathcal{G}\rangle = 0$. We note that the above condition imposed at $t=0$ continues at all times since the bond fermion numbers are conserved. We then have,

$$g_{\langle ij\rangle_\alpha}(t) \quad = \quad \langle \mathcal{M}_{\mathcal{G}}|\langle \mathcal{G}|\ ic_i(t)\chi^\dagger_{\langle ij\rangle_\alpha}(t)\chi_{\langle ij\rangle_\alpha}(0)\ c_j(0)|\mathcal{G}\rangle|\mathcal{M}_{\mathcal{G}}\rangle \tag{4.14}$$

The time dependence of evolution can be expressed in terms of the Hamiltonian and noting that it is diagonal in the number operators $\chi^\dagger\chi$, we get,

$$g_{\langle ij\rangle_\alpha}(t) = \langle \mathcal{M}_{\mathcal{G}}|e^{iH[\mathcal{G}^{i\alpha}]t}ic_i(0)e^{-iH[\mathcal{G}^{i\alpha}]t}(-1)c_j(0)|\mathcal{M}_{\mathcal{G}}\rangle \tag{4.15}$$

where $H[\mathcal{G}^{i\alpha}]$ is the tight binding Hamiltonian in the background of the static gauge field configuration $\mathcal{G}^{i\alpha}$. The (-1) factor is the eigenvalue of $u_{\langle ij\rangle_\alpha}$. This expression can be re-written in the following way,

$$\begin{aligned} g_{\langle ij\rangle_\alpha}(t) \quad &= \quad \langle \mathcal{M}_{\mathcal{G}}|ic_i(t)T\left(e^{-2J_\alpha\int_0^t u_{\langle ij\rangle_\alpha}c_i(\tau)c_j(\tau)d\tau}\right) \\ &\qquad u_{\langle ij\rangle_\alpha}c_j(0)|\mathcal{M}_{\mathcal{G}}\rangle \end{aligned} \tag{4.16}$$

The above equation is written in an arbitrary gauge. We see that the calculation of time dependence correlation function for the ground state corresponds to solving a single impurity problem. But here the word 'impurity' means breaking of a translation invariance on a particular bond which has opposite sign for hopping element compared to the rest of the bonds.

4.3 Fractionalisation and deconfinement

We have thus derived a simple but exact expression for the spatial dependence of the two spin dynamical correlation function. We have also obtained an exact expression for the time dependence in terms of the correlation functions of non-interacting Majorana fermions in the background of static Z_2 gauge fields. Eq. (4.16) represents the propagation of a Majorana fermion in the presence of two injected fluxes.

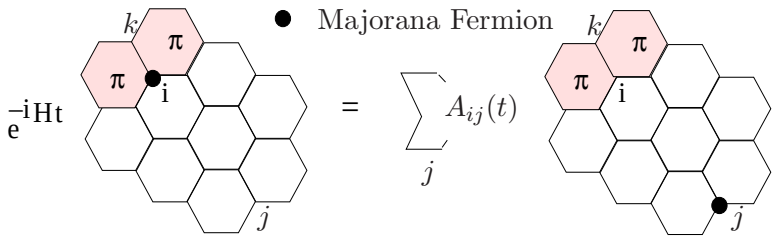

Figure 4.4: Time evolution and fractionisation of a spin flip at t = 0 at site 'i', into a π-flux pair and a propagating Majorana fermion.

The notion of Fractionalisation of spin-flip quanta is the natural interpretation of our results [55, 76]. Now let us discuss in detail the time evolution of a single 'spin-flip' at site 'i' given in Eq. (4.12). Using the notation introduced in Eq. (4.9) we have,

$$\sigma_i^{\alpha}|\hat{\Psi}\rangle \equiv ic_i(t)T(e^{2u_{\langle ik\rangle_\alpha}J_\alpha\int_0^t c_i(\tau)c_k(\tau)d\tau})\hat{\pi}_{\langle ik\rangle_{\alpha 1}}\hat{\pi}_{\langle ik\rangle_{\alpha 2}}|\hat{\Psi}\rangle \tag{4.17}$$

A spin-flip at site 'i' at time t = 0, is a sudden perturbation to the matter (Majorana fermion) sector, as it adds two static π-fluxes to adjoining plaquette. The time ordered expression represents how a bond perturbation term($i2u_{\langle ik\rangle_\alpha}J_\alpha c_i c_k$) evolves the Majorana fermion state, in 'interaction representation'. At long time scale the resulting 'shakeup' is simple and represents

a rearrangement (power law type for gapless case) of the Majorana fermion vacuum to added static π-flux pairs. The Majorana fermion, produced by a spin-flip, $c_i(t)$ propagates freely, as a function of time.

As spin-flip at site 'i' is a composite of a Majorana fermion and π-flux pair (Eq. (4.9)), two spin correlation function defines the probability that we will detect the added composite at site 'j' after a time 't. As the added π-flux pair do not move, the above probability is identically zero, unless sites 'i' and 'j' are nearest neighbours and spin components are identical, i.e, $a = b$. This is why the spatial dependence of two spin correlation functions are sharply cut off at nearest neighbour separation. The asymptotic response to an added π-flux pair and free dynamics of the added Majorana fermion control the long time power law behaviour of our only non vanishing nearest neighbour two spin correlation function.

Further, for a given pair of nearest neighbour sites, only one Ising spin pair of a corresponding component is non-zero. Other pairs and cross correlation functions vanish. More specifically, for a given bond the only non zero two spin correlation function is the bond Hamiltonian.

What is unusual is that the above result is true for all eigen-states of the Kitaev Model, irrespective of their relative energies. It follows that it is valid for thermal averages too. This is an unusual result, indicating exact fractionalisation occurring at all energy scales. In known models such as 1D repulsive Hubbard model or spin half Heisenberg chain, fractionisation is only a low energy asymptotic phenomenon. Our results show the *all energy scale exact confinement* of the spin-flip quanta, and exact *Deconfinement* of the Majorana fermions in the Kitaev model.

Kitaev model supports non-abelian anyons in the presence of uniform external magnetic field. Non-abelian anyons are believed to be fundamental in topological quantum computation. Even though we can not calculate correlation functions exactly in the presence of external magnetic field, we find that the short range character of spin-spin correlation and quantum number fractionalisation phenomenon continues. A major difference is that π fluxes acquires their own dynamics and have a band like motion.

4.4 Dimer-Dimer Correlation

Though the two spin-correlation is short range and vanishes beyond nearest neighbour, certain dimer-dimer spin correlations can be long range. In the case of two-spin correlation we have noticed that the combination of two nearest-neighbour spins which preserves the flux configuration yields a non-vanishing correlation. Now let us consider a pair of such two nearest-

neighbour as shown in Fig. (4.5), then obviously it would not change flux configuration and hence will be non vanishing. But unlike two-spin correlation function here we need to evaluate average of four Majorana fermion term.

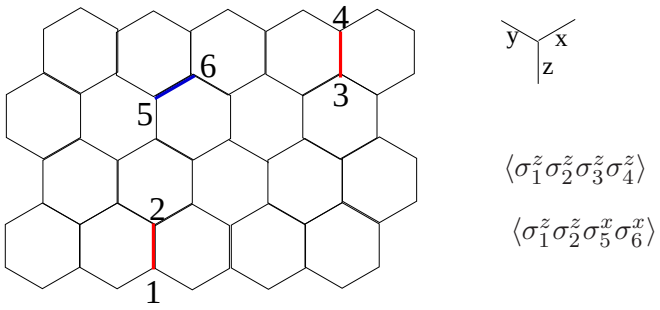

Figure 4.5: Some example of non vanishing long range dimer-dimer correlations. As shown in the figure a combination of two spin pair where each spin pair is nearest neighbour, gives rise to non vanishing long range dimer-dimer spin correlations .

Like two spin correlations, the dimer-dimer correlation functions can be expressed as the product of Hamiltonian interaction terms for two links arbitrarily separated. Taking one bond to be at the origin and the other at some location $\mathbf{R}$, the dimer-dimer correlation for such dimers is given by,

$$\langle\sigma^\alpha_{a,0}\sigma^\alpha_{b,0}\sigma^\beta_{a,\mathbf{R}}\sigma^\beta_{b,\mathbf{R}}\rangle = \langle G|ic_{a,0}c_{b,0}(2\chi_0^{\alpha\dagger}\chi_0^\alpha - 1)ic_{a,\mathbf{R}}c_{b,\mathbf{R}}(2\chi_{\mathbf{R}}^{\beta\dagger}\chi_{\mathbf{R}}^\beta - 1)|G\rangle \tag{4.18}$$

Here α and β can be x, y and z depending on whether the dimer lives on x, y or z bonds. The terms in the parenthesis yields unity for the ground state as all the gauge fermions occupation number is 1. Though Eq (4.18) can be evaluated for any two dimer, we take two z-dimers for simplicity. Then we get the following expression for $\langle\sigma^z_{a,0}\sigma^z_{b,0}\sigma^z_{\mathbf{a},\mathbf{R}}\sigma^z_{\mathbf{b},\mathbf{R}}\rangle$,

$$\begin{aligned}\langle\sigma^z_{a,0}\sigma^z_{b,0}\sigma^z_{\mathbf{a},\mathbf{R}}\sigma^z_{\mathbf{b},\mathbf{R}}\rangle &= 2\int\int \mathbf{dkdk'}\{\cos(\theta_{\mathbf{k}}+\theta_{\mathbf{k'}}) + \cos((\mathbf{k}-\mathbf{k'}).\mathbf{R}) - \\ &\quad \cos((\theta_k+\theta_{k'}) + (\mathbf{k}-\mathbf{k'}).\mathbf{R})\}\end{aligned} \tag{4.19}$$

Here $\theta_k = \epsilon_k/\sqrt{\epsilon_k^2+\delta_k^2}$ and

$$\epsilon_k = 2\mathrm{J_x cosk_1} + 2\mathrm{J_y cosk_2} + 2\mathrm{J_3} \tag{4.20}$$

$$\delta_k = 2\mathrm{J_x sink_1} + 2\mathrm{J_y sink_2} \tag{4.21}$$

Where k_1 and k_2 is given by,

$$k_1 = \vec{k}.(\frac{1}{2}\vec{e_x} + \frac{\sqrt{3}}{2}\vec{e_y}) \; ; \quad k_2 = \vec{k}.(-\frac{1}{2}\vec{e_x} + \frac{\sqrt{3}}{2}\vec{e_y}) \tag{4.22}$$

Here we give a qualitative analysis of how dimer dimer correlations depends on the distance between two dimers. We find a power law behaviour for the case $J_x = J_y = J_z$ which can be easily extended to all over the gapless phase. To do this we do long wavelength approximations. The zero for spectrum is obtained at $k_1 = 2\pi/3 = -k_2$. We take $k_1 = 2\pi/3 + q_1$ and $k_2 = -2\pi/3 + q_2$ then expanding around the zeros we get $\cos\theta_k = -q_x/|q|$ and $\sin\theta_k = -q_y/|q|$ where $q_{x,y}$ is the component along Cartesian x and y axis. Here 'q' denotes small momentum around the spectral minima.

Now in the expression for dimer-dimer correlation function(Eq. (4.19)) first term is $\mathbf{R}$ independent. Let us look at the second term which can be written as (in the long wave length limit $\lambda << \mathbf{R}$)

$$\begin{aligned} \int\int \mathbf{dkdk'} &= \int\int \mathbf{dqdq'} \\ &= Re(\int e^{i\mathbf{q}.\mathbf{R}}\mathbf{dq})(\int \mathbf{e^{-iq'.R}dq'}) \end{aligned} \tag{4.23}$$

Now we take $\mathbf{R}$ to be along the x-axis. Then each integral becomes,

$$\begin{aligned} I &= \int_0^{\lambda}\int_0^{2\pi} e^{iqR\cos\theta_q} qdqd\theta_q \\ &= \frac{1}{R^2}2\pi\int_0^{\lambda R} J_0(x)xdx \end{aligned} \tag{4.24}$$

Where x=qR. Thus as each term varies as R^{-2} , the second term gives R^{-4}. Similarly the last term in Eq. (4.19), can be factorised in to many terms. Each term is a product of two integral, one over 'q' and another over q' and each has the following form,

$$I = \frac{1}{R^2}\int_0^{\lambda R}\int_0^{2\pi} \cos\theta e^{ix\cos\theta} xdxd\theta \tag{4.25}$$

Thus this also give R^{-4} variation. This power law behaviour of dimer-dimer correlation is true for all over the gapless phase in the parameter space [81]. A more detailed analysis of dimer-dimer spin correlation can be found in [81] which shows that in gapped phase the dimer-dimer correlation function decays exponentially.

4.5 Multi spin correlations

Multi spin correlation functions can also be calculated in our formalism. We have already seen that only non vanishing two spin correlations are those spin combinations which preserve the flux configuration. We found that it is the bond Hamiltonian which does this. The multi-spin correlation functions is just the extension of this fact. It follows that any multi-spin correlations to exist among a certain number of site , it must be expressed as the product of the bond Hamiltonians among the sites. In the picture below we elaborate this fact.

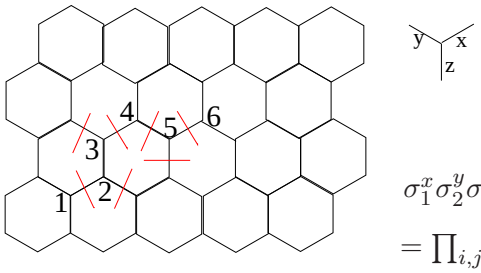

Any spin-spin correlation that preserves flux configuration is non zero

Figure 4.6: Only non-vanishing multi-spin correlations among the sites 1 to 6 is obtained by taking product of bond Hamiltonians containing the sites.

In the Fig (4.6) we have shown a string like multi-spin correlations among the site (1,2,3,4,5,6). We easily find that only non-vanishing multi-spin correlations among these sites are,

$$S_m = \sigma_1^x\sigma_2^y\sigma_3^y\sigma_4^z\sigma_5^z\sigma_6^y = \prod_{i,j} h_{ij}. \tag{4.26}$$

Where h_{ij} is the bond Hamiltonian for the bond $\langle ij\rangle$. It is straightforward to show that equal time multi-spin correlations for a string like path as shown in the figure above is equal to

$$S_T \equiv c_i c_f \tag{4.27}$$

Where 'i' and 'f' denotes the initial and final site of the strings. What follows directly from the Eq. (4.27) is that for a close loop, where $i = j$, we get $S_T \equiv 1$. But this is nothing but the product of B_p which should be ± 1 depending on the flux configurations of the gauge sector. For the ground state it is 1.

4.6 Fractionalisation in other Kitaev like model

The method we employ here can be applied to all models containing Kitaev like interactions [85–87]. In all these model we see similar nature of two-spin correlations and the multi-spin correlations, basically it should be products of bond Hamiltonians. Again in all these model we notice fractionalisation to occur but the notion of fractionalization depends on the details of the lattice. To summarise, we have shown certain exact analytical results for the spin dynamics and a spin-flip fractionisation scheme for the Kitaev model. As this non-trivial spin model has been proposed for possible implementation of topological quantum computation, our exact results should provide insights into qu-bit dynamics and possible ways of generating emergent topological qubits. Our formalism, which uses the factorised character of the eigen-functions in the extended Hilbert space, is easily adapted to the calculation of multi-spin correlation functions, which is a key step in the calculation and understanding of quantum entanglement properties.

Prisoner, tell me, who was it that wrought this unbreakable chain?'
'It was I,' said the prisoner, 'who forged this chain very carefully.
Prisoner-Rabindranath Tagore

Chapter 5

Quantum entanglement study on Kitaev model

In this chapter we present our studies on quantum entanglement in the Kitaev model. We know that the entanglement arises out of the non-local correlations of quantum states. In the vicinity of quantum phase transition it is natural to expect that various parts of the system get entangled in a nontrivial way. The relation between quantum phase transition and entanglement has been investigated in the seminal works [28, 111–114] dealing with one dimensional systems. Among many entanglement measures that exist for a many body system the entanglement entropy and the concurrence is well known [123, 124, 126] . This measure is defined by dividing the systems into two subsystems 'A' and 'B' and then calculating reduced density matrix of one subsystem only (e.g $\rho_A = tr_B\rho$ obtained by tracing over degrees of freedom of B subsystem) . After this one looks into the quantity called von-Neumann entropy (S_A) which is defined as,

$$S_A = -tr[\rho_A ln \rho_A] \tag{5.1}$$

It is to be noted that by definition $\rho_A = \rho_B$. The matrix ρ_B contains the residual entanglement information between the subsystem 'A' and 'B'. In case of concurrence the partition of the system is done in a subsystem of 'two particles' and the rest of the system excluding those 'two particles' . In case of block entanglement one usually divides the total system into a square block with length 'L' and the rest of the system. In the later case one generally looks at the scaling of S_A with respect to size 'L'. Concurrence and the entanglement entropy is known to either diverge or show some jump at a quantum phase transition [112–116, 118, 121–123]. For a critical fermionic system with gapless excitation, the bulk entanglement entropy is shown

to vary as $S \sim L^{d-1}logL$. Away from the criticality, it varies as $\sim L^{d-1}$ [126, 126, 127]. Here we calculate concurrence and binary entropy for Kitaev model. Both of the above entanglement measures was shown to capture the presence of quantum phase transitions [121, 123, 124] . However for Kitaev model we find concurrence to be zero for any two sites. We argue that binary entropy shows the presence of phase transition in Kitaev model.

5.1 Concurrence

We can write the reduced density matrix ρ_{12} for two arbitrary site '1' and '2' is given by,

$$\rho_{12} = \begin{pmatrix} v & 0 & 0 & u \\ 0 & w & y & 0 \\ 0 & y & w & 0 \\ u & 0 & 0 & v \end{pmatrix} \tag{5.2}$$

The above reduced density matrix is derived in the standard z-basis [116]. The various parameter appearing in the above equation is given by [120],

$$v = \frac{1}{4}(1 + \langle\sigma_1^z\sigma_2^z\rangle) \tag{5.3}$$

$$w = \frac{1}{4}(1 - \langle\sigma_1^z\sigma_2^z\rangle) \tag{5.4}$$

$$y = \frac{1}{4}(\langle\sigma_1^x\sigma_2^x\rangle + \langle\sigma_1^y\sigma_2^y\rangle) \tag{5.5}$$

$$u = \frac{1}{4}(\langle\sigma_1^x\sigma_2^x\rangle - \langle\sigma_1^y\sigma_2^y\rangle) \tag{5.6}$$

The definition of the concurrence is the following [116]. Let us construct a matrix C given by,

$$C = \rho_{12}\tilde{\rho_{12}}, \quad \text{where} \quad \tilde{\rho_{12}} = \sigma_1^{\mathrm{y}} \otimes \sigma_2^{\mathrm{y}} \rho_{12} \sigma_1^{\mathrm{y}} \otimes \sigma_2^{\mathrm{y}}. \tag{5.7}$$

The above transformation causes partial transpose of the matrix ρ_{12} with respect to element '2' . The concurrence is defined as :$C = \max\{0, \lambda_1 - \lambda_2 - \lambda_3 - \lambda_4\}$. Here λ_i's are the eigenvalues of the matrix C and they are ordered in decreasing order. If the quantity C is positive then concurrence is finite otherwise it is zero. In Kitaev model, for a pair of sites which is joined by a z-bond we get $u = y = 0$. Then we have for C (for such two sites joined by z-bond) ,

$$C = \begin{pmatrix} v^2 & 0 & 0 & 0 \\ 0 & w^2 & 0 & 0 \\ 0 & 0 & w^2 & 0 \\ 0 & 0 & 0 & v^2 \end{pmatrix} \tag{5.8}$$

From the definition of C, we find that concurrence is zero as we have v^2 and w^2 positive or zero. Similarly it can be easily shown that concurrence between any two sites is zero.

5.2 Binary entropy

We can easily calculate the von-Neumann entropy for this two spin subsystem as we can easily diagonalise the reduced density matrix ρ_{12} in this case. This entropy which is also called binary entropy is defined as,

$$S_{12} = -\sum_i \lambda_i ln\lambda_i \tag{5.9}$$

where λ_is are the eigenvalues of the reduced density matrix ρ_{12}. The von-Neumann entropy for two nearest neighbour site is given by,

$$S^a_{12} = -\frac{1}{2}\{(1+p)ln(1+p) + (1-p)ln(1-p)\} + 2ln2 \tag{5.10}$$

where $p = \langle \sigma^a_1 \sigma^a_2 \rangle$ and $a = x, y, z$ depending on the bond. This is always finite as in complete parameter space we have, $1 \leq p \geq 0$. For the sites which are not nearest neighbour the von-Neumann entropy is $2ln2$, a constant. The above result is consistent with the fact that in the Kitaev model, the phase transition is not associated with any long range spin-spin correlations. Thus the binary entropy is expected to be finite all over the parameter space. Below we present how the binary entropy behaves as a function of J_z. For simplicity we take $J_x = J_y$.

From the Fig (5.1), we observe that binary entropy is maximum at $J_z = 0$. This limit corresponds to isolated 1 dimensional chain and there is no coupling between two sites joined by a z-bond. It just reproduces the constant term in the r.h.s of Eq. (5.10). At $J_z = 1$, we have $J_x = J_y = 0$ and the two spins of a z-bond are either in ferromagnetic or anti ferromagnetic alignment and entanglement entropy reaches a minima here. However it is interesting to note that the gradient of the binary entropy reaches maximum at $J_z = 0.5$

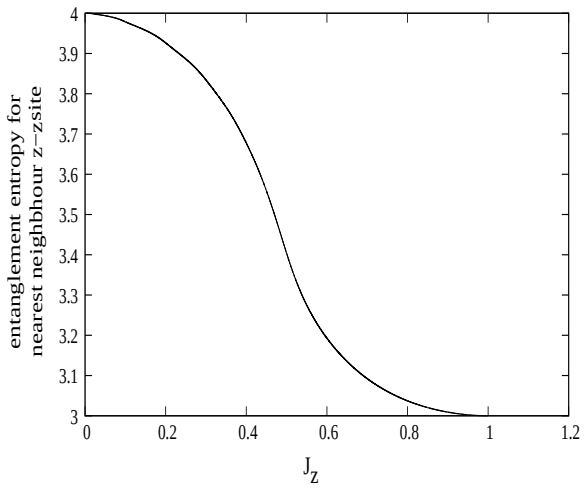

Figure 5.1: Along the horizontal axis we plot the strength of J_z and along the vertical axis we plot the binary entropy.

which is the transition point from gapless to gapped phases in Kitaev model. Thus it is evident that binary entropy is able to capture the presence of phase transition as corroborated in other investigations [117, 121].

Bee! I'm expecting you!
Was saying Yesterday
To Somebody you know
That you were due –
Bee! I'm expecting you!-Emily Dickinson

Chapter 6

Toric code limit of 2D Kitaev model

One of the basic properties which characterises fundamental particles or quasi-particles in many real systems is exchange statistics obeyed by them. Let us consider a two body wave function of such two particles, $\psi(\mathbf{x_1}, \mathbf{x_2})$. When one particle is taken around another particle completely, the wave function in general get multiplied by a phase, i.e, we get for the new wave function $e^{i\phi}\psi(\mathbf{x_1}, \mathbf{x_2})$. For bosons we have, $\phi = 2\pi$ and for fermions $\phi = \pi$. In 3 or higher dimension only possible statistics among elementary particles or among quasi-particle excitations of certain system can only be either fermionic or bosonic. However in 2 spatial dimension mutual statistics between two quasi-particles are special and here ϕ can be anything in between 0 to 2π. These special excitations or particles are termed anyons whose exchange statistics interpolate the statistical behaviour intermediate between bosonic and fermionic statistics [41, 42]. There are examples where they are predicted to exist in real condensed matter systems. One of the ready example is Laughlin state [70] in the Fractional Quantum Hall Systems at filing factor $n = 1/3$. It carries abelian anyons with exchange phase $\phi = \pi/3$ and electric charge $\pm 1/3$. The fractional charge has also been experimentally seen in shot noise measurements [71, 73]. The Kitaev model which is defined in 2 Dimension also supports anyons in some regions of the parameter space. It has been shown that in the presence of magnetic field the gapless phase opens up a gap and it has non-abelian anyons as excitations [33]. On the other hand the gapped phase is described by abelian anyons. In this chapter we will be discussing the effective Hamiltonian in the toric code limit($J_z \gg J_x, J_y$) and examine the effective Hamiltonian obtained in terms of Jordan-Wigner fermions. This toric code Hamiltonian has been investi-

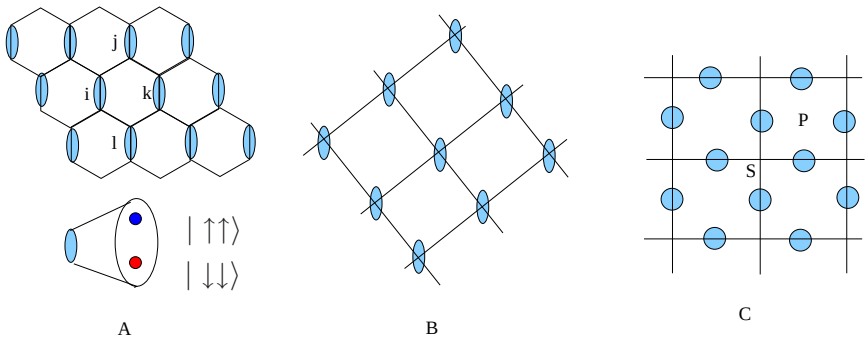

Figure 6.1: Reduction of the Kitaev model in toric code limit. Strong links in the original model (A) constitute effective spins (B) , which are associated with the links of a new lattice (C). The lattice in Fig C can be obtained from the lattice of Fig B by a bond to site and site to bond transformations.

gated in other important works [45, 46, 49]revealing many insightful results on Kitaev model. At first we briefly outline the main results obtained in [33]. The Hamiltonian we investigate is the following,

$$\begin{aligned} H &= H_0 + H' \\ H_0 &= -\sum_{z-\text{link}} J_z \sigma_i^z \sigma_j^z \\ H' &= -\sum_{x-\text{link}} J_x \sigma_i^x \sigma_j^x - \sum_{y-\text{link}} J_y \sigma_i^y \sigma_j^y \end{aligned} \tag{6.1}$$

In the above equation we have $J_z \gg J_x, J_y$. This is why we write Hamiltonian into two separate parts. H_0 describes the unperturbed Hamiltonian and H' is treated as a perturbation to H_0. The ground state configuration for the unperturbed Hamiltonian H_0 corresponds to spin states $|\uparrow\uparrow\rangle$ or $|\downarrow\downarrow\rangle$ at every z-bond. If we are having a system with a total of N_z z-bond the ground sector has a degeneracy of 2^{N_z}. In perturbation theory it has been observed that first nontrivial contribution appears only in fourth order [32]. Without going into details we write the results obtained in [32]. We denote by τ the effective spin operator in the ground state sub space of each z-bond (spanned by the state $|\uparrow\uparrow\rangle$ and $|\downarrow\downarrow\rangle$), then the effective Hamiltonian is given by(in appendices E, we derive the effective Hamiltonian in detail.),

$$H_{eff} = -\frac{J_x^2 J_y^2}{16|J_z|^3} \sum Q_p, \qquad Q_p = \tau_i^y \tau_j^z \tau_k^y \tau_k^z \tag{6.2}$$

The above Hamiltonian is defined on a square lattice which is obtained from hexagonal lattice after replacing each z-bond by a site as shown in Fig. (6.1). Now if we do a unitary transformation such that for all the horizontal links of the effective lattice (Fig. 6.1 B) we replace $\tau^y \rightarrow \tau^z$ and for all the vertical links $\tau^y \rightarrow \tau^x$, then we can write referring to the Fig. (6.1 C) , the following Hamiltonian,

$$H_{eff} = -J_{eff} \left(\sum_{vertices} Q_s + \sum_{plaquettes} Q_p \right) \tag{6.3}$$

where $Q_s = \Pi_{star(s)} \tau_j^x$ and $Q_p = \Pi_{boundary(p)} \tau_j^z$. Here the star denotes the vertices of the square lattice. This is the famous toric code Hamiltonian and has been extensively studied in the references [32, 33]. Ground state of this Hamiltonian is obtained by having all $Q_s = 1$ and all $Q_p = 1$. It has been shown that on a torus all the Q_p satisfy the constraint $\Pi_p Q_p = 1$. All Q_s satisfy similar constraint. These two constrains give rise to four fold ground state degeneracies. From the above constraints we also notice that on a torus one can only create the excitations in pair. By excitations we mean a state with eigenvalue of some Q_p or Q_s to be -1. It has been shown [32, 33] that when one Q_p excitation goes around another Q_p excitation, the wave function does not pick up any phase and the same is true for Q_s. But if a Q_p excitation goes around another Q_s the global wave function picks up a phase -1.s Thus all Q_ps (and Q_s) are Bosons among themselves but mutually they behave like Semions.

Below we present the effective Hamiltonian in the Jordan-Wigner formalism. In Jordan Wigner formalism we are able to write down explicitly the four fold degenerate ground states. We show that when two quasi particles are being exchanged the wave function itself get mapped from one degenerate ground state to another degenerate ground state. This proves that wave function behaves as multicomponent object revealing the characteristics of anyonic system. Also we demonstrate that the matrix representing the effect of exchanging two quasi particles along horizontal direction and vertical direction commute with each other. This conforms, in a most elementary way, the one dimensional nature of braid group representation associated with this exchange operation. This is in conformity with the abelian nature of the quasi particles in the large J_z limit.

6.1 Toric code limit in Jordan-Wigner formalism

In Jordan-Wigner formalism the effective Hamiltonian becomes quite simple and specifying the four ground sector can be done easily. Let us write the Hamiltonian in terms of ψ and χ fermion, as written in equations (3.46, 3.47, 3.48). Again we work in a particular gauge choices which corresponds to the J-W path given in Fig (3.3). Similar to Eq. (6.1), we write the Hamiltonian into two parts, H_0 which is given by $z-z$ interaction and H' which contains $x-x$ and $y-y$ interaction and is treated as perturbation to H_0. Further, depending on whether a bond is on the side boundary or in interior we separate H_0 (and H') into H_{0b} and H_{0i} (H'_b and H'_i). Thus we have ,

$$
\begin{aligned}
H_0 &= H_{0b} + H_{0i} + H_{end} && (6.4)\\
H_{0b} &= -\sum_{mn} J_z(2\chi^\dagger_{mn}\chi_{mn} - 1)(2\psi^\dagger_{mn}\psi_{mn} - 1) && (6.5)\\
H_{0i} &= -\sum_{mn} J_z(2\psi^\dagger_{mn}\psi_{mn} - 1); \quad H_{end} = -\mathcal{S}J_z(2\psi^\dagger_{MN}\psi_{MN} - 1) && (6.6)
\end{aligned}
$$

In above H_{end} denotes the bond interactions where Jordan-Wigner paths end points meet each other (referring to the Fig. 6.2, it is given by bond joining site '1' and '32'). We rewrite H' in the following way,

$$
\begin{aligned}
H' &= H'_b + H'_i && (6.7)\\
H'_b &= \sum_{mn} J_x(\psi^\dagger_{m,n} + \psi_{m,n})(\psi^\dagger_{m+1,n+1} - \psi_{m+1,n+1})\\
&+ \sum_{mn} J_y(\psi^\dagger_{m,n} + \psi_{m,n})(\psi^\dagger_{m,n+1} - \psi_{m,n+1})\\
H'_i &= \sum_{m,n} J_y U_{\substack{m,n\\m,n+1}}(\psi^\dagger_{m,n} + \psi_{m,n})(\psi^\dagger_{m,n+1} - \psi_{m,n+1}) && (6.8)
\end{aligned}
$$

In above equations subscript 'b' and 'i' refers to boundary bonds and internal bonds respectively. $U_{\substack{m,n\\m,n+1}}$ is defined on each slanted y-link connecting site (m,n) and (m,n+1) and is given by,

$$
U_{\substack{m,n\\m,n+1}} = (2\chi^\dagger_{\substack{m,n\\m,n+1}}\chi_{\substack{m,n\\m,n+1}} - 1). \qquad (6.9)
$$

Now looking at the Hamiltonian H_0 we can very easily find the ground state subspace by specifying the χ and ψ fermion occupation numbers on

each link. It is clear from Eq. (6.5) that for every internal z-bond we have two degenerate states minimising the bond energy. They corresponds to states where both ψ and χ fermion are present or absent. Moreover except the end z-bond all the other boundary z-bonds have ψ fermion occupation number 1. Thus there is no degeneracy associated with these bonds. This also imposes a constraint on the number of ψ fermions which is given by,

$$\Pi_{mn}\rho_{\substack{m,n\\m,n+1}} = 1 \qquad \rho_{\substack{m,n\\m,n+1}} = \mathrm{U}_{\substack{m,n\\m,n+1}} \tag{6.10}$$

Now we write down the effective Hamiltonian obtained in fourth order of perturbation. For convenience we separate the plaquette operators into two parts, one which is in the interior of the lattice and the rest which shares boundary.

$$\begin{aligned} H_{eff} &= -J_{eff}\sum_{p_i} Q_{p_i} - J_{eff}\sum_{p_b} Q_{p_b} - J_{eff}Q_{end} && (6.11)\\ Q_{p_i} &= n_{m,n}n_{m+1,n} \qquad \mathrm{n_{m,n}} = (2\psi^{\dagger}_{\mathrm{m,n}}\psi_{\mathrm{m,n}} - 1) && (6.12)\\ Q_{p_b} &= n_{m,n}n_{m+1,n}\rho_{\substack{m,n\\m,n+1}} \qquad \rho_{\substack{m,n\\m,n+1}} = \mathrm{U}_{\substack{m,n\\m,n+1}} && (6.13) \end{aligned}$$

The expression for Q_{end} is that of Q_{p_b} multiplied by $\mathcal{S}$. 'p_i' and 'p_b' refer to the interior and boundary plaquettes respectively. Every internal z-links are associated with one χ fermion and one ψ fermion. They appear in the effective Hamiltonian as $\rho_{m,n}$ and $n_{m,n}$ respectively. Every boundary z-links are associated with one ψ fermion which appears as $n_{m,n}$ in effective Hamiltonian. All slanted boundary y-links are associated with one χ fermion operators which appear as $\rho_{\substack{m,n\\m,n+1}}$. The effective plaquette operators are just the product of above mentioned density operators appropriately (obtained in perturbation theory). An internal plaquette operator is given by the product of $n_{m,n}$ of two z-links associated with this plaquette. Thus it is very easy to construct eigenstates of these plaquette operators, we only need to specify the fermion occupation numbers on each z-bonds. We have already discussed that there are four ways to make all effective plaquette operators eigenvalues to be 1. In the table below we specify the eigenvalues of density operators corresponding to four degenerate ground state wave functions.

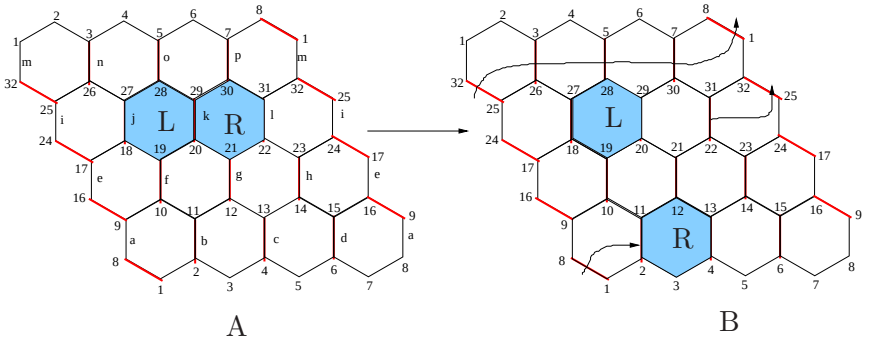

Figure 6.2: (A) A pair of plaquette excitations have been created on plaquette 'L' and 'R'. This is done by applying t_k on the ground state. (B) The plaquette excitation 'R' has been moved to a new position by the application of suitable string operator.

	$\mathcal{S}$	$n_{0,N}$ m $\neq$ N	$n_{0,m}$	$\rho\ {}^{m,n}_{m,n+1}$ n $\neq 0$	$\rho_{m,n}(n_{m,n})$ n $\neq 0$	$\rho_{n,M}$
$\|\mathcal{G}\rangle_1$	1	1	1	1	1	1
$\|\mathcal{G}\rangle_2$	1	1	1	-1	-1	-1
$\|\mathcal{G}\rangle_3$	-1	-1	1	1	1	-1
$\|\mathcal{G}\rangle_4$	-1	-1	1	-1	-1	1

6.2 Excitations and more

Excitations over these ground states can be easily represented by changing the occupation number of fermions consistent with the boundary conditions. The characterisation of excited states are also straightforward. Here we discuss some elementary braiding properties of such excitations. Braiding properties of excitations has been discussed in detail in [32, 33]. Here we take a small lattice and study the braiding properties in terms of Jordan Wigner fermions. Namely we elaborate to show the multicomponent nature of ground state wave function. We take a 4×4 lattice and try to see the braiding properties of excitations. We start with ground state $|\mathcal{G}\rangle_1$. We remember that the choice 1 ensures a state which is denoted by all density operator to have eigenvalue 1 which means at every dimer all the ψ fermions are present. Moreover the χ fermions on the internal z-bonds and on the slanted y-bonds are also occupied. This ensures that $\mathcal{S} = 1$. It is to be noticed that we can not change the $\psi_{0,m}(m \neq N)$. This is clear from the Eq. (6.4). If we do so we get a state which is outside the ground state

manifold. The Ground state for this sector(choice 1) can be written as,

$$|\mathcal{G}\rangle_1 \quad = \quad \Pi_{i,j}\psi_i^\dagger\chi_j^\dagger|0\rangle \tag{6.14}$$

In the above equation products go over all normal bonds. Other ground states can also be written easily by fixing the occupation number for all the fermions at every z bond following the above table. Now we create a pair of excitations above the Ground state and examine the effect of exchanging these excitations over the torus. For this we take the ground state given by Eq. (6.14). The operator $(\psi_{mn}\chi_{mn} + \psi_{mn}^\dagger\chi_{m,n}^\dagger)$ acting on $|\mathcal{G}\rangle_1$ creates a pair of excitations at the plaquette shared by the z-bond labelled by (m,n). In Fig. (6.2 A), the operator, $t_k = \psi_k\chi_k + \psi_k^\dagger\chi_k^\dagger$ produces a pair of flux excitations shown by shaded plaquettes labelled by 'L' and 'R'. Now we move the plaquette excitation 'R' and bring it to a new position as shown in (6.2 B). The operator which does this operation is given by,

$$S_{lb} = t_l t_{i,m} t_n t_o t_p t_{ma} t_b. \tag{6.15}$$

Here $t_{i,m}$ is given by , $t_{i,m} = (\chi_{i,m} + \chi_{i,m}^\dagger)$, same is true for t_{ab}. They are defined on slanted normal bonds connecting the z-dimer 'i' and 'm' (and 'a' and 'b' respectively). Now to exchange the 'L' and 'R' excitation, we bring 'R' excitation to the initial position of 'L' excitation and then bring the 'L'-excitation to the initial position of 'R' excitation. The operator which does this complete operation is given by,

$$\Sigma_h = \Pi_{i,\langle j,k\rangle} t_i t_{j,k} \tag{6.16}$$

Here the product goes over all the z-links of the lattice. However we find that $\Sigma_h|\mathcal{G}\rangle_1 = |\mathcal{G}\rangle_2$ where $|\mathcal{G}\rangle_2$ is the ground state wave function corresponding to choice 2. Similarly it can be checked that $\Sigma_h|\mathcal{G}\rangle_3 = |\mathcal{G}\rangle_4$. Up to now all operators correspond to a particular Jordan-Wigner path(which we call Hamilton path) which winds the lattice in Horizontal direction. We can define another Jordan-Wigner path which corresponds to vertical winding for which we also obtain four degenerate ground state $|\mathcal{G}\rangle_i'$. We can make a connection between this two sets of Ground states and get one to one mapping between these two sets of ground state. For the vertical winding, we see that after a full translation the state $\Sigma_v|\mathcal{G}\rangle_1$ goes to $= |\mathcal{G}\rangle_3$ and $\Sigma_v|\mathcal{G}\rangle_1$ goes to $= |\mathcal{G}\rangle_3$. We denote by $\mathcal{W}_h$ the operator which summarises complete exchange effects in two different directions. Thus we can write,

$$\begin{pmatrix} |\mathcal{G}\rangle_1 \\ |\mathcal{G}\rangle_2 \\ |\mathcal{G}\rangle_3 \\ |\mathcal{G}\rangle_4 \end{pmatrix} \rightarrow \mathcal{W}_h \begin{pmatrix} |\mathcal{G}\rangle_1 \\ |\mathcal{G}\rangle_2 \\ |\mathcal{G}\rangle_3 \\ |\mathcal{G}\rangle_4 \end{pmatrix}; \mathcal{W}_h = \begin{pmatrix} 0 & 1 & 0 & 0 \\ 1 & 0 & 0 & 0 \\ 0 & 0 & 0 & 1 \\ 0 & 0 & 1 & 0 \end{pmatrix} \tag{6.17}$$

Similarly for the vertical winding we can write,

$$\begin{pmatrix} |\mathcal{G}\rangle_1 \\ |\mathcal{G}\rangle_2 \\ |\mathcal{G}\rangle_3 \\ |\mathcal{G}\rangle_4 \end{pmatrix} \rightarrow \mathcal{W}_t \begin{pmatrix} |\mathcal{G}\rangle_1 \\ |\mathcal{G}\rangle_2 \\ |\mathcal{G}\rangle_3 \\ |\mathcal{G}\rangle_4 \end{pmatrix}; \mathcal{W}_t = \begin{pmatrix} 0 & 0 & 1 & 0 \\ 0 & 0 & 0 & 1 \\ 1 & 0 & 0 & 0 \\ 0 & 1 & 0 & 0 \end{pmatrix} \tag{6.18}$$

Now it is easy to check that $\mathcal{W}_h$ and $\mathcal{W}_t$ commutes. It is important to note that toric code Hamiltonian is obtained from original spin Hamiltonian at 4th order of perturbation theory. All the terms in the effective Hamiltonian describe noninteracting abelian anyons. However a more detail study [47, 74] in toric code limit which extends beyond 4th order of perturbation shows presence of emergent fermions and interacting anyons. It is to be noted that Refs. [47, 74] use perturbative continuous unitary transformations (PCUT) instead of J-W transformations (or Majorana fermions) as analytical method.

One day the Nouns were clustered in the street.
An Adjective walked by, with her dark beauty.
The Nouns were struck, moved, changed.
The next day a Verb drove up, and created the Sentence.
Permanently-Kenneth Koch

Chapter 7

Stability of Kitaev Model against Ising perturbations

In chapter 2 we have seen that the exact solution of Kitaev model was possible because original spin Hamiltonian was mapped to a non-interacting Hamiltonian describing nearest neighbour hopping interactions for Majorana fermions. Moreover the gauge fields coupled to the hopping matrix elements were static. These two facts rendered the original spin Hamiltonian quadratic in Majorana fermions which was exactly solvable. In this chapter we study the dynamics of gauge fields in an elementary way. We make the gauge fields dynamic by adding suitable interactions to the original Hamiltonian of Kitaev model. When gauge fields are not conserved then a generic term in the Hamiltonian describes interaction among four Majorana fermions. There are many possible ways to introduce such dynamics to Z_2 gauge fields in Kitaev model. One way to achieve this is to add a Zeeman term to Kiteav Hamiltonian which has already been treated in [33]. It has been shown that addition of such interaction to original Kitaev model causes gapless phase to acquire a gap. But this study was done primarily to investigate the topological nature of the model rather than investigating the gauge field dynamics. Here we introduce dynamics to the gauge fields by adding a nearest neighbour Ising interactions to Kitaev Hamiltonian. We show that depending on the strength of the Ising interaction the Hamiltonian describes a spin liquid regime where Z_2 gauge fields are static (conserved) and a magnetic ordered state where Z_2 gauge fields are dynamic. A quantum phase transition is observed between these two phases as we vary the strength of Ising interactions.

7.1 Kitaev-Ising(K-I) model

The Hamiltonian we study is, $H_{K-I} = H_K + H_I$ where H_K refers to the original Kitaev interactions and H_I refers to Ising interactions.

$$H_K = -J_\alpha \sum_{\alpha-\text{bond}} \sigma_i^\alpha \sigma_j^\alpha, \alpha = x, y, z \; ; \quad H_I = -\lambda \sum_{\text{all bond}} \sigma_i^z \sigma_j^z \quad (7.1)$$

If the coupling constant λ is positive then the coupling of Ising Hamiltonian is ferromagnetic otherwise it is anti-ferromagnetic. We study both the cases. Let us explain how the Ising interaction introduces gauge field dynamics. We know that the Kitaev model (i.e, $\lambda = 0$) contains conserved operators (B_p) (Eq. 2.3) associated with each plaquette of honeycomb lattice . It can be readily checked that B_p does not commute with the Ising interactions of H_{K-I}. We know that when we fermionise the spin operators B_p can be re-expressed as a product of appropriate Z_2 gauge fields associated with the bonds of the plaquette 'p'. We will show that this Z_2 gauge fields are no longer conserved as they do not commute with the resulting fermionised interaction terms derived from Ising perturbations.

7.2 Classical ground states

Before proceeding further with the fermionic Hamiltonian obtained from H_{K-I}, first we discuss about the possible classical ground states of the Hamiltonian (7.1) so that we can describe appropriate mean field analysis around these classical minima. For λ positive (ferromagnetic Ising interaction), the classical minima is obtained by aligning all the spins in the positive z direction or in the negative z direction [83]. The classical energy density per unit cell for such configuration is,

$$E_{\text{FM}} = -(3\lambda + 1). \quad (7.2)$$

However for λ negative, there exist two classical minima depending on the relative magnitudes of J and λ. In the Fig (7.1), we have drawn these two classical configurations. The left one is called dimer state and the right one is the familiar Neel state.

Classical energy density for these two configurations are given by ,

$$E_{\text{Dimer}} = -J - \lambda; \quad E_{\text{Neel}} = -3\lambda + J \quad (7.3)$$

$$E_{\text{Dimer}} - E_{\text{Neel}} = 2(\lambda - J) \quad (7.4)$$

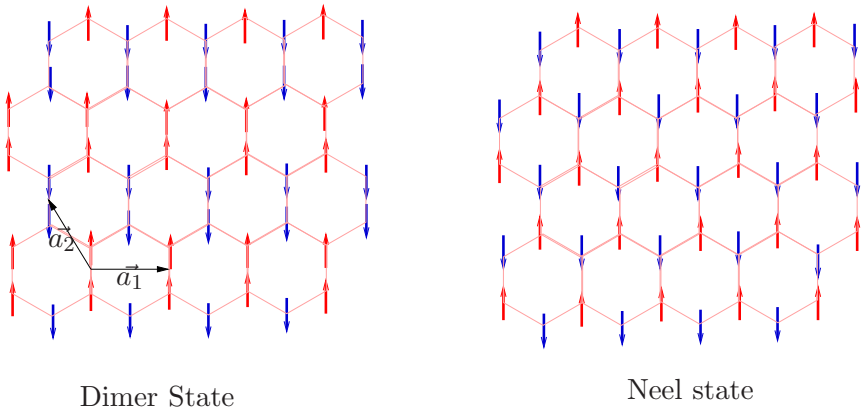

Dimer State Neel state

Figure 7.1: Two different classical configurations minimising the classical energy density at different parameter regime. For $\lambda \leq J$, the dimer state minimises the classical energy. For $\lambda \geq J$, Neel state yields the minimum classical energy density.

Thus it is clear that for $\lambda \leq J$, it is the Dimer state which corresponds to classical minima.

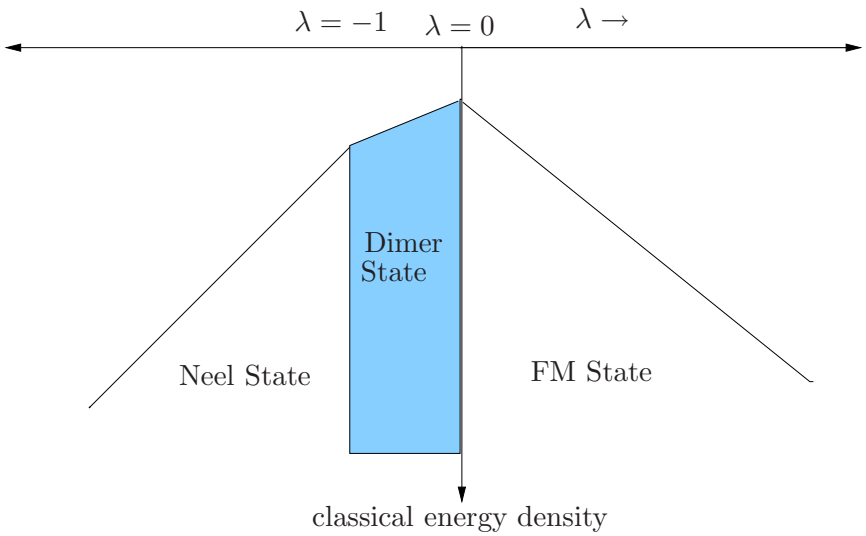

Figure 7.2: The classical phase diagram for the Hamiltonian (7.15). For λ negative we expect a transition from Dimer state to Neel state at $\lambda = -1$. We have taken $J = 1$.

Having discussed the classical configurations of spins which minimises H_{K-I}, we proceed with the Hamiltonian given in Eq. (7.1). We will develop appropriate mean field analysis around these classical configurations. Now we discuss the fermionised form of the spin Hamiltonian given by Eq. (7.1).

7.3 Fermionisation of Kitaev-Ising model

Following Kitaev's Majorana fermionisation [33], we substitute the spin-1/2 operators in terms of appropriate combination of Majorana fermions, namely, $\sigma_i^\alpha = ic_i b_i^\alpha$, then we get,

$$H_k = \sum_{x-\text{link}} J_x i b_i^x b_j^x i c_i c_j + \sum_{y-\text{link}} J_y i b_i^y b_j^y i c_i c_j + \sum_{z-\text{link}} J_z i b_i^z b_j^z i c_i c_j \quad (7.5)$$

$$H_I = \sum_{\text{all}-\text{link}} i b_i^z b_j^z i c_i c_j \quad (7.6)$$

Where the b_i^α and c_i are Majorana fermions. Here the index 'i' belongs to sub lattice '1' and 'j' belongs to sub lattice '2'. In previous chapters we have used 'a' and 'b 'as the sub-lattice indices, here we use '1' and '2' as the sub-lattice index as here we use the letter 'b' to denote gauge fields.

We see that the terms $(ib_i^x b_j^x)$ and $(ib_i^y b_j^y)$ (which are nothing but the Z_2 gauge fields appearing on x and y bonds) commute with the Hamiltonian as before. But the gauge fields $ib_i^z b_j^z$ appearing on z-bonds no longer commute with Hamiltonian. If we apply the Jordan-Wigner formalism we get the gauge fields on x and y bonds set to 1. Then we are left with the following Hamiltonian,

$$H_{kitaev} = \sum_{x-\text{link}} J_x i c_i c_j + \sum_{y-\text{link}} J_y i c_i c_j + \sum_{z-\text{link}} J_z i b_i^z b_j^z i c_i c_j \quad (7.7)$$

$$H_{ising} = \sum_{\text{all link}} i b_i^z b_j^z i c_i c_j \quad (7.8)$$

We have already mentioned that addition of Ising interactions to Kitaev model makes the flux operator B_p not to commute with the Hamiltonian H_{k_i}. In terms of fermions this is obvious from the fact that the quantity $ib_i^z b_j^z$ on z-bonds do not commute with the Hamiltonian. Working with the open boundary condition, we get the expression of B_p as,

$$B_p = i b_{1,i}^z b_{2,i}^z i b_{1,j}^z b_{2,j}^z \quad (7.9)$$

where '1' and '2' refers to the sub-lattice index and 'i' and 'j' denote the two z-bonds shared by a plaquette.

7.4 Mean-field decomposition

Looking at the equations (7.7) and (7.8), we observe the following facts. The Hamiltonian contains terms quatric in Majorana fermions. In the absence of Ising interactions Hamiltonian effectively reduces to quadratic in 'c' fermions as the combination $ib_i^z b_j^z$ in each quatric term commute with the Hamiltonian and also commute among themselves. But this is not the case in the presence of Ising interactions. Thus the 'b' fermions also acquire their own dynamics. To proceed further with this situations, we make appropriate mean field decompositions for each four fermion terms of the Hamiltonian given in Eq. (7.7) and in Eq. (7.8). Let us write the mean field decomposition for one of the generic term in the Hamiltonian,

$$\begin{aligned} ib_i^z b_j^z ic_i c_j &= \langle ib_i^z b_j^z\rangle ic_i c_j + ib_i^z b_j^z \langle ic_i c_j\rangle \\ &\quad -\langle ic_i b_i^z\rangle ic_j b_j^z - \langle ic_j b_j^z\rangle ic_i b_i^z \\ &\quad -\langle ib_i^z b_j^z\rangle\langle ic_i c_j\rangle + \langle ic_i b_i^z\rangle\langle ic_j b_j^z\rangle \end{aligned} \tag{7.10}$$

We introduce following order parameters which will be used in subsequent analysis,

$$\langle ic_i b_i^z\rangle = \Delta_z^1 \tag{7.11}$$
$$\langle ic_j b_j^z\rangle = \Delta_z^2 \tag{7.12}$$
$$\langle ib_i^z b_j^z\rangle = \gamma_\alpha \qquad \alpha = x, y, z \tag{7.13}$$
$$\langle ic_i c_j\rangle = \gamma_{0\alpha} \qquad \alpha = x, y, z \tag{7.14}$$

We observe that by doing this mean field decomposition we reduce the Hamiltonian into one which contains terms quadratic in majorana fermion operator. γ_α can be identified with the previously mentioned gauge field (conserved for only Kitaev Hamiltonian). The term Δ_z^1 is nothing but $\langle\sigma_i^1\rangle$ and hence measures the spin-order of the system. Here the index '1' and '2' refer to sub-lattice index. From the symmetry of our problem we expect $\gamma_x = \gamma_y$ and we call it γ_h. Similarly we put $\gamma_{0x} = \gamma_{0y} = \gamma_{0h}$. A nonzero value of Δ_z^1 implies the emergence of spin-order due to the Ising Interaction. On the other hand, a non-vanishing value of γ_α is a measure of residual conserved Z_2 gauge fields associated with pure Kitaev model. Inserting the Eq. (7.10) into Eq. (7.7) and in Eq. (7.8) we get,

$$
\begin{aligned}
H_{K-I} &= \sum_{x-\text{link}} J_x i c_i c_j + \sum_{y-\text{link}} J_y i c_i c_j \\
&+ (J_z+\lambda)\left(\sum_{z-\text{link}} \gamma_z i c_i c_j + \gamma_{0z} i b_i b_j - \Delta_z^1 i c_j b_j - \Delta_z^b i c_i b_i + N_z(\Delta_z^1\Delta_z^2 - \gamma_z\gamma_{0z})\right) \\
&+ \lambda\left(\sum_{x-\text{link}} \gamma_h i c_i c_j + \gamma_{0h} i b_i b_j - \Delta_z^a i c_j b_j - \Delta_z^b i c_i b_i + N_x(\Delta_z^1\Delta_z^2 - \gamma_h\gamma_{0h})\right) \\
&+ \lambda\left(\sum_{y-\text{link}} \gamma_h i c_i c_j + \gamma_{0h} i b_i b_j - \Delta_z^1 i c_j b_j - \Delta_z^2 i c_i b_i + N_x(\Delta_z^1\Delta_z^2 - \gamma_h\gamma_{0h})\right) \quad (7.15)
\end{aligned}
$$

From now on we set $J_x = J_y = J_z = 1$ and $N_x = N_y = N_z = N$ for convenience without loss of generality.

7.5 Mean field ansatz around classical minima

First we derive mean field solutions for the spectrum around ferromagnetic state and Neel state. For this we substitute in Eq. (7.15) , $\Delta_i^1 = \Delta^1$ and $\Delta_j^2 = \Delta^2$, where the index 'i' belongs to sub-lattice '1' and 'j' belong to sub-lattice '2'. Ferromagnetic state and Neel state can be obtained by putting $\Delta^1 = \Delta^2$ and $\Delta^1 = -\Delta^2$ respectively..

Then rearranging the terms of Eq. (7.15), we get the following,

$$
\begin{aligned}
H_{K-I} &= \sum_{x-\text{link}} (1+\lambda\gamma_h) i c_i c_j + \sum_{y-\text{link}} (1+\lambda\gamma_h) i c_i c_j + \sum_{z-link} \gamma_z(1+\lambda) i c_i c_j \\
&+ \sum_{x-\text{link}} \lambda\gamma_{0h} i b_i b_j + \sum_{y-\text{link}} \lambda\gamma_{0h} i b_i b_j + \sum_{z-\text{link}} \gamma_{0z}(1+\lambda) i b_i b_j \\
&- \sum_{i\in' 1'} (1+3\lambda)\Delta_z^2 i c_i b_i - \sum_{i\in' 2'} (1+3\lambda)\Delta_z^1 i c_i b_i \\
&+ N(1+3\lambda)\Delta_z^2\Delta_z^1 - 2N\lambda\gamma_h\gamma_{0h} - N(1+\lambda)\gamma_z\gamma_{0z} \quad (7.16)
\end{aligned}
$$

The first line in the above equation describes the hopping Hamiltonian for the 'c' Majorana fermions (which we describe as the matter field for only Kitaev model). The second line describes the hopping interactions for 'b' (referred as gauge fields) Majorana fermions. The last line describes a coupling between 'b' fermions(gauge fields) and 'c' fermions(matter fields).

For future references we define following parameters,

$$\begin{aligned} J_{ch} &= (1+\lambda\gamma_h) \quad ; \; J_{cz} = \gamma_z(1+\lambda) \\ J_{bh} &= \lambda\gamma_{0h} \quad ; \; J_{bz} = \gamma_{0z}(1+\lambda) \\ t_1 &= (1+3\lambda)\Delta_z^1 \quad ; \; t_2 = (1+3\lambda)\Delta_z^2 \end{aligned} \tag{7.17}$$

To proceed with the mean field Hamiltonian (Eq. (7.16)), we go to momentum space by introducing usual Fourier transformation for the fermionic field operators.

$$c_{i,1} = \frac{1}{\sqrt{M}} \sum_k e^{ir_i k} c_{k,1}, c_{j,2} = \frac{1}{\sqrt{M}} \sum_k e^{ir_j k} c_{k,2} \tag{7.18}$$

with $c_k = c_{-k}^\dagger$ to ensure that c_i's are Majorana fermions. Substituting (7.18) in (7.16) and simplifying we get,

$$\begin{aligned} H &= \sum_{k\in \mathrm{HBZ}} \begin{pmatrix} c_{1,k}^\dagger & c_{2,k}^\dagger & b_{1,k}^\dagger & b_{2,k}^\dagger \end{pmatrix} \begin{pmatrix} 0 & if_k & -it^2 & 0 \\ -if_k^* & 0 & 0 & -it^1 \\ it^2 & 0 & 0 & ig_k \\ 0 & it^1 & -ig_k^* & 0 \end{pmatrix} \begin{pmatrix} c_{1,k} \\ c_{2,k} \\ b_{1,k} \\ b_{2,k} \end{pmatrix} \\ &+ M^2(1+3\lambda)\Delta_z^2\Delta_z^1 - 2M^2\lambda\gamma_h\gamma_{0h} - M^2(1+\lambda)\gamma_z\gamma_{0z} \end{aligned} \tag{7.19}$$

Where g_k and f_k are given by,

$$f_k = J_{ch}e^{ik_1} + J_{ch}e^{ik_2} + J_{cz} \tag{7.20}$$

$$g_k = J_{bh}e^{ik_1} + J_{bh}e^{ik_2} + J_{bz} \tag{7.21}$$

After diagonalising the Hamiltonian we get the dispersions as ,

$$E_{1-4} = \pm\frac{1}{\sqrt{2}}\left(|f_k|^2 + |g_k|^2 + t_1^2 + t_2^2 \pm \delta_k\right)^{\frac{1}{2}} \tag{7.22}$$

In the above equation we have wrote the 4 bands of the spectrum in a compact way. where δ_k is given by,

$$\delta_k = \{4({f^*}_k g_k - t_1 t_2)(-f_k {g^*}_k + t_1 t_2) + (|f_k|^2 + |g_k|^2 + t_1^2 + t_2^2)^2\}^{1/2} \tag{7.23}$$

7.5.1 Spectrum for Mean field around FM and Neel State

To get the ground state energy for mean field ansatz around FM state, we substitute $\Delta_1^z = \Delta_2^z$ and for Neel State we substitute $\Delta_1^z = -\Delta_2^z$. From the Eq. (7.19) we can write for ground state energy density E_g per unite cell as given below,

$$E_g = -\frac{1}{M^2}\sum_k (E_{k,1} + E_{k,2}) + a(1+3\lambda)\Delta_z^1\Delta_z^1 - 2\lambda\gamma_h\gamma_{0h} - (1+\lambda)\gamma_z\gamma_{0z} \tag{7.24}$$

where $a = 1$ corresponds to ground state energy around FM state and $a = -1$ is the ground state energy around Neel state. Taking thermodynamic limit we convert the summation to integral in Eq. (7.24) and then performing change of variables we obtain for ground state energy,

$$\begin{aligned} E_g = &-\frac{1}{2\pi^2}\int_0^{\frac{\pi}{2}} dk_x \int_0^{2\pi} dk_y \,(E_{k,1} + E_{k,2}) \\ &+a(1+3\lambda)\Delta_z^1\Delta_z^1 - 2\lambda\gamma_h\gamma_{0h} - (1+\lambda)\gamma_z\gamma_{0z}, \end{aligned} \tag{7.25}$$

where $E_{k,1}$ and $E_{k,2}$ have been defined earlier and $|f_k|$, $|g_k|$ are given by,

$$\begin{aligned} |f_k| &= \sqrt{(\epsilon_{ck}^2 + \Delta_{ck}^2)} \;\; ; \;\; |g_k| = \sqrt{(\epsilon_{bk}^2 + \Delta_{bk}^2)} \\ \delta_k &= \{(|f_k|^2 - |g_k|)^2 + 4t^2|f_k + g_k|^2\}^{1/2} \\ \epsilon_{ck} &= J_{cz} - 2J_{ch}\cos k_x \sin k_y \;\; ; \;\; \Delta_{ck} = 2J_{ch}\cos k_x \cos k_y \\ \epsilon_{bk} &= J_{bz} - 2J_{bh}\cos k_x \sin k_y \;\; ; \;\; \Delta_{ck} = 2J_{bh}\cos k_x \cos k_y \end{aligned} \tag{7.26}$$

In the next section we derive the ground state energy density around Dimer state.

7.5.2 Spectrum for Mean field around dimer state

From the discussions made in Section (7.2), we get the following spatial dependency for the spin-order parameter Δ for Dimer state,

$$\Delta_i^{1,2} = e^{i\vec{R}_i.\vec{G}}\Delta \quad \text{where} \quad \vec{G_2} = \frac{4\pi}{\sqrt{3}}\hat{e}_y \tag{7.27}$$

Here $\vec{G_2}$ is the reciprocal lattice vector corresponding to the lattice translation vector $\vec{a_1}$ and $\vec{a_2}$ shown in Fig (7.1). After inserting Eq. (7.27) in

Eq. (7.15) and then performing Fourier transformation we get the k-pace Hamiltonian as follows,

$$\begin{aligned} H &= \sum_k \left(i f_k c_k^{\dagger a} c_k^b + i g_k b_k^{\dagger a} b_k^b + t i c_k^{\dagger a} b_{k+G_2/2}^a + t i c_k^{\dagger b} b_{k+G_2/2}^b \right) \\ &+ N(J-\lambda)\Delta^2 - 2N\lambda\gamma_h\gamma_{0h} - N(1+\lambda)\gamma_z\gamma_{0z} \end{aligned} \tag{7.28}$$

Where f_k and g_k are given by (7.20) and $t = (J - \lambda)$. N is the number of unit cells. We get the following dispersions,

$$E_{1-4} = \pm\frac{1}{\sqrt{2}} \left(|f_k|^2 + |l_k|^2 + 2t^2 \pm \sqrt{(|f_k|^2 - |l_k|^2)^2 + 4t^2|f_k + l_k|^2} \right)^{\frac{1}{2}} \tag{7.29}$$

$$E_{5-8} = \pm\frac{1}{\sqrt{2}} \left(|g_k|^2 + |h_k|^2 + 2t^2 \pm \sqrt{(|g_k|^2 - |h_k|^2)^2 + 4t^2|g_k + h_k|^2} \right)^{\frac{1}{2}} \tag{7.30}$$

Where g_k and f_k are as before and h_k and l_k are given by,

$$h_k = -J_{ch}e^{ik_1} - J_{ch}e^{ik_2} + J_{cz} \tag{7.31}$$

$$l_k = -J_{bh}e^{ik_1} - J_{bh}e^{ik_2} + J_{bz} \tag{7.32}$$

Similar to Eq. (7.25), we can easily write down the ground state energy density per unit cell for the Dimer state. Having derived the spectrum for mean field solutions around each classical configurations we proceed to obtain self consistent solutions for various order parameters given in equations (7.11,7.12,7.13,7.14).

7.6 Minimisation of ground state energy

To calculate the various order parameters (corresponding to various mean field ansatz) we minimise the respective ground state energy with respect to each order parameter and solve for resulting equations self-consistently. Here below we write the self consistent equations for various order parameter for FM and Neel state. Solutions corresponding to Dimer state can be found in a similar way.

$$\gamma_h = \frac{1}{2\pi^2}\int_0^{\frac{\pi}{2}} dk_x \int_0^{2\pi} dk_y \left(\frac{\partial E_{k,1}}{\partial J_{cz}} + \frac{\partial E_{k,2}}{\partial J_{cz}}\right) \tag{7.33}$$

$$\gamma_z = \frac{1}{2\pi^2}\int_0^{\frac{\pi}{2}} dk_x \int_0^{2\pi} dk_y \left(\frac{\partial E_{k,1}}{\partial J_{ch}} + \frac{\partial E_{k,2}}{\partial J_{ch}}\right) \tag{7.34}$$

$$\gamma_{0h} = \frac{1}{2\pi^2}\int_0^{\frac{\pi}{2}} dk_x \int_0^{2\pi} dk_y \left(\frac{\partial E_{k,1}}{\partial J_{bz}} + \frac{\partial E_{k,2}}{\partial J_{bz}}\right) \tag{7.35}$$

$$\gamma_{0z} = \frac{1}{2\pi^2}\int_0^{\frac{\pi}{2}} dk_x \int_0^{2\pi} dk_y \left(\frac{\partial E_{k,1}}{\partial J_{bh}} + \frac{\partial E_{k,2}}{\partial J_{bh}}\right) \tag{7.36}$$

$$\Delta = -\frac{a}{4\pi^2}\int_0^{\frac{\pi}{2}} dk_x \int_0^{2\pi} dk_y \left(\frac{\partial E_{k,1}}{\partial t} + \frac{\partial E_{k,2}}{\partial t}\right) \tag{7.37}$$

In the last equation 'a' is 1(-1) for solution around FM(AFM) state. After evaluating all the parameters self consistently we calculate mean value of B_p (the flux operator). We know that the flux operator is given by,

$$B_p = ib_{1,i}b_{2,i}ib_{1,j}b_{2,j} \tag{7.38}$$

Where 'i' and 'j' are two z-bonds shared by the hexagonal plaquette 'p' and 1, 2 refers the sub lattice indices. $\langle B_p\rangle$ denotes the average value of flux operator and a non-vanishing value of this signifies a spin liquid phase (which we also refer as Kitaev phase). In the following section we present the behaviour of $\langle B_p\rangle$ and Δ as a function of λ to explain the possible phases of H_{KI}.

7.7 Numerical results

7.7.1 For FM Ising interaction

We begin with positive λ corresponding to ferromagnetic Ising perturbations to the Kitaev Hamiltonian. First we plot the spin-order parameter and flux-order parameter in the figure below. We see from Fig (7.1) that at $\lambda = 0.07$, spin order parameter Δ takes a finite value discontinuously. At the same

value of λ the flux order parameter also goes to zero from 1. It is evident that this marks phase transition from spin liquid phase to magnetically ordered state. The Kitaev phase which is characterised by a finite flux order parameter is stable up to $\lambda = 0.07$. This transition is first order as indicated by the Fig. (7.4) where we plot ground-state energy density as a function of λ.

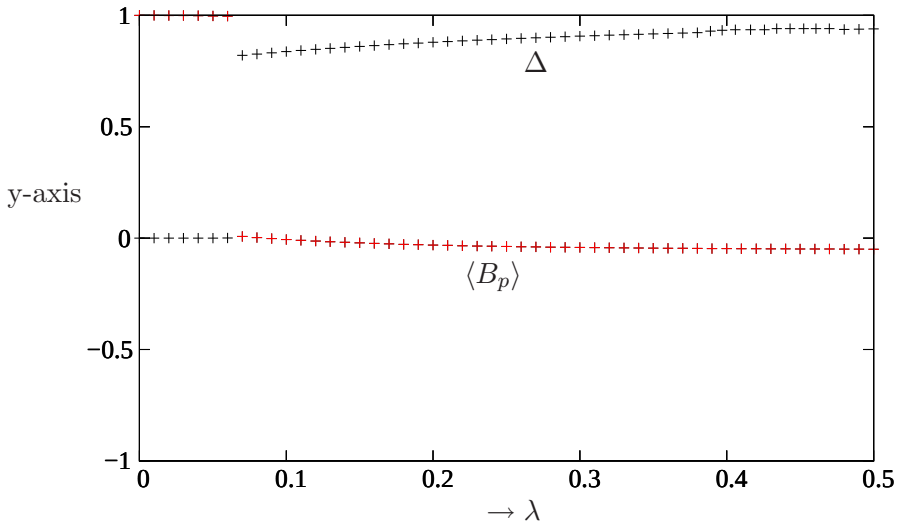

Figure 7.3: The red points corresponds to flux order parameter and black points corresponds to spin-order parameter. Both of them undergoes a discontinuous change around $\lambda = 0.1$

7.7.2 For AFM Ising interaction

We have already discussed that for small λ it is the Dimer state which corresponds to true classical minima. This is also evident from the ground state energy densities as shown in Fig. (7.6). In Fig. (7.5), we plotted $\langle B_p \rangle$ and Δ verses λ. In this case we also observe a discontinuous change of flux order parameter $\langle B_p \rangle$ and Δ around $\lambda = -0.1$.

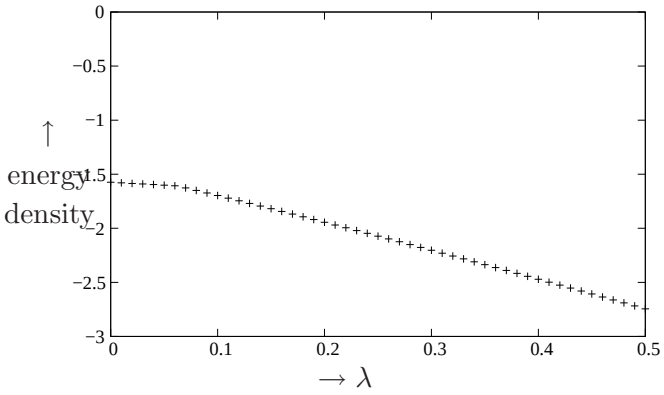

Figure 7.4: Here we plot the ground state energy density vs λ . The behaviour of energy density suggests a first order phase transition at $\lambda = 0.07$.

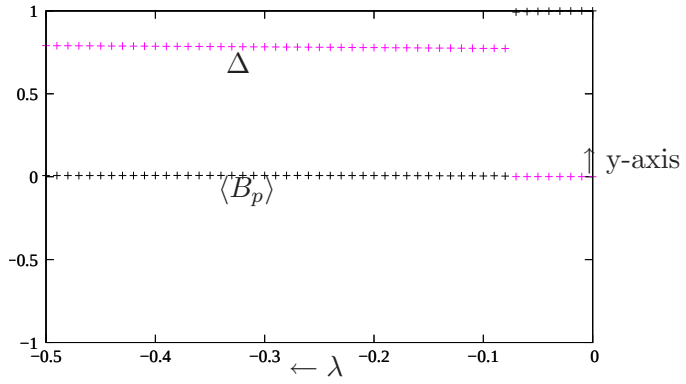

Figure 7.5: The pink points correspond to flux-order and black points correspond to spin-order parameter. We observe discontinuous changes for both the order parameters as λ is being varied

7.8 Discussion

From the above results we conclude that around $\lambda = 0$, there is a small region(of about 10 percent of J) where Kitaev model is stable and flux order parameter is non-zero describing a spin liquid state. As we increase λ further the system undergoes a 'first order' transition at mean field level to a magnetic state and flux-order parameter vanishes. The stability of Kitaev phase around $\lambda = 0$ might be important from the view point of experimental realisation of Kitaev model [96, 97]. Because there may have trace of other kind of interactions to be present when realizing Kiteav interaction experi-

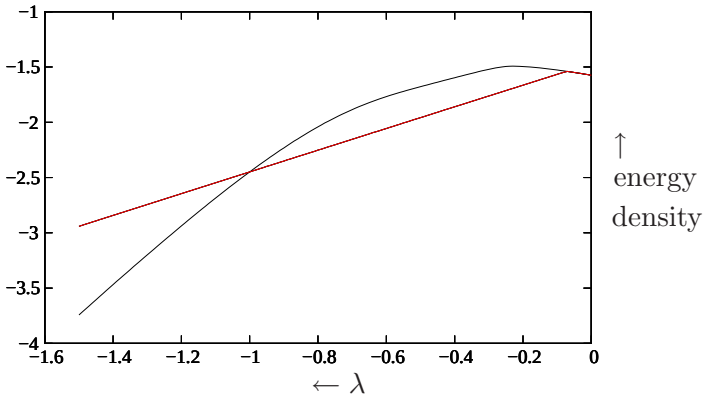

Figure 7.6: Here we plot the ground state energy density vs λ . The black line corresponds to energy density for Neel state and red line corresponds to energy density for Dimer state. We see that for intermediate value of λ it is the Dimer state which corresponds to true minima.

mentally. Our analysis gives a first hand measure of how much impurity of interaction may be acceptable in practical realisation of Kitaev model.

If the red slayer think he slays,
Or if the slain think he is slain,
They know not well the subtle ways
I keep, and pass, and turn again.
Brahma-Ralph Waldo Emerson

Chapter 8

3D Kitaev model

8.1 Introduction

In previous chapters we have been studying various many body aspects of the 2 dimensional Kitaev model. We have seen that this spin 1/2 model can be solved exactly. It is very remarkable in the sense that exactly solvable models are not very common [137–139]. We have also seen that this spin model represents a quantum spin liquid state. It supports anyonic excitations which can be useful in quantum computation. Given the novelty of this 2 dimensional model, it is very natural to search for other possible Kitaev like models. Thus it is no surprise that following Kitaev model, a number of exactly solvable models have been proposed in 2 dimension as well as in 3 dimension with Kitaev like interactions [85–89]. Apart from the exact solvability one is also interested to examine how the dimensionality and the difference in underlying lattice structures yield new topological order and nontrivial statistics of excitations (if any) in all these models. In this chapter we introduce a 3 dimensional generalisation of the Kitaev model [87]. We have seen that exact solution of 2D Kitaev model was possible as it could be mapped to non-interacting Majorana fermion hopping problem with background static Z_2 gauge fields. This feature remains intact in all the models with Kitaev like interactions. However depending on underlying lattice on which the model is defined, it possesses many new features compared to original Kitaev model. We first give details of the 3D lattice on which our 3 Dimensional Kitaev model has been defined.

8.2 The 3D lattice

We note two features of the honeycomb lattice that are very important to the construction of the 3D lattice : (1) The coordination number of the lattice is 3. (2) The three types of links x, y and z are distributed in such a way that two links of the same type do not touch each other. In the figure (8.1, A) we have drawn a part of the 3D lattice. Let us explain how to construct this 3D lattice in steps. We can describe the 3D lattice as a connected 2D lattices parallel to $x-y$ plane. We first explain how to construct the 2D lattices parallel to $x-y$ plane. Then we will show how to connect these 2D lattices in z-directions to get the complete 3D lattice. Every 2D plane repeats itself after every fourth plane in the z-directions.

Let us first construct the 2D lattice on the plane $z = 0$. This 2D lattice, essentially, contains disconnected 1 dimensional chains parallel to x-axis. In the Fig. (8.1), the red lines, r_1, r_2 and r_3 denote such 1 Dimensional chain. It is to be noticed that these 1D chains are completely disconnected. If the distance between two sites in a given chain is unity then the distance between two parallel disconnected chains are of 2 units. We can write for the position of the sites of this 1D chains as,

$$\vec{r} = r_x\hat{x} + 2r_y\hat{y} \; ; \quad r_x, \; r_y \in \text{integer} \tag{8.1}$$

Now let us construct the 2nd plane which is defined by $z = 1$. Similar to the 1st plane it also contains disconnected 1D chains but here the disconnected 1D chains are parallel to y-axis. In the Fig. (8.1), they are represented by pink lines, p_1 and p_2, etc. The co-ordinates for the sites of the 2nd layer are,

$$\vec{p} = 2p_x\hat{x} + p_y\hat{y} + \hat{z} \; ; \quad p_x, \; p_y \in \text{integer} \tag{8.2}$$

The third plane is specified by $z = 2$. It is identical to the first plane but only shifted by 1 unit in y-direction. The black lines b_1 and b_2 denotes such 1D chains. The co-ordinates of the sites for this plane are given by,

$$\vec{b} = b_x\hat{x} + (2r_y + 1)\hat{y} + 2\hat{z} \; ; \quad b_x, \; b_y \in \text{integer} \tag{8.3}$$

Similarly the fourth plane is given by $z = 3$ and it is a repetition of 2nd plane but shifted along x-direction by unite distance. Thus we can write for the sites of this plane,

$$\vec{l} = (2l_x + 1)\hat{x} + l_y\hat{y} + 3\hat{z} \; ; \quad l_x, \; l_y \in \text{integer} \tag{8.4}$$

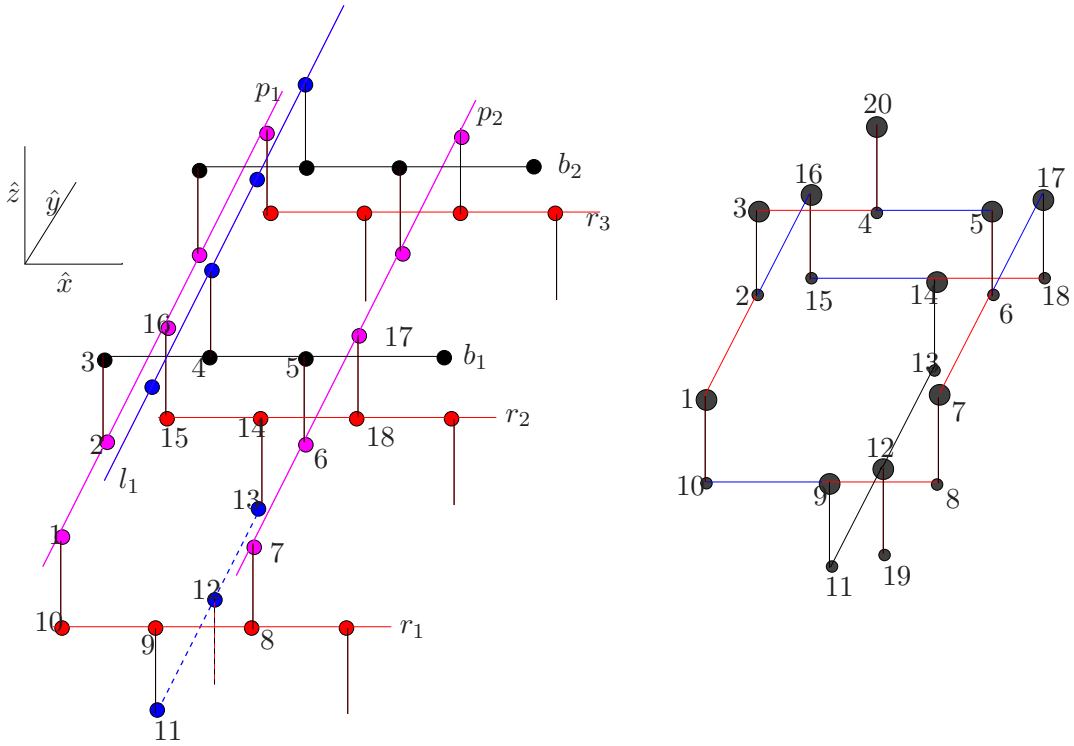

Figure 8.1: In the right side we show a part of the 3D lattice. In the left an elementary structure of 3D lattice has been shown. The complete 3D lattice can also be constructed by suitably pudding up this elementary object. The red bonds are x-bonds, blue bonds are y-bonds and the vertical bonds are z-bonds. Sites 1 to 10 constitute an elementary loop in the lattice. Sites 1 to 18 form an elementary object mentioned before. An elementary object contains four elementary loops. These loops are associated with conserved quantities of the 3D Kitaev model which are analogous to B_p in 2D Kitaev model. This 3D lattice is a bipartite one and we have shown this in the right side of the figure. The small black points and the big black points indicate different sub-lattices.

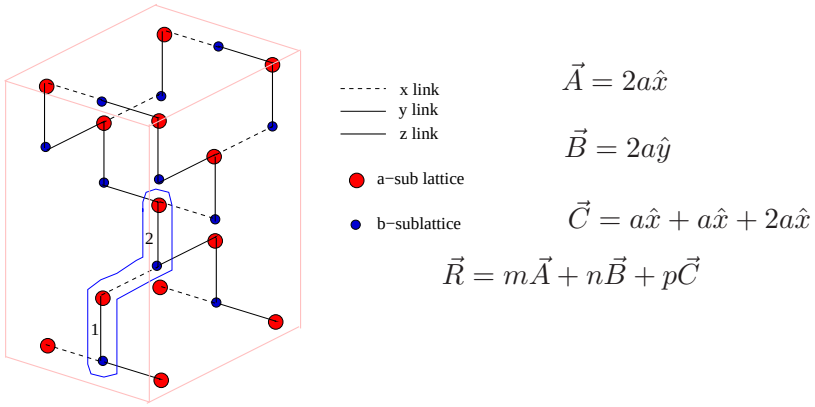

Figure 8.2: The 3D lattice. The four sites inside the closed loop constitute a unit cell.

Now the fifth plane is exactly on top of the first plane and situated at $z = 4$. After every four plane the patterns repeat. We can easily construct the 3D lattice by suitably connecting the sites of different planes. The rule is the following. Connect all the sites which are at unit distance from each other. This will suffice to describe the 3D lattice. To see how this makes the 3D lattice completely connected let us see the above figure. In each 1D chain alternative sites are connected with the sites belonging to the plane just above and below respectively. This is true for each 1D chain.

Now we can parameterise the lattice sites completely. For this purpose we note that the unit cell contains four sites. Since the lattice is bipartite, it is convenient to introduce two indices to label the sites within a unit cell; $\mu = 1, 2$ denotes the dimer to which a site belongs and $\alpha(= a, b)$ denotes the sub lattice (see Fig. (8.2)) indices. The position vector of a unit cell is given by,

$$\mathbf{r} = m\mathbf{a}_1 + n\mathbf{a}_2 + p\mathbf{a}_3, \quad m, n, p \in \text{integer}, \tag{8.5}$$

$$\mathbf{a}_1 = 2\hat{\mathbf{x}}, \quad \mathbf{a}_2 = 2\hat{\mathbf{y}}, \quad \mathbf{a}_3 = \hat{\mathbf{x}} + \hat{\mathbf{y}} + 2\hat{\mathbf{z}}. \tag{8.6}$$

Where $\hat{\mathbf{x}}, \hat{\mathbf{y}}$ and $\hat{\mathbf{z}}$ are unit vectors along x, y and z directions respectively. The location of the sites $\{(\mu, \alpha)\}$ in the unit cell at $\mathbf{r}$ are given as follows:

$$(1, a) \rightarrow \mathbf{r} - \frac{\hat{\mathbf{y}}}{2} - \hat{\mathbf{z}} \tag{8.7}$$

$$(1, b) \rightarrow \mathbf{r} - \frac{\hat{\mathbf{y}}}{2} \tag{8.8}$$

$$(2,a) \quad \rightarrow \quad \mathbf{r} + \frac{\hat{\mathbf{y}}}{2} \tag{8.9}$$

$$(1,b) \quad \rightarrow \quad \mathbf{r} + \frac{\hat{\mathbf{y}}}{2} + \hat{\mathbf{z}} \tag{8.10}$$

8.3 The 3D Kitaev model

In the Fig. (8.2), we have labelled 4 different sites which belong to a unit cell. Dashed bonds refer to x-interaction, solid horizontal links refer to y-interaction and vertical bonds refer to z-interactions. We have taken 2 z-bonds inside the unite cell. This lattice is a bipartite lattice. We denote the coordinate of unit cell as (i,j,k) where 'i' stands for 'x' co-ordinate and so on. The length of each $x/y/z$ bond is taken to be of unity. Then the Hamiltonian is given by,

$$\begin{aligned} H \quad = \quad & \sum -J_x \sigma^x_{i,j,k,1a}\sigma^x_{i,j,k-1,2b} - J_y \sigma^y_{i+1,j,k-1,2b}\sigma^y_{i,j,k,1a} \\ & -J_x \sigma^x_{i,j,k,2a}\sigma^x_{i,j,k,1b} - J_y \sigma^y_{i,j,k,2a}\sigma^y_{i,j+1,k,1b} \\ & -J_z(\sigma^z_{i,j,k,1a}\sigma^z_{i,j,k,1b} + \sigma^z_{i,j,k,2a}\sigma^z_{i,j,k,2b}) \end{aligned} \tag{8.11}$$

Similar to 2D Kitaev model, 3D Kitaev model also have conserved loop operators associated with each plaquette. The conserved quantity associated with the plaquette 'p' as shown in Fig. (8.1, B), is given by,

$$W_p \quad = \quad \sigma^x_1\sigma^y_2\sigma^y_3\sigma^y_4\sigma^z_5\sigma^x_6\sigma^y_7\sigma^y_8\sigma^y_9\sigma^z_{10} \tag{8.12}$$

Like before the conserved quantity associated with each plaquette is the product of out going sigma matrices of each sites of the plaquette. It is easy to check that like 2D Kitaev model $[W_p, W_q] = 0$ and $[W_p, H] = 0$. Thus they form a complete set of commuting operators.

8.4 Fermionization of spin operators.

In the next step, following Kitaev, we use a representation of Pauli matrices in terms of Majorana fermions to obtain a fermionic Hamiltonian from Eq. (8.11). In chapter 2, section (2.1) we have discussed it in detail, here we present the final form of the fermionised Hamiltonian.

$$\begin{aligned} H &= \frac{i}{2}\sum_{j,k}\hat{A}_{jk}c_jc_k, \\ \hat{A}_{jk} &= \begin{cases} J_{\alpha_{jk}}\hat{u}_{jk} & \text{if } j \text{ and } k \text{ are linked,} \\ 0 & \text{otherwise,} \end{cases} \\ \hat{u}_{jk} &= ib_j^{\alpha_{jk}}b_j^{\alpha_{jk}}. \end{aligned} \tag{8.13}$$

In the above equation c_i and $b_j^{\alpha ik}$ are the Majorana fermions. We note that $\hat{u}_{jk} = -\hat{u}_{kj}$, and in the sum the links are treated as directed and therefore counted twice. We use a hat to emphasise that $\hat{u}_{jk}$ is an operator; u_{jk} is the corresponding eigenvalue and takes values ± 1. Further,

$$[H, \hat{u}_{jk}] = 0,\ [\hat{u}_{jk}, \hat{u}_{lm}] = 0\ \forall\ j,k,l,m. \tag{8.14}$$

Therefore, the Hilbert space breaks up into various sectors, each corresponding to a particular set $\{u_{jk}\}$; the matrix elements of $\widetilde{H}$ between states belonging to different sectors are zero. The Hamiltonian in a given sector is obtained by replacing the $\hat{u}_{jk}$ operators with the corresponding eigenvalues, u_{jk}.

$$H_u = \frac{i}{2}\sum_{j,k}A_{jk}c_jc_k. \tag{8.15}$$

We notice that the spin model has conserved quantities associated with all closed loops, where as the Majorana fermionised Hamiltonian 8.15 has a conserved quantity on each link. The projection of $\hat{u}_{jk}$ on the physical subspace is zero, as consistency would demand. The gauge invariant physical conserved quantities in the extended space are

$$W_l = \prod_{<j,k>\in l}\hat{u}_{jk}, \tag{8.16}$$

where l, as before, is an arbitrary closed loop and $< j,k >$'s are the links which, strung together, forms l.

8.5 Gauge fixing and solving the model

In chapter 2 when studying 2 dimensional Kitaev model, we have seen that the gauge sector where all the gauge fields $\hat{u}_{ij}$ are 1, is the ground state sector. This follows from a beautiful theorem by Lieb in [110]. It studied problem of free fermions hopping on a d-Dimensional hyper cubic lattice

with hopping strength $|t_{ij}|e^{i\theta_{ij}}$ between nearest neighbour sites i and j. It was shown that, if $|t_{ij}|$ is reflection symmetric about planes which does not contain any sites, then in the ground state the flux of the phase along elementary loops, $\Phi \equiv \sum_{<ij>} \theta ij$, equals to π if the length of the loop is 0 mod 4, and equals to 0 if the length is 2 mod 4. Unfortunately, Lieb's result cannot be directly applied to our case because the lattice does not have reflection symmetry about planes which does not contain sites. We have studied the Hamiltonian in Eq. (8.15) numerically and found that the ground state has a uniform flux configuration of $\Phi = 0$ for all the elementary loops. We have taken a lattice of 500 sites and compared the ground state energy of the uniform flux configuration with other chosen configuration of fluxes for sufficiently large number of times and we always found that the uniform flux 1 corresponds to the universal minima. This is consistent with Lieb's result since the elementary loop in our lattice has length 10, which is 2 mod 4. In terms of the loop operators, $W_l = 1, \quad \forall l$. This is satisfied if $u_{jk} = 1$, for all links $< j, k >$. (Of course, any configuration related to this one by a gauge transformation will also satisfy the above condition on W_l.) The Hamiltonian in this sector in its explicit form is

$$\begin{aligned} H &= i\sum_{\mathbf{r}} \Big[J_x c_{1a}(\mathbf{r}) c_{2b}(\mathbf{r}+\mathbf{a}_3) + J_y c_{1a}(\mathbf{r}) c_{2b}(\mathbf{r}+\mathbf{a}_1+\mathbf{a}_3) + J_x c_{2a}(\mathbf{r}) c_{1b}(\mathbf{r}) \\ &\quad + J_y c_{2a}(\mathbf{r}) c_{1b}(\mathbf{r}+\mathbf{a}_2) + J_z c_{1a}(\mathbf{r}) c_{1b}(\mathbf{r}) + J_z c_{2a}(\mathbf{r}) c_{2b}(\mathbf{r}) \Big], \end{aligned} \tag{8.17}$$

where $\mathbf{r}$ and $\mathbf{a}_i$ are given in Eqs. (8.5) and (8.6). Next we define the Fourier transformation in the following way,

$$c_{\mathbf{r},\mathbf{j}\alpha} = \frac{1}{\sqrt{PQR}} \sum_{\mathbf{r}} e^{-i\mathbf{r}.\mathbf{k}} c_{\mathbf{k},\mathbf{j}\alpha} \tag{8.18}$$

Where 'j' can take value 1 to 4 and $\alpha = a, b$. c_k has the property, $c_{-k} = c_k^\dagger$. PQR is the size of the lattice where 'P', 'Q' and 'R' denote the number of unit cells taken in each three direction of lattice translations.

$$\begin{aligned} \mathbf{r} &= i\vec{a_1} + j\vec{a_2} + k\vec{a_3} \\ \vec{a_1} &= (2,0,0) \\ \vec{a_2} &= (0,2,0) \\ \vec{a_3} &= (1,1,2) \end{aligned} \tag{8.19}$$

$\vec{a_j}$ is the lattice translation vector. With this definition we get,

$$\begin{aligned} H &= \sum_k ie^{-ik_3}(J_x + J_y e^{ik_1}) c_{\mathbf{k,1a}} c_{-\mathbf{k,2b}} \\ &\quad + i(J_x + J_y e^{ik_2}) c_{\mathbf{k,2a}} c_{-\mathbf{k,1b}} \\ &\quad + iJ_z(c_{\mathbf{k,1a}} c_{-\mathbf{k,1b}} + c_{\mathbf{k,2a}} c_{-\mathbf{k,2b}}) \end{aligned} \tag{8.20}$$

k_1, k_2, k_3 are the components of $\mathbf{k}$ along the three translation vectors. Using the property of $c_{-k} = c_k^\dagger$ and replacing $\mathbf{k} = -\mathbf{k}$ we rewrite it,

$$\begin{aligned} H &= \sum_k \frac{i}{2}(e^{-ik_3}\delta_{1k} c_{\mathbf{k,1a}} c^\dagger_{\mathbf{k,2b}} + e^{ik_3}\delta^*_{1k} c^\dagger_{\mathbf{k,1a}} c_{\mathbf{k,2b}}) \\ &\quad + \frac{i}{2}(\delta_{2k} c_{\mathbf{k,2a}} c^\dagger_{\mathbf{k,1b}} + \delta^*_{2k} c^\dagger_{\mathbf{k,2a}} c_{\mathbf{k,1b}}) \\ &\quad + \frac{i}{2} J_z(c^\dagger_{\mathbf{k,1a}} c_{\mathbf{k,1b}} + c^\dagger_{\mathbf{k,2a}} c_{\mathbf{k,2b}}) \end{aligned} \tag{8.21}$$

Here δ_{1k} and δ_{2k} is given by,

$$\delta_{1k} = (J_x + J_y e^{ik_1}), \quad \delta_{2k} = (J_x + J_y e^{ik_2}) \tag{8.22}$$

Eq. (8.21) looks like following when written in matrix form.

$$H = \sum_k \begin{pmatrix} \xi_1^\dagger & \xi_2^\dagger \end{pmatrix} \begin{pmatrix} 0 & A \\ A^T & 0 \end{pmatrix} \begin{pmatrix} \xi_1 \\ \xi_2 \end{pmatrix} \tag{8.23}$$

Where

$$\xi_1 = \begin{pmatrix} c_{\mathbf{k,1a}} \\ c_{\mathbf{k,2a}} \end{pmatrix} \tag{8.24}$$

$$\xi_2 = \begin{pmatrix} c_{\mathbf{k,1b}} \\ c_{\mathbf{k,2b}} \end{pmatrix} \tag{8.25}$$

and

$$A = \frac{i}{2} \begin{pmatrix} J_z & e^{i(k_3)}\delta^*_{1k} \\ \delta^*_{2k} & J_z \end{pmatrix} \tag{8.26}$$

The eigenvalue equation of A is given by,

$$\begin{pmatrix} 0 & A \\ A^T & 0 \end{pmatrix} \begin{pmatrix} \eta_1 \\ \eta_2 \end{pmatrix} = \lambda \begin{pmatrix} \eta_1 \\ \eta_2 \end{pmatrix} \tag{8.27}$$

Here η_1 and η_2 are two component column matrices. These equations yield the following conditions,

$$\begin{aligned} A\eta_2 &= \lambda\eta_1 \quad A^T\eta_1 = \lambda\eta_2 \quad \text{or} \\ A^TA\eta_2 &= \lambda^2\eta_2 \quad AA^T\eta_1 = \lambda^2\eta_1 \end{aligned} \tag{8.28}$$

Solving above equations would give $\eta_1, \eta_2, \lambda^2$. Then the actual eigenvectors of Hamiltonian with eigenvalue $\pm\lambda$ can be made of $\begin{pmatrix} \eta_1 \\ \eta_2 \end{pmatrix}$ and $\begin{pmatrix} \eta_1 \\ -\eta_2 \end{pmatrix}$ Solving for the λ we get the eigenvalues as,

$$E_k = \frac{\pm 1}{2\sqrt{2}} \left(\Delta_k \pm \Delta_{3k}\right)^{\frac{1}{2}} \tag{8.29}$$

The various parameters appearing in the above equation are given by,

$$\Delta_k = |\delta_{1k}|^2 + |\delta_{2k}|^2 + 2J_z^2 \tag{8.30}$$

$$\Delta_{3k} = \sqrt{(\Delta_{12k}^2 + +4J_z^2(|\delta_1^{2k}| + |\delta_2^{2k}| + (\delta_{1k}\delta_{2k}e^{-i(k_3)} + c.c))} \tag{8.31}$$

$$\Delta_{12k} = (|\delta_{1k}|^2 - |\delta_{2k}|^2) \tag{8.32}$$

It is clear that E_k is gapless when Δ_{3k} is equal to Δ_k. This condition gives following equation,

$$2J_z^2\delta_{1k}\delta_{2k}e^{-i(k_3)} = |\delta_{1k}|^2|\delta_{2k}|^2 + J_z^4 \tag{8.33}$$

To solve the above equation, we substitute $x = \delta_{1k}\delta_{2k}e^{-i(k_3)}$ and obtain

$$\begin{aligned} J_z^4 + x^2 - 2J_z^2x &= 0 \\ x &= J_z^2 \end{aligned} \tag{8.34}$$

Thus we get the following condition for gapless spectrum,

$$\begin{aligned} \delta_{1k}\delta_{2k}e^{-i(k_3)} &= J_z^2 \\ \delta_{1k}^*\delta_{2k}^*e^{i(k_3)} &= J_z^2 \end{aligned} \tag{8.35}$$

The above equation can be written as,

$$J_z^2 = \left(J_x^2 + J_y^2 + 2J_yJ_x\cos k_1\right)^{1/2}\left(J_x^2 + J_y^2 + 2J_yJ_x\cos k_2\right)^{1/2} \tag{8.36}$$

We notice that the maximum value r.h.s of the above equation can produce is $(J_x + J_y)^2$. If J_z is greater than $J_x + J_y$, Eq. (8.36) can not be satisfied. Thus gapless region is obtained for $J_z \leq J_x + J_y$. Now we look at the other end. The minimum value r.h.s can produce is given by $(J_x - J_y)^2$. Thus if J_z is less than $J_x - J_y$, Eq. (8.36) can not be satisfied for any value of k_1 and k_2. So we get another condition, $J_z \geq J_x - J_y$ or $J_x \leq J_z + J_y$. Similarly we would get $J_y \leq J_x + J_z$.

In summary, we can write the condition for the gapless spectrum as,

$$J_z \quad \leq \quad J_x + J_y; \;\; J_x \leq J_z + J_y; \;\; J_y \leq J_x + J_z \tag{8.37}$$

We note that this condition is identical to the gapless condition for the 2d Kitaev model. The above condition for gapless spectrum is derived assuming that all J's are positive. If this is not the case then equation (8.37) should be rewritten as,

$$|J_z| \leq |J_x| + |J_y|; \;\; |J_x| \leq |J_z| + |J_y|; \;\; |J_y| \leq |J_x| + |J_z| \tag{8.38}$$

Below we have given the phase diagram for positive J's. The shaded region is the gapless region. We have also shown the value of 'k' for which minimum occurs in the gapped phase.

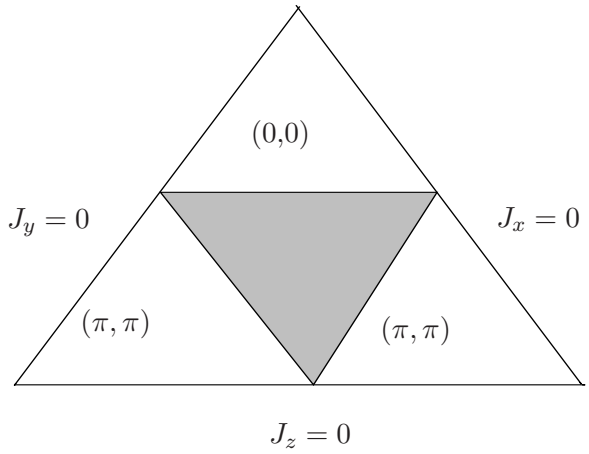

Figure 8.3: Phase diagram for 3d Kitaev model in the parameter space of J_x, J_y, J_z. The shaded region is gapless. The value of the k_x and k_y for which spectrum is minimum in the gapped region is specified.

After presenting the formal solutions of the model we proceed to discuss some many body aspects of this model. We start with a discussion on spin-spin correlations.

8.6 Spin correlations

Various spin correlations can also be calculated following the way we did for 2D Kitaev model. And no wonder that like Kitaev model and other Kitaev like model here also correlation function is short range and follows exactly the same nature as seen in other Kitaev like model. In other words, the only non-zero correlations are those of operators which are a product of an arbitrary number of the terms that appear in the Hamiltonian. We notice that, quite remarkably, this is true for all eigenstates of H, not just the ground state. In particular, the only non-vanishing two-spin correlations are those of the terms in the Hamiltonian; it vanishes identically beyond nearest neighbours. Moreover, this is a general result that holds for both the gapped as well as the gapless phases. This suggests that the transition between the two phases cannot be characterised by a local order parameter. But here a single spin fractionalises into a Majorana fermion and a number of π fluxes in the elementary loops.

8.7 Excitations

Original Kitaev model which has been defined in 2 Dimensions has anyonic excitations, i.e., there are particle-like excitations which obey nontrivial exchange statistics. Anyons are very specific to two dimensions and cannot exist in higher Dimensions—the fundamental reason being that in D $>$ 2 there are no nontrivial paths which take a particle around another. However in three dimensions, excitations localised on loops may show nontrivial exchange statistics. We will now explain that such excitations may exist in our model.

In Sec 8.4, we have seen that the link variables $\hat{u}_{jk}$ are static. Further, in Sec 8.5, we have explained that numerically we found that in the ground state, W_l, the product of $\hat{u}_{jk}$'s along the loop l takes the value 1 for all closed loops l. It then follows that the excitations are of two types:

1. Configurations of $\hat{u}_{jk}$ which violate the condition $W_l = 1$; i.e., $W_l = -1$ for some of the loops. It can be looked upon as creating a π flux over those loops.

2. Fermionic excitations of the field c_j in the background of static configurations of $\hat{u}_{jk}$.

We will next show that the excitations of the first type are localised on closed 'loops'.

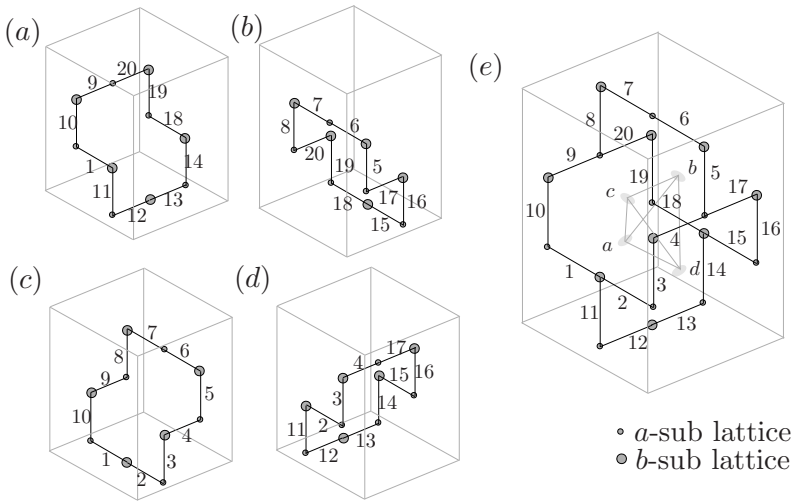

Figure 8.4: (a)-(d) The four elementary loops. (e) Part of the lattice involving four such adjacent loops; the corresponding operators give rise to a constraint. The ellipses, labelled a to d, respectively represent each of the loops and they form a tetrahedron.

Earlier, we mentioned that not all W_l's are independent; now we will find the constraints among them. Note that the most elementary loop consists of 10 sites; let B_α denote the loop operator corresponding to such a loop. There are four types of such loops—labelled a, b, c and d—which are distinguished by their orientation (see Fig. 8.4 a-d). For an open system, W_l for any closed loop l can be written in terms of B_α's. To find the constraints among B_α's we consider a part of the lattice, shown in Fig. 8.4e, which consists of four adjacent elementary loops—each a different type. Let the corresponding loop operators be B_a, B_b, B_c, and B_d, respectively. Here the links are labelled 1 to 20 (this is different from our earlier notation where links were labelled in terms of the sites). In this notation, the B_α operators corresponding to

the four loops are

$$\begin{aligned} B_a &= u_{11}u_{12}u_{13}u_{14}u_{18}u_{19}u_{20}u_9u_{10}u_1, \\ B_b &= u_{15}u_{16}u_{17}u_5u_6u_7u_8u_{20}u_{19}u_{18}, \\ B_c &= u_1u_2u_3u_4u_5u_6u_7u_8u_9u_{10}, \\ B_d &= u_{11}u_{12}u_{13}u_{14}u_{15}u_{16}u_{17}u_4u_3u_2. \end{aligned} \tag{8.39}$$

where u_m, as defined in Eq. (8.13), is understood to be the product of the c Majorana fermions at the two sites that form the link m, with the convention that the operator belonging to the a-sub lattice comes to the left. Since $u_m^2 = 1$,

$$B_aB_bB_cB_d = 1. \tag{8.40}$$

The above constraint can be graphically understood using Fig. (8.4,e): it represents the left hand side of Eq. (8.40); evidently, each link m is shared by two of the B_α's and therefore every u_m appears twice in the product, which makes the latter 1. For open boundary conditions, relations such as Eq. (8.40) exhaust all the constraints. [For periodic boundary conditions, it is easy to check that the number of independent B_α's is $(2N + 1)$, where N is the number of unit cells.]

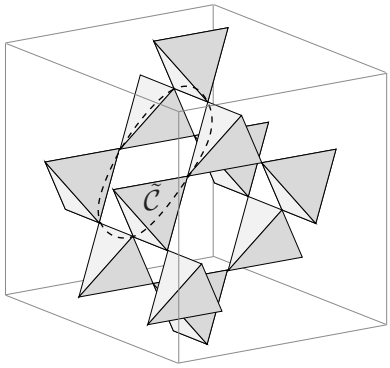

Figure 8.5: The lattice $\mathfrak{L}$ formed by the elementary loops—the pyrochlore lattice. The dashed curve $\tilde{\mathcal{C}}$, which goes through 6 sites, is the shortest possible loop in $\mathfrak{L}$ that lies within the tetrahedra. The minimum energy flux configuration has $B_\alpha = -1$, if $\alpha \in \tilde{\mathcal{C}}$, and $B_\alpha = 1$, otherwise.

To find the configurations of $\{B_\alpha\}$ which satisfy all the constraints, it is instructive to consider a lattice obtained by representing each elementary loop by a single site. An elementary loop has a step like structure, which consists of two rectangles perpendicular to the $x - y$ plane connected

by another rectangle on the $x-y$ plane. Each loop can be uniquely represented by a point at the centre of the rectangle on the $x-y$ plane (in Fig. 8.4e such points are marked by ellipses). Let $\mathfrak{L}$ be the new lattice thus obtained—topologically, it is the pyrochlore lattice, which is an arrangement of corner-sharing tetrahedra (see Fig. (8.5)). In this description, the four elementary loops that give rise to the constraint in Eq. (8.40) are the four sites of a tetrahedron, and each tetrahedron corresponds to an independent constraint. Therefore, any configuration satisfying all the constraints will have an even number of B_α taking value -1 in each tetrahedron, where α is now the site index in $\mathfrak{L}$. Now it is clear how to obtain such configurations: Draw a closed loop $\mathcal{C}$ which does not cross itself and which lies entirely within the tetrahedra, and let

$$B_\alpha = \begin{cases} -1, & \text{if } \alpha \in \mathcal{C}, \\ 1, & \text{otherwise.} \end{cases}$$

Any closed, self-avoiding loop contains an even number of sites (0, 2 or 4) belonging to any particular tetrahedron; hence all the constraints are satisfied. There is a one-to-one correspondence between the set of all allowed configurations $\{B_\alpha\}$ and the set of all closed loops (including multiple ones, but which do not cross each other). We have thus shown that, topologically, the flux excitations have the structure of loops in the lattice $\mathfrak{L}$.

8.8 Counting of Conserved Quantities

Here we calculate the number of independent conserved quantities of 3D Kitaev model using gauge invariance principle. We will also be giving a simple arguments using Jordan-Wigner transformation as we have done for 2D Kitaev model. In the Kitaev model, we have Z_2 gauge field, u_{ij}, which lives on the bond connecting the sites i and j and take values ± 1. The total number of states is 2^{N_b}, where N_b is the number of bonds. Then we can define a gauge transformation (GT) given by,

$$\tilde{u}_{ij} = W_i u_{ij} W_j, \tag{8.41}$$

where W_i is ± 1. All states related to each other by a GT represent the same physical state. The total number of gauge transformations is 2^{N_s}, where N_s is the number of sites. There are two GT's under which u_{ij}'s are invariant—$W_i = +1,\ \forall i$ and $W_i = -1,\ \forall i$. Therefore number of states representing one physical state is 2^{N_s-1}. And the total number of physical states, D_{phys}, is given by

$$D_{phys} = 2^{(N_b - N_s + 1)}. \tag{8.42}$$

Any loop operator is gauge invariant and also takes values ± 1; therefore the number of independent loop operators is,

$$N_l = N_b - N_s + 1. \tag{8.43}$$

Counting of independent loop operators for 3D Kitaev model

Let us repeat the above calculation for 3D Kitaev model. Let N be the number of unit cells. Then $N_s = 4N$ and $N_b = 6N$. Using Eq. (8.43), number of independent loops,

$$N_l = 6N - 4N + 1 = 2N + 1. \tag{8.44}$$

Now we calculate the number of independent loops by finding total number of loops which exist and then subtracting from them total number of constraints among them. If there are N_t number of loops and N_c number of constraints among them, then the number of independent loops, 'N_i', is given by,

$$N_i = N_t - N_c \tag{8.45}$$

Let us consider a lattice with N_x, N_y and N_z number of unit cell in x, y and z directions respectively. We know that each unit cell has four sites, then total number of sites is $4N_xN_yN_z$. From the Fig. (8.6), we find that each pair of unit cells constitute a loop of a particular type. Then we have total number of a particular type of elementary loops as $N_xN_yN_z$. As there are four different type of elementary loops, we have in total $4N_xN_yN_z$ number of local loops. Moreover we have three topologically nontrivial global loops which wind around the three directions. Thus the total number of loops which is given by,

$$N_t = 4N_xN_yN_z + 3 \tag{8.46}$$

Now, let us find the total number of constraints. We have already seen in Fig. (8.4) that every four different type of loops which constitute an elementary object 'A' gives a local constraint. Again each elementary loop is part of two different elementary object 'A'. Thus total number of independent 'A' objects is $4N_xN_yN_z/2 = 2N_xN_yN_z$. But all of these local constraints is not independent. Due to the periodic boundary condition, we have one global constraint among these local constraints, thus the total number of independent local constraints is $2N_xN_yN_z - 1$. Apart from these local constraint we have other global constraints as well. A particular type of loop in a given plane gives rise to a constraint. We call them planar constraints. There are

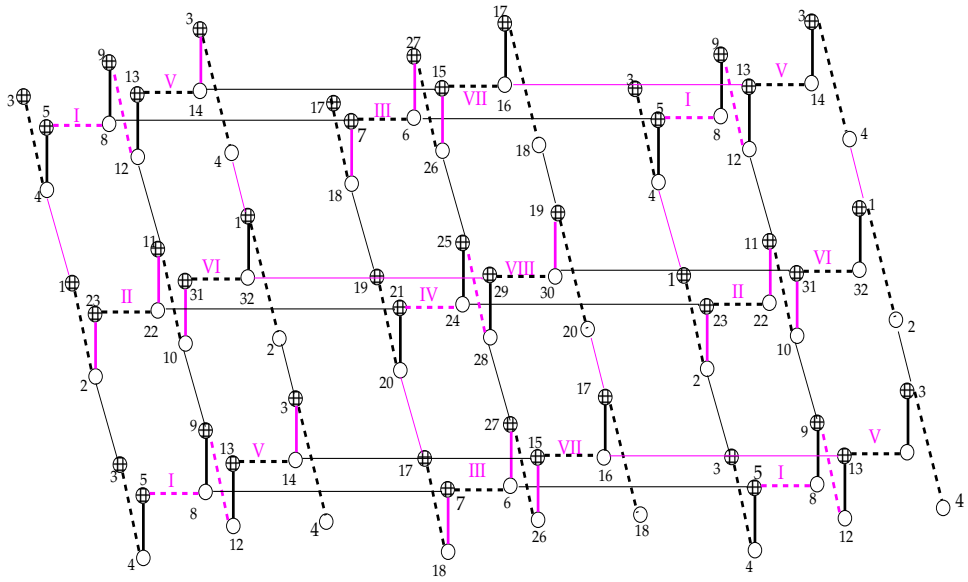

Figure 8.6: Jordan Wigner Path for 3d Kitaev lattice with periodic boundary condition. We have taken a system with $2 \times 2 \times 2$ unite cell. Numerical number gives the sequences of Jordan Wigner path. The pink links constitute the normal bonds and black links are tangential path.

'3' such planer constraints corresponding to three different orthogonal plane that exists in three dimensions. Thus total number of constraints N_c is,

$$N_c = 2N_xN_yN_z - 1 + 3 = 2N_xN_yN_z + 2 \tag{8.47}$$

Then from equation (8.45), we get the total number of independent loop as,

$$N_i = 4N_xN_yN_z + 3 - (2N_xN_yN_z + 2) = 2N_xN_yN_z + 1 \tag{8.48}$$

Having presented in detail the complete account of the independent conserved quantities we now show that this result can be easily reached if we consider Jordan-Wigner fermionisations. In chapter 3, we have outlined a general procedure for Jordan-Wigner Transformations(JWT) which can be used in any Kitaev type of model defined on a lattice with co-ordination number three. In the Fig. (8.6), we have shown a J-W path for the 3D lattice. We know that to define JWT on such lattice we need to define normal bonds such that it contains all sites without sharing sites among themselves. For a lattice with N site, we must have N/2 Normal bonds. Then according

to the construction given in section (3.2.4), there will be a conserved quantities on each such normal bonds. So we have N/2 such conserved quantities. Apart from that we will be having one more conserved quantity analogous to Eq. (3.18) which fixes the total number of fermions. Thus we must have, (N/2+1= $2N_xN_yN_z$+1), number of conserved quantity. This is fully consistent with equations (8.44) and (8.48). In the next chapter we briefly discuss toric code limit of this 3D Kitaev model which corresponds to the limit $J_z >> J_x, J_y$.

And write my old adventures with the pen
Which on the first day drew,
Upon the tablets blue,
T h e dancing Pleiades and eternal men.
Bacchus-Ralph Waldo Emerson

Chapter 9

Toric code limit of 3D Kitaev model

In this chapter, we study the limit, $J_z >> J_x, J_y$, for the 3D Kitaev model discussed previous chapter. We derive the effective Hamiltonian at lowest nontrivial order and present a short account of the various properties of the elementary excitations of the effective Hamiltonian. We show that the effective Hamiltonian is very similar to that of 2D toric code Hamiltonian [32]. Following 2D Kitaev model [33] , we start from a Hamiltonian, $H = H_0 + V$, where H_0 and V are given by,

$$H_0 = -J_z \sum_{z-\text{link}} \sigma_j^z \sigma_k^z, \qquad V = -J_x \sum_{x-\text{link}} \sigma_j^x \sigma_k^x - J_y \sum_{y-\text{link}} \sigma_j^y \sigma_k^y \tag{9.1}$$

Like 2D Kitaev model it is clear that in the limit, $J_z \gg J_x, J_z$, the low energy subspace of H is governed by the state $|\uparrow\uparrow\rangle$ or $|\downarrow\downarrow\rangle$ at every z-bond. Here the state $|\uparrow\uparrow\rangle$ ($|\downarrow\downarrow\rangle$) represents a state where the two spins on a z-bond aligned in the positive (negative) z-direction. We denote these subspace by Υ. To find out whether the Hamiltonian, H, admits any " effective Hamiltonian " within ground state subspace we work out the perturbation theory. The "effective Hamiltonian" can be derived by examining the self-energy, $\sum(E)$. The self-energy can be computed by the standard green function formalism. Let, $G_0'(E) = \left((E - H_0)^{-1}\right)'$ be the unperturbed Green function for the excited states of H_0. The 'prime' sign indicates that the operator $\left((E - H_0)^{-1}\right)'$ acts on excited states in the natural way but vanishes on ground states. Then

$$\sum(E) = \Upsilon^\dagger (V + VG_0'V + VG_0'VG_0'V + VG_0'VG_0'VG_0'V + ...)\Upsilon. \tag{9.2}$$

Here Υ is a map which maps the effective Hilbert space onto ground state subspace of H_0. Setting $E = E_0$ and computing, $H_{\text{eff}} = E_0 + \sum$, at different orders we get the following, (in appendix E, we give a detailed derivation of the effective Hamiltonian),

- $H^1_{eff} = \Upsilon^\dagger V \Upsilon = 0$
- $H^2_{eff} = \Upsilon^\dagger V G'_0 V \Upsilon = \text{constant}$
- $H^3_{eff} = \Upsilon^\dagger V G'_0 V G'_0 V \Upsilon = 0$
- $H^4_{eff} = \Upsilon^\dagger V G'_0 V G'_0 V G'_0 V \Upsilon = \text{constant}$
- $H^5_{eff} = \Upsilon^\dagger V G'_0 V G'_0 V G'_0 V G'_0 V \Upsilon = 0$
- $H^6_{eff} = \Upsilon^\dagger V G'_0 V G'_0 V G'_0 V G'_0 V G'_0 V \Upsilon$
  $= \text{constant} - \sum \frac{a J_x^4 J_y^2}{J_z^5} B_1 - \sum \frac{a J_y^4 J_x^2}{J_z^5} B_2$

Here B_1 and B_2 are operators associated with two different kind of plaquettes in the 3D lattice. They differ in the distribution of x and y bonds along the respective plaquettes. In the Fig. (9.1) B and C, we have drawn these two kinds of plaquettes. In operator form we have following expressions for B_1 and B_2,

$$B_1 = \tau_i^x \tau_j^z \tau_k^y \tau_l^x \tau_m^z \tau_n^y \tag{9.3}$$
$$B_2 = \tau_i^y \tau_j^z \tau_k^x \tau_l^y \tau_m^z \tau_n^x \tag{9.4}$$

In the above equations subscripts refer to indices for 'z-bonds'(refer to Fig. (9.1 B and C)) and superscripts denotes the components of effective spin operators (τ) defined on each z-bonds. The numerical number, $a = 0.02734$, is obtained by summing the contributions from $6! = 720$ terms that appear in calculating H^6_{eff}. It is at the sixth order, we get first nontrivial contribution to the effective Hamiltonian. As the higher order terms are less significant we confine our analysis to H^6_{eff}. Omitting all the constant term in the effective Hamiltonian we write the Hamiltonian in the $J_z \gg J_x, J_y$ limit as,

$$H = -J_{e1} \sum_p B_{1,p} - J_{e1} \sum_q B_{2,q} \quad J_{e1} = \frac{a J_x^4 J_y^2}{J_z^5} \quad , \quad J_{e2} = \frac{a J_y^4 J_x^2}{J_z^5} \tag{9.5}$$

where the sum over 'p' and 'q' refers the sum over two different type of plaquettes described before.

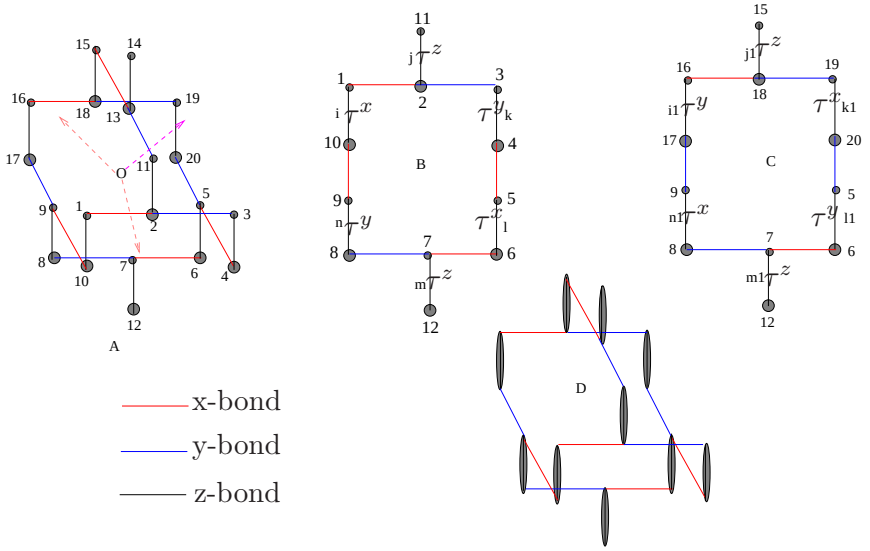

Figure 9.1: In figure A we have shown an elementary objects containing two kind of elementary plaquettes which has been redrawn separately in fig B and C. These two different kind of plaquette differ in the distribution of x and y bonds along respective plaquettes.

The easy way to remember the effective plaquette operators present in the effective Hamiltonian is the following. For a given plaquette the contribution from a z-dimer in the expression of effective loop operator depends on the bonds just behind it and after it. If these two bonds are identical then the z-dimer contributes a τ_x to the effective plaquette operator otherwise it contributes a τ_y operator. This can be understood easily from effective spin representation in the subspace Υ. Let us consider the dimer 'k' in Fig. (9.1) B which contains two sites 3 and 4. The effective spin representations (τ's) in the subspace $|\uparrow\uparrow\rangle$ or $|\downarrow\downarrow\rangle$ are given by,

$$\begin{aligned} \sigma_3^x \otimes \sigma_4^x &= \tau_k^x, \quad \sigma_3^y \otimes \sigma_4^y = -\tau_k^x, \quad \sigma_3^x \otimes \sigma_4^y = \sigma_3^y \otimes \sigma_4^x = \tau_k^y \\ \sigma_3^z &= \sigma_4^z = \tau_k^z, \quad \sigma_3^z \otimes \sigma_4^z = I \end{aligned} \tag{9.6}$$

Now using the above representations we show that the effective plaquette operators which appear in H_{eff} are nothing but the old plaquette conserved quantities expressed in the low energy subspace. Let us look at the Fig. (9.1), B. The conserved quantity associated with this elementary plaquette

is given by(written in terms of original spin variables σs),

$$B = \sigma_1^y \sigma_2^z \sigma_3^x \sigma_4^y \sigma_5^y \sigma_6^y \sigma_7^z \sigma_8^x \sigma_9^y \sigma_{10}^y \tag{9.7}$$

Now using the relations given in equation (9.6) for each dimer associated with the plaquette B in figure (9.1) we get,

$$B = \tau_i^x \tau_j^z \tau_k^y \tau_l^x \tau_m^z \tau_n^y \tag{9.8}$$

In the same way it can be shown that all the effective plaquette operators which appear in the effective Hamiltonian are respective plaquette conserved quantities. The ground state for this H_{eff} is characterised by the state $|G\rangle$ for which $B_{1,p}|G\rangle = |G\rangle$ and $B_{2,q}|G\rangle = |G\rangle$ for all 'p' and 'q'. This fact is consistent with the numerical results that for arbitrary J_x, J_y, J_z uniform flux configuration 1 corresponds to ground state sector of the Majorana fermion hopping Hamiltonian in the presence of background Z_2 gauge fields. Excitations can be created by creating the state $|\psi\rangle$ such that for some plaquette 'p', $B_{1,p}|\psi\rangle = -|\psi\rangle$. However due to the presence of local constraints, a single flux excitation is not possible. The minimum number of fluxes which can be excited is 8. We already discussed that in the pyrocholore lattice representation plaquettes are replaced by a site. Thus 8 flux configuration forms a loop of 8 sites in the pyrocholore lattice representation. This 8-flux excitations can be created by applying τ_i^z on the ground state. It turns that 6 flux excitation(due to the constraint given by Eq. (8.40)) which is the minimum for loop excitation we mentioned in the previous chapter, is forbidden here. We recall that in the 3D Kitaev model if we apply σ_i^x on the ground state (which is flux free state) it creates a 6 flux excitation. But σ_i^x has vanishing matrix element in the ground state subspace i.e,

$$\Upsilon' \sigma_i^x \Upsilon = 0 \tag{9.9}$$

where Υ' and Υ are two eigenvectors of the H_0 in Eq. (9.1). For this reason creation of isolated single six flux excitation is forbidden. We have not found any local or non local operator which creates a single 6-flux excitation. However six flux excitations can be created in pair. In the next section we discuss in detail the correspondence between the original lattice (in which 3D Kitaev model has been defined) to the pyrocholore lattice in order to explain the excitations systematically.

9.1 Loop Excitations

We have seen that 3D lattice on which the 3d Kitaev model is defined is topologically equivalent to pyrochlore lattice. Each basic object(I) which is

formed by 4 types of basic loop(F) touching each other, is equivalents to a tetrahedron(T) in the pyrochlore lattice. A smallest closed basic loop(F) in the 3D lattice is replaced by a site in the pyrochlore lattice. In the limit $J_z >> J_x, J_y$, the effective lattice is formed by the location of z-bonds only, nonetheless the pyrochlore structure of the basic objects(I) remains unchanged because effective Hamiltonian contains terms defined on each plaquettes which are the sites of the pyrochlore lattice. We also observe that a z-bond has a 4 nearest-neighbour z-bonds and it shared 10 basic objects(I) and 12 basic loops(F). Though the elementary plaquettes of the original lattice is replaced with sites in the pyrochlore lattice, we need to identify the corresponding τ operators associated with the z-bonds of the original lattice in the pyrochlore lattice. In the pyrochlore lattice we identify such an object which has the above characteristics of the z-bonds in the original 3D lattice . We refer this object as U' and it represent z-bonds of the original 3D lattice. This basic object U' is assigned with an index 'i'. In the Fig. (9.1), we have represented such a basic objects in fig (1a) and (1b). The pyrochlore lattice can be built with this objects too. We see that each of this objects contains four six-site close loop and each two six-site close loop gives a 8-site closed loop. Thus we have three 8-site loops in together. Any two 8-site close loop yield the remaining 8-site loop. For this reason we anticipate that this object U' can be associated with the z-link. Three τ operator for this z-bond will create three 8-sight loops which can be associated with the $\tau_\alpha, \alpha = 1, 2, 3$. There is a unique point in such 'U's which can be used to label these basic objects(hence it will correspond to z-bonds of the original 3D Kitaev model). In figure 9.1, point 'p' and 'q' denote such points. The point p' is the intersection point of the line joining K,L and M,N.

Next question is how to represent and label the loops. We assign two indices to every closed 6-site loop. We see that pyrochlore lattice can also be described by four different 2D kagome lattice intersecting each other. We will call this parallel plane as $0, x, y, z$ planes. Referring to the Fig. (9.1) 1b, the plane formed by the points (9,10,4,5,11,12) lie on the z-kogome plane. The plane formed by (11,12,8,7,1,13) is on the 0-kagome plane. The sites (1,2,3,4,5,6) are on the y-kagome plane. And the sites (7,8,9,10,3,2) are on the x-kagome plane. The first index given to a 6-site loop corresponds to the plane it resides. Secondly a six-site loop is shared by two basic object U for example 'p' and 'q' which can be assigned to a 6-loop. Thus we can represent a 6-site loop by $\mathcal{L}^6_{p,\alpha}$ or $\mathcal{L}^6_{q,\alpha}$. Where α is a kagome plane shared by the basic object 'p' and 'q'. It is understood that $\mathcal{L}^6_{p,\alpha} \equiv \mathcal{L}^6_{q,\alpha}$.

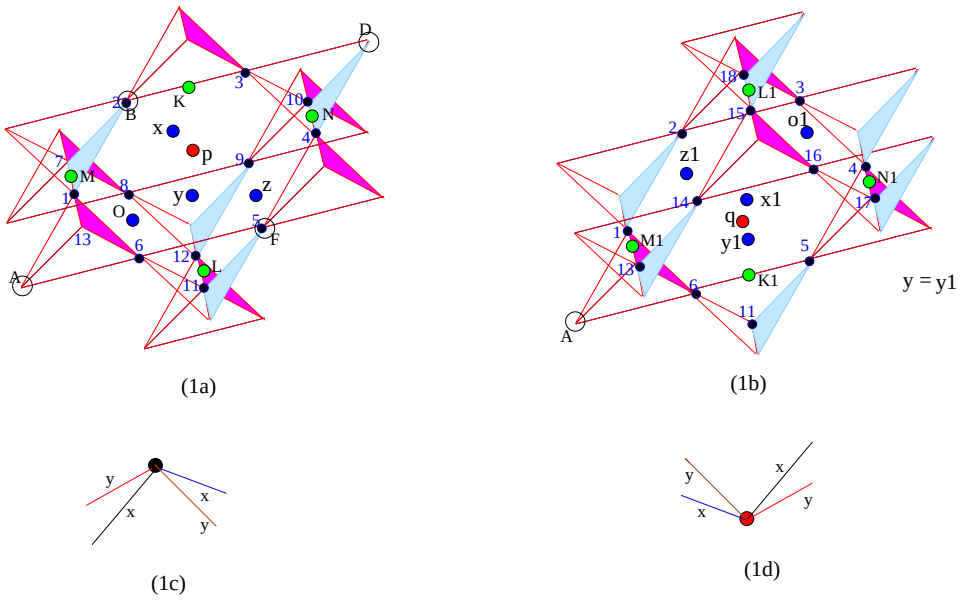

Figure 9.2: The objects (1a) and (1b) are equivalent to z-bonds of the original lattice. We represent these objects by the point 'p' and 'q' respectively. The straight line joining blue point and p' (and q') connects p' with its nearest neighbour. This has been shown schematically in (1c) and (1d). A object like (1c) (or 1a) is surrounded by four (1d) (or 1b). By this way we can construct the effective lattice formed by these objects.

We know that the ground state of the effective model at large J_z have no loop excitations (which corresponds to the site of the pyrochlore lattice). For excited states, some of the loops are excited. We also discussed that it is forbidden to create a single six-site loop $\mathcal{L}^6$. However they can be created in pairs. The smallest single closed loop we can create is a 8-site loop. If we apply τ_p^z on the ground state $|\mathcal{G}\rangle$, it corresponds to a state with 8-site closed loop excitations $\mathcal{L}^8$ in the pyrochlore lattice. Any 8-site closed loop can be made out of two overlapping six-site closed loops with two sites common in between them. These two 6-site loops must belong to same unit cell U'. For this reason we denote $\mathcal{L}^8$ as a product of two $\mathcal{L}^6$ belonging to same unite cell. Thus referring to the unite cell 'p' we denote the action of τ_p^α on the ground state as follows,

$$\mathcal{L}^8_{p,\alpha} = \mathcal{L}^6_{p,\alpha} \otimes \mathcal{L}^6_{p,0}, \qquad \alpha \;=\; x, y, z \tag{9.10}$$

We notice that though a single closed $\mathcal{L}^6$ is shared by two unit cell and a $\mathcal{L}^8$ is shared by one unit cell only. Thus there is no ambiguity in representing the $\mathcal{L}^8$ in the above way. We wish to determine the statistics of loop excitations $\mathcal{L}^8$ and $\mathcal{L}^6$. First we derive the statistics between two $\mathcal{L}^6$.

9.2 Statistics of the elementary excitations

Now we proceed to derive the statistics of the loop excitations. Effective Hamiltonian has no dynamics in its own, in the sense that it contains conserved operators commuting with each other. To generate a dynamics we can add a simple Zeeman perturbation to it. Thus we study,

$$H \;=\; H_0 - \sum_{\alpha=x,y,z} B_\alpha \sum_i \tau_{i,\alpha} \tag{9.11}$$

Here H_0 is the original effective Hamiltonian and second term describes the Zeeman interactions. Now the Zeeman part of the Hamiltonian anti-commute with the loop operators of H_0, thus bringing a dynamics among them. The basic excitations which satisfy all the constraints are $\mathcal{L}^8$ and two separated $\mathcal{L}^6$. If we restrict ourselves to the low energy excitations comprising $\mathcal{L}^8$ and a pair of $\mathcal{L}^6$, the effective Hamiltonian can be described by hopping operators represented by the 2nd term of the Eq. (9.11), where the coefficient B_α represents the hopping energy and $\sigma_{i,\alpha}$ causes the loop excitations to hop. Two separated $\mathcal{L}^6$ excitations are created by successive

application of suitable nearest $\mathcal{L}^8$ excitations. Below we write down the hopping rules for $\mathcal{L}^6$ excitations.

$$\mathcal{L}^6_{p,0} \rightarrow \mathcal{L}^6_{p,\alpha} \sim \tau^\alpha_q, \quad \alpha = x,y,z \tag{9.12}$$
$$\mathcal{L}^6_{p,\alpha} \rightarrow \mathcal{L}^6_{p,0} \sim \tau^\alpha_q, \quad \alpha = x,y,z \tag{9.13}$$
$$\mathcal{L}^6_{p,\alpha} \rightarrow \mathcal{L}^6_{p,\beta} \sim \tau^\beta_q \tau^\alpha_q, \quad \alpha\ ,\beta = x,y,z\ ,\alpha \neq \beta \tag{9.14}$$

The above rules for intra-cell hopping are consistent with each other and can be derived from each other. Moreover this definition also removes the possibility of any residual gauge field/source bringing any unphysical phases associated with the hopping of loops.

Now we derive the statistics of two well separated $\mathcal{L}^6$ using the above hopping rules. In Fig. (9.2), we represented a cartoon picture of four unit cells labelled by i,j,k and l. The well separated loops are $\mathcal{L}^6_{0,i}$ and $\mathcal{L}^6_{y,k}$. We take the following steps for interchanging them [74, 75]. First we move $\mathcal{L}^6_{y,k}$ to some other location. Next we bring $\mathcal{L}^6_{0,i}$ to the original position of $\mathcal{L}^6_{y,k}$. Finally we bring $\mathcal{L}^6_{y,k}$ to the original position of $\mathcal{L}^6_{0,i}$. For the step one we take $\mathcal{L}^6_{y,k}$ to $\mathcal{L}^6_{0,l}$ via the path $y_k \rightarrow 0_k \rightarrow z_l \rightarrow 0_l$. Here 0_i denotes the '0'th six-site loop of the cell unit 'i'. The second step is achieved via the path $0_i \rightarrow 0_j \rightarrow y_k$. The final step is achieved via the path $0_l \rightarrow z_l \rightarrow 0_j \rightarrow x_j \rightarrow 0_i$. The operators which are required for these three steps are given by ,

$$T_1 = \tau^y_l \tau^z_l \tau^z_j \tau^y_j \tau^y_k \tau^z_k \tag{9.15}$$
$$T_2 = \tau^z_k \tau^y_k \tau^y_j \tau^x_j \tau^x_i \tag{9.16}$$
$$T_3 = \tau^x_i \tau^x_j \tau^y_j \tau^y_j \tau^z_j \tau^z_l \tau^y_l \tag{9.17}$$

We find that $T_3 T_2 T_1 = -1$, which proves that mutual statistics between loops excitations $\mathcal{L}^6_{0,i}$ and $\mathcal{L}^6_{y,k}$ are fermionic. Using the same procedure one can easily prove that all $\mathcal{L}^6$ are fermions. Similarly we find mutual statistics between any two $\mathcal{L}^8$ excitations are Bosonic. This is no surprise as a $\mathcal{L}^8$ is comprised of two $\mathcal{L}^6$. Besides these two basic excitations, there are more complex and extended loop operators which can be constructed out of these basic excitations.

9.3 Overview of the basic excitations of 3D Kitaev model

To summarise, we have shown that the 3D Kitaev model has 2 different kind of low energy excitations. Firstly, fermionic excitations for a given

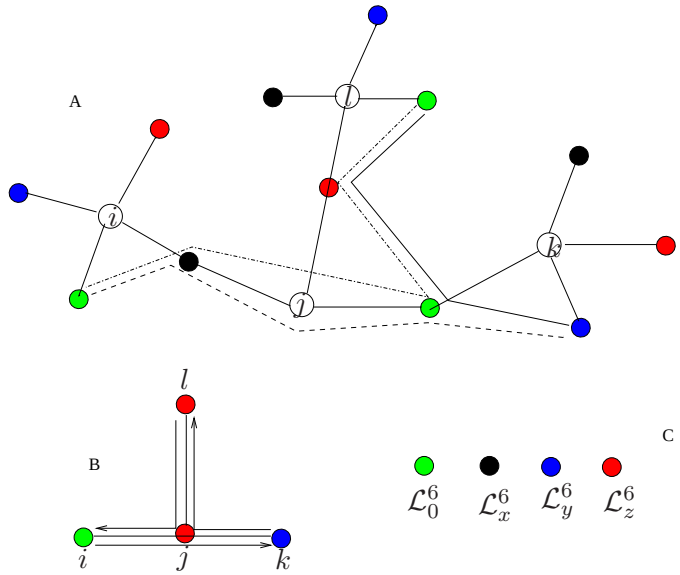

Figure 9.3: See text for detail explanation. In this cartoon picture we have represented the exchange of two $\mathcal{L}^6$ which are represented by green circle at site 'j' and blue circle at site 'k'. We have taken the exchange path such that it does not encircle any closed area. This forbids the inclusion of any gauge field in the determination of the statistics. In the B we have schematically represented then exchange procedure. A six site loop $\mathcal{L}^6$ is represented by a coloured circle, four different colour represent four different type of $\mathcal{L}^6$, as shown in C. In fig B we have given a simplified description of exchange processes of fig A.

background distribution of conserved operators W_l. Secondly, we have loop excitations where the eigenvalues of some 'W_l' is -1. The ground state corresponds to vortex free sector(meaning eigenvalue for all W_l is 1). Fermionic spectrum can be gapless and gapped depending on the parameters used in the model. In gapless phase the low energy excitations are fermionic excitations over this vortex free configuration, as discussed in previous chapter. In the gapped phase the low energy excitations are the loop excitations where the eigenvalues of some 'W_l' is -1. In this chapter we have studied the low energy excitations in the gapped phase in the limit $J_z >> J_x, J_y$. In pyrochlore lattice representations the description of loop excitations becomes easy and each site of the pyrochlore lattice corresponds to a given basic loop, 'W_l', of the original model. The basic loop excitations, which satisfy all the constraints, corrrespond to a pair of loop excitations of 6-sites ($\mathcal{L}^6$) and a single loop excitation of 8-sites ($\mathcal{L}^8$) in pyrochlore lattice. Mutual exchange statistics between two '$\mathcal{L}^6$' is fermionic, whether mutual statistics between two '$\mathcal{L}^8$' are bosonic. Moreover one can have membrane excitations also in the effective Hamiltonian [19, 21, 22]. However the detail properties of these exotic excitations are being carried out now and will be presented elsewhere.

They are all gone away,
T h e House is shut and still,
There is nothing more to say.
-The House on the Hill-E A Robinson

Chapter 10

Summary and Discussion

In this thesis, we have presented some theoretical investigations on 2D Kitaev model [32] and some of its generalisations. We have presented an alternative solution to 2D Kitaev model using Jordan-Wigner fermionisation(JWF) [77–80]. The application of Jordan-Wigner transformation to solve this model is significant for two reasons. Firstly, to out knowledge, it is the first two dimensional model where JWF is shown to solve the model exactly(it may be noted that JWF was successfully applied to other 2d Kitaev like model which was proposed after Kitaev's original work [32]). Secondly JWF is exact in the sense that it did not bring any unphysical states like the fermionisation procedure used in [32]. The four fold degeneracy of the ground state was explicitly derived using JWF in the thermodynamic limit.

Next, spin-spin correlation functions have been studied for the Kitaev model. Extending Kitaev's fermionisation procedure we showed that the two spin correlation function vanishes beyond nearest neighbour [76]. The correlation functions are anisotropic and bond dependent. This proves that the Kitaev model is an example of a quantum spin liquid. In our bond-fermion formalism introduced in [76], the calculation of spin-spin correlation function becomes straightforward. Existence of string type multi-spin correlations have also been shown. A spin is shown to undergo fractionalisation into two static Z_2 static π fluxes and a dynamic Majorana fermion. Our formalism to calculate the spin-spin correlation function can be easily applied to calculate spin-spin correlation functions of other Kitaev-like model.

We have discussed the toric code limit of the Kitaev model in terms of gauge invariant Jordan-Wigner fermions. We have calculated four degenerate ground states explicitly and have demonstrated the multicomponent

nature of the ground state wave functions. Further we have calculated concurrence and von-Neuman entropy for kitaev model.The exact calculation of spin-spin correlation function enables us to calculate these quantities exactly. While concurrence is zero for the Kitaev model in complete phase space, binary entropy is finite throughoout the phase space.

The stability of Kitaev model and the Z_2 gauge dynamics against a Ising perturbation has been studied within the mean field theory and it revealed that Kitaev phase is stable up to 10 percent (of J, where J is the strength of Kitaev interaction) against an Ising interaction [101]. Our analysis shows that in the presence of Ising interaction, the system undergoes a quantum phase transition from a spin liquid state to a magnetically ordered state. The nature of magnetically ordered state depends on the nature of Ising interactions. If the Ising interaction is ferromagnetic then the magnetically ordered state is a ferromagnetic state. On the othehand for intermediate antiferromagnetic Ising interaction, the magnetically orderded state is a dimer state. For stronge antiferromagnetic interaction the magnetically ordered state is Neel state.

We have introduced an exactly solvable 3D Kitaev model and solved it exactly [87]. It has all the key features of the 2D Kitaev model and an example of 3D quantum spin liquid. Like Kitaev model it has conserved operator W_l associated with every basic loops ('l') of the model. Low energy excitations of this 3D spin model have been classified. It consists of two kind of excitations. Firstly, fermionic excitations for a given background distribution of conserved operators W_l. Secondly we have loop excitations where the eigenvalues of some 'W_l' is -1. We have shown that our 3D lattice is topologically equivalent to pyrochlore lattice. In pyrochlore lattice representations the description of loop excitations becomes easy and each site of the pyrochlore lattice corresponds to a given basic loop 'W_l' of the original model. The basic loop excitations which satisfy all the local constraints corrrespond to a loop excitation of 6-sites ($\mathcal{L}^6$) and 8-sites ($\mathcal{L}^8$) in pyrochlore lattice. In the chapter 9, we have studied the large J_z limit of this 3d kitaev model. We have shown that the elementary excitations of the effective Hamiltonian at this limit are loop excitations and they are explained in pyrochlore lattice representations. Mutual statistics between two '$\mathcal{L}^6$' is fermionic, whether mutual ststistics between two '$\mathcal{L}^8$' are bosonic.

Appendix A

J-W Transformation for OBC

In this appendix we briefly outline the details of Jordan-Wigner transformation (JWT) applied to open boundary geometry for the Kitaev model. For this we first need to specify a suitable lattice geometry on which JWT can be applied.

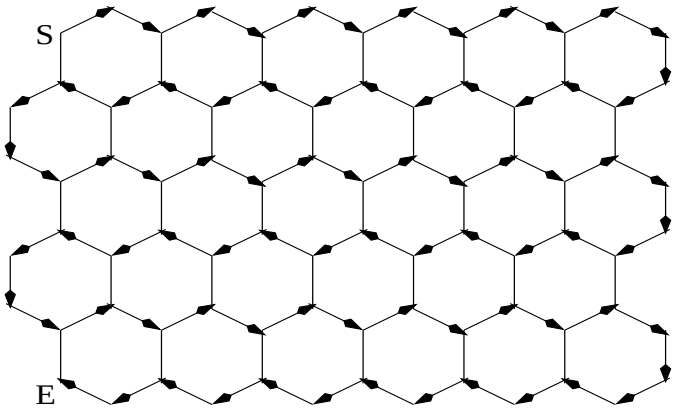

Figure A.1: Jordan-Wigner path for a lattice with open boundary condition. It starts at the site 'S' and follows the directions given arrows and ends at site 'E'.

In the above figure we have drawn a finite honeycomb lattice which is used for open boundary Kitaev model. The upper and lower boundaries are of zig-zag boundary and the sides are of arm-chair boundary. This finite lattice can be extended to an infinite one without loosing generality. We

know that the Jordan-Wigner transformation needs an one dimensional path (Hamilton path) which passes through all the sites of the lattice exactly once, i.e, the path does not cross to itself anywhere. The above geometry of the lattice enables us to find such an one dimensional path. This path starts at the site labelled by 'S' and follows the directions of arrows and ends at site 'E'. Though the above path is shown for a finite lattice, it can be extended easily for an infinite lattice. Now we explain how this particular lattice geometry helps us to find a appropriate fermionic Hamiltonian to be solved easily. Since the vertical bonds contain only $J_z\sigma_j^z\sigma_k^z$ interaction, we can choose such one dimensional Jordan-Wigner path that is made-up of only x and y bonds (except at the edges) and cover the 2D lattice. We need to adhere this kind of boundary to define the Jordan-Wigner transformations. Further the vertical bonds that connect neighbouring zig-zag chains do not transfer Jordan-Wigner fermions from a chain to its neighbouring chain, this is due to the fact that all the vertical bonds are having z-z interactions and in Jordan-Wigner transformations the expression for z-component of spin is local. Thus we end up with fermions hopping along the 1-D chain that covers the 2-D lattice. However there is a "density-density" interaction along the vertical bonds that makes the problem 2-dimensional. Now we give the details of fermionisations in JWT.

We define the fermionization by the following way,

$$\begin{aligned} \sigma_i^{a,x} &= (c_i^a + c_i^{a\dagger})\mu_i^a \\ \sigma_i^{a,y} &= i(c_i^a - c_i^{a\dagger})\mu_i^a \\ \sigma^{a,z} &= (2c_i^{a\dagger}c_i^a - 1) \end{aligned} \tag{A.1}$$

In the above equation 'a' represents sub-lattice index. 'μ' is the Jordan Wigner tail which is given by,

$$T_i = \Pi_{\text{forall}j<i}\sigma_j^z \tag{A.2}$$

Here 'i' stands for all the sites which resides behind the site 'j' in the sequence of Jordan-Wigner path as shown in the figure A.1. It is easy to note that in defining the above transformations we did not enlarge the original fock space dimension of the spin problem. The dimension of the spin space and the fermionic space is identical. Now plugging the transformations given by equation (A.1) in the Kitaev Hamiltonian, we get the fermionised Hamiltonian as,

$$\begin{aligned} H &= \sum_{m,n} -J_x(c^{a\dagger}_{m,n} - c^a_{m,n})(c^{b\dagger}_{m+1,n+1} + c^b_{m+1,n+1}) \\ &- J_y(c^{a\dagger}_{m,n} - c^a_{m,n})(c^{b\dagger}_{m,n+1} + c^b_{m,n+1}) \\ &+ J_z(2c^{a\dagger}_{m,n}c^a_{m,n} - 1)(2c^{b\dagger}_{m,n}c^b_{m,n} - 1) \end{aligned} \tag{A.3}$$

Before diagonalising the above Hamiltonian we introduce two complex fermions, χ and ψ, on all z-bonds and define the following transformations,

$$c^a_{m,n} = \frac{1}{2}\{(\chi_{m,n} + \chi^\dagger_{m,n}) - i(\psi_{m,n} + \psi^\dagger_{m,n})\} \tag{A.4}$$

$$c^b_{m,n} = \frac{1}{2}\{(\chi^\dagger_{m,n} - \chi_{m,n}) - i(\psi_{m,n} - \psi^\dagger_{m,n})\}. \tag{A.5}$$

The inverse transformation is given by,

$$\chi_{m,n} = \frac{1}{2}\{(c^a_{m,n} + c^{a\dagger}_{m,n}) - (c^b_{m,n} - c^{b\dagger}_{m,n})\} \tag{A.6}$$

$$\psi_{m,n} = \frac{i}{2}\{(c^a_{m,n} - c^{a\dagger}_{m,n}) + (c^b_{m,n} + c^{b\dagger}_{m,n})\} \tag{A.7}$$

Then the Hamiltonian given by equation (A.3) reduces to,

$$\begin{aligned} H = \sum_{(m,n)} &-J_x(\psi_{m,n} + \psi^\dagger_{m,n})(\psi_{m+1,n+1} - \psi^\dagger_{m+1,n+1}) \\ &-J_y(\psi_{m,n} + \psi^\dagger_{m,n})(\psi_{m,n+1} - \psi^\dagger_{m,n+1}) + \\ &J_z(2\psi^\dagger_{m,n}\psi_{m,n} - 1)(2\chi^\dagger_{m,n}\chi_{m,n} - 1) \end{aligned} \tag{A.8}$$

Looking at the above equation, it can be readily verified that $\chi^\dagger_i\chi_i$ on any z-bond commutes with the Hamiltonian. Thus it is a conserved operator. Moreover $\chi^\dagger_i\chi_i$ defined on each z-bond mutually commutes. For a given occupancy of χ fermion, Hamiltonian reduces to a bilinear one in ψ fermions. However the ground state sector corresponds $\chi^\dagger\chi = 0$ for every site for the following reason. The plaquette conserved quantity B_p's are made out of $\chi^\dagger\chi$. Let us call, $\rho = (2\chi^\dagger\chi - 1)$. Then for all plaquettes, $B_p = \rho_i\rho j$ where the label 'i' and 'j' denote the label of two z-bond associated with a plaquette. Now we know that ground state sector belongs to $B_p = 1$ which can be obtained by taking all ρ to be ± 1. For the choice $\rho = 1$, Hamiltonian becomes,

$$\begin{aligned} H = \sum_{(m,n)} &-J_x(\psi_{m,n} + \psi^\dagger_{m,n})(\psi_{m+1,n+1} - \psi^\dagger_{m+1,n+1}) \\ -J_y(\psi_{m,n} + \psi^\dagger_{m,n})(\psi_{m,n+1} - \psi^\dagger_{m,n+1}) &- J_z(2\psi^\dagger_{m,n}\psi_{m,n} - 1). \end{aligned} \tag{A.9}$$

Now let us look back to the Chapter 1, Eq. (2.18). The Eq. (2.18) can be brought to the form of Eq. (A.9) easily with the following transformations,

$$c^a_{m,n} \;=\; \psi_{m,n} + \psi^\dagger_{m,n} \;;\; c^b_{m,n} = \frac{1}{i}(\psi_{m,n} - \psi^\dagger_{m,n}) \tag{A.10}$$

Now let us define the Fourier Transformations , $\psi_i = \frac{1}{\sqrt{MN}} \sum_k e^{i\vec{k}.\vec{r}} \psi_k$, then equation (A.9) becomes,

$$H = \sum (\epsilon_k \psi^\dagger_k \psi_k + i\frac{\delta_k}{2}\psi^\dagger_k \psi^\dagger_{-k} - i\frac{\delta_k}{2}\psi_{-k}\psi_k) \tag{A.11}$$

Where $\epsilon_k = 2(J_x \cos k_1 + J_y \cos k_2 + J_z)$ and $\delta_k = 2(J_x \sin k_1 + J_y \sin k_2)$. Where k_1 and k_2 has been defined before. Following Bogoliubov transformation diagonalizes this Hamiltonian,

$$\psi_k = \cos\frac{\theta_k}{2}\alpha_k + i \sin\frac{\theta_k}{2}\alpha^\dagger_{-k} \tag{A.12}$$

where $\cos\theta_k = \epsilon_k/\sqrt{(\epsilon^2_k + \delta^2_k)}$ with $\theta_k = -\theta_{-k}$ and the diagonalised Hamiltonian reads as,

$$H = E_k \alpha^\dagger_k \alpha_k + E_0 \tag{A.13}$$

E_0 is the ground state energy and is given by,

$$E_0 = \sum_k \frac{1}{2}(\epsilon_k - \sqrt{\epsilon^2_k + \delta^2_k} - N_z J_z) \tag{A.14}$$

.

$N_z = MN$ is the number of z-bond. E_k is given by ,

$$E_k = \sqrt{\epsilon^2_k + \delta^2_k} \tag{A.15}$$

The inverse Bogoliubov transformation is given by,

$$\alpha_k = \frac{1}{\cos\theta_k}(\cos\frac{\theta_k}{2}\psi_k - i\sin\frac{\theta_k}{2}\psi^\dagger_{-k}) \tag{A.16}$$

This completes our short discussions of JWT for open boundary conditions.

Appendix B

The gauge fixing algorithm and J-W gauge

In this appendix we show a correspondence between the fermionised Hamiltonian obtained in chapter 2 and the fermionised Hamiltonian obtained in chapter 3. In chapter 3 we explained that JWT can be thought of as a gauge fixing procedure and showed it for a particular Jordan-Wigner path called Hamiltonian Path. Here we show how one can obtain this gauge fixed Hamiltonian starting from fermionised Hamiltonian obtain in chapter 2. We also present details of derivation of fermionic Hamiltonian in Jordan-Wigner gauge.

Let us recall the fermionic Hamiltonian (2.14), which is given by,

$$H = \sum_{x-\text{link}} J_x u^x_{i,j} i c^a_i c^b_j + \sum_{y-\text{link}} J_y u^y_{i,j} i c^a_i c^b_j + \sum_{z-\text{link}} J_z u^z_{i,j} i c^a_i c^b_j \quad \text{(B.1)}$$

Here c_i's are Majorana fermions and $u^\alpha_{i,j}$ are Z_2 conserved gauge fields which can take values ± 1. These Z_2 gauge fields appear on every links. In the contrary we have seen in chapter 3 that Jordan-Wigner transformation yields a fermionic Hamiltonian where Z_2 gauge fields appear only on the normal bonds fixed by the Hamiltonian path. Now we will show that these two are completely equivalent by reducing Eq. (B.1) to the same form as in J-W gauge after suitable gauge transformations.

From the Fig. (B.1), we write for the Hamiltonian for all the bonds that appear in the figure,

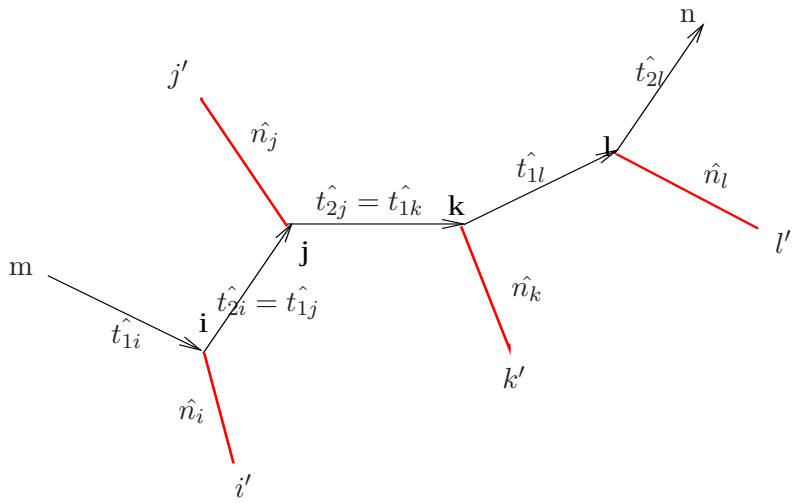

Figure B.1: A part of the Jordan-Wigner path. Black arrows follow the Jordan-Wigner path and they constitute the tangent bonds. The red links constitute the normal bonds.

$$\begin{aligned} H &= u_{m,n}J_{mn}ic_mc_i + u_{i,j}J_{ij}ic_ic_j + u_{j,k}J_{jk}ic_jc_k + u_{k,l}J_{kl}ic_kc_l \\ &+ u_{i,i'}J_{i,i'}ic_ic_{i'} + u_{j,j'}J_{j,j'}ic_jc_{j'} + u_{k,k'}J_{k,k'}ic_kc_{k'} + u_{l,l'}J_{l,l'}ic_lc_{l'} \end{aligned} \tag{B.2}$$

In the first line we have written the Hamiltonian for the tangential bonds and in the second line we have written the Hamiltonian for the normal bonds. Now we do the following gauge transformation.

$$c_i \rightarrow u_{m,i}c_i \tag{B.3}$$
$$c_j \rightarrow u_{i,j}u_{m,i}c_j \tag{B.4}$$
$$c_k \rightarrow u_{j,k}u_{i,j}u_{m,i}c_k \tag{B.5}$$
$$c_l \rightarrow u_{k,l}u_{j,k}u_{i,j}u_{m,i}c_l \tag{B.6}$$
$$\tag{B.7}$$

The above gauge transformations keep all the fermionic commutation relations unchanged. After inserting these transformations into Eq. (B.2),

we get the following form of the Hamiltonian,

$$\begin{aligned} H &= J_{mn} i c_m c_i + J_{ij} i c_i c_j + J_{jk} i c_j c_k + J_{kl} i c_k c_l \\ &+ u'_{i,i'} J_{i,i'} i c_i c_{i'} + u'_{j,j'} J_{j,j'} i c_j c_{j'} + u'_{k,k'} J_{k,k'} i c_k c_{k'} + u'_{l,l'} J_{l,l'} i c_l c_{l'} \end{aligned} \tag{B.8}$$

Now from the Eq. (B.8), we see that gauge fields only appear on the normal bonds. The new Z_2 gauge fields appearing only on the normal bonds are given by,

$$u'_{i,i'} = u_{i,i'} u_{m,i} \tag{B.9}$$

$$u'_{j,j'} = u_{j,j'} u_{i,j} u_{m,i}, \text{ and so on} \tag{B.10}$$

$$\tag{B.11}$$

The above method can be easily generalised for an infinite or finite lattice once we find a Hamilton path which is nothing but the Jordan-Wigner path. For a finite lattice size, if there are in total 'N' sites, we label the site of the lattice by i_n $n = 1, N$. Here the labelling of the sites are done by their position on the Hamilton path. Then the following gauge transformations reduce the Hamiltonian (Eq. (2.1)) to the same form obtained in Jordan-Wigner gauge.

$$c_{i_n} \rightarrow u_{i_1,i_2} u_{i_2,i_3} ... u_{i_r,i_{r+1}} .. u_{i_{n-1},i_n} c_n \tag{B.12}$$

B.1 Jordan-Wigner gauge

Now we give details of the Jordan-Wigner gauge mentioned in chapter 3. First we write the normal and tangent vectors for each site as defined by Eq. (3.7). We notice that for $m \neq 0$,

$$\begin{aligned} \hat{\mathbf{t}}^a_{1m,n} = \hat{y};\ \hat{\mathbf{t}}^a_{2m,n} = \hat{x};\ \hat{\mathbf{n}}^a_{1m,n} = -\hat{z} \\ \hat{\mathbf{t}}^b_{1m,n} = \hat{x};\ \hat{\mathbf{t}}^b_{2m,n} = \hat{y};\ \hat{\mathbf{n}}^a_{1m,n} = \hat{z} \end{aligned} \tag{B.13}$$

And for $m = 0$,

$$\begin{aligned} \hat{\mathbf{t}}^a_{1m,n} = \hat{z};\ \hat{\mathbf{t}}^a_{2m,n} = \hat{x};\ \hat{\mathbf{n}}^a_{1m,n} = -\hat{y} \\ \hat{\mathbf{t}}^b_{1m,n} = \hat{x};\ \hat{\mathbf{t}}^b_{2m,n} = \hat{z};\ \hat{\mathbf{n}}^b_{1m,n} = -\hat{y} \end{aligned} \tag{B.14}$$

Then starting with the $z - z$ interactions of the Hamiltonian we get, for $m = 0, n = 0$,

$$-\sigma^{az}_{0,0} \sigma^{bz}_{0,0} = -i \eta^a_{0,0} \eta^b_{0,0} \mathcal{S} \tag{B.15}$$

For $m \neq 0$

$$-\sigma^{az}_{m,n}\sigma^{bz}_{m,n} = -i\eta^{a}_{m,n}\eta^{b}_{m,n}(i\xi^{a}_{m,n}\xi^{b}_{m,n}) \tag{B.16}$$

now for $m = 0, n \neq 0$

$$-\sigma^{az}_{0,n}\sigma^{bz}_{0,n} = i\eta^{a}_{0,n}\eta^{b}_{0,n} \tag{B.17}$$

The above three equations give complete description of all the $z-z$ interactions of Kitaev model.

Now for the y-bond we get for $m = 0$

$$-\sigma^{ay}_{0,n}\sigma^{by}_{0,n+1} = -i\eta^{a}_{0,n}\eta^{b}_{0,n+1}(i\xi^{a}_{0,n}\xi^{b}_{0,n+1}) \tag{B.18}$$

For $m \neq 0$ we get

$$-\sigma^{ay}_{m,n}\sigma^{by}_{m,n+1} = i\eta^{a}_{m,n}\eta^{b}_{m,n+1} \tag{B.19}$$

Finally we writethe Hamiltonian terms for $x-x$ interactions. For $m = 0$

$$-\sigma^{ax}_{0,n}\sigma^{bx}_{1,n+1} = -i\eta^{a}_{0,n}\eta^{b}_{1,n+1} \tag{B.20}$$

And for $m \neq 0$ we get,

$$-\sigma^{ax}_{m,n}\sigma^{bx}_{m+1,n+1} = -i\eta^{a}_{m,n}\eta^{b}_{m+1,n+1} \tag{B.21}$$

Now we make the following gauge transformation which we call Jordan-Wigner gauge.

$$\eta^{r}_{m,n} \to (-1)^{m}\eta^{r}_{m,n} \tag{B.22}$$

After this, we choose for each normal bond, $U_{i,j} = -i\xi^{a}_{i}\xi^{b}_{j}$. This gives the Jordan-Wigner Hamiltonian given by Eq. (3.43) to Eq. (3.45). Then we define complex fermion, $\chi_{m,n}$, on each normal internal z-bonds in the following way,

$$\xi^{a}_{m,n} = (\chi_{m,n} + \chi^{\dagger}_{m,n})\ ;\ \xi^{b}_{m,n} = \frac{-1}{i}(\chi_{m,n} - \chi^{\dagger}_{m,n}) \tag{B.23}$$

Similarly on each normal slanted y-bond which is joined by the z-bond (m,n) and (m,n+1), we define,

$$\xi^{a}_{m,n+1} = (\chi_{\substack{m,n\\ m,n+1}} + \chi^{\dagger}{}_{\substack{m,n\\ m,n+1}})\ ;\ \xi^{b}_{m,n} = \frac{-1}{i}(\chi_{\substack{m,n\\ m,n+1}} - \chi^{\dagger}{}_{\substack{m,n\\ m,n+1}}) \tag{B.24}$$

With this we have always, $U_{i,j} = (2\chi^{\dagger}_{i,j}\chi_{i,j} - 1)$. Finally on each z-link we define ψ fermions in the following way,

$$\eta^{a}_{m,n} = (\psi_{m,n} + \psi^{\dagger}_{m,n})\ ;\ \eta^{b}_{m,n} = \frac{1}{i}(\psi_{m,n} - \psi^{\dagger}_{m,n}) \tag{B.25}$$

This gives the Eq. (3.46) to Eq. (3.50). This completes the details of Jordan-Wigner gauge used in chapter 3.

Appendix C

Notes on Spin-Spin Correlation

C.1 Corelation function in Physical Subspace

In Chapter 4, we have derived the spin-spin correlation functions for Kitaev model. However we have worked in the fermionisation procedure adopted by Kitaev [33]. We have seen that this fermionisation procedure enlarges the local Hilbert space dimension. But we argued that as the spin operators are gauge invariant, the results obtained in enlarged Hilbert space is identical with the results one should have obtained in physical Hilbert space. In this appendix, we explain this. We have seen that the operator D_i defined in equation chapter 1 at the site 'i' does following operation,

$$\begin{aligned} D_i|s_i\rangle &= |s_i\rangle, \qquad |s_i\rangle \in \text{physical subspace} \\ D_i|s_i\rangle &= -|s_i\rangle, \qquad |s_i\rangle \in \text{physical subspace.} \end{aligned} \tag{C.1}$$

Where $|s_i\rangle$ is any one of the four states defined in terms of two complex fermion at the site 'i'. The projection operator P_i can be easily defined as $P_i = (1 + D_i)/2$, then it follows that the global projection operator is,

$$P = \prod_i P_i \tag{C.2}$$

where the product runs over all the sites of the lattice. We have seen that an eigenstate of the Hamiltonian can be written as $|\mathcal{M}_\mathcal{G}\rangle \otimes |\mathcal{G}\rangle$, where $|\mathcal{G}\rangle$ represents the configuration of gauge sector which can be written as,

$$|\mathcal{G}\rangle = |\chi_x\rangle \otimes |\chi_y\rangle \otimes |\chi_z\rangle \tag{C.3}$$

The state $|\chi_\alpha\rangle$ ($\alpha = x, y, z$) gives a full description of the occupation number of χ_α fermions on every α-bonds. We have seen that for the ground state all the χ_α fermion occupation number is 1. Now we can easily write down the normalized ground state wave function belonging to the physical subspace as follows,

$$|\psi_{Phy}\rangle = 2^{M-1} \prod_i \frac{(1+D_i)}{2} |\psi_{ext}\rangle \tag{C.4}$$

Where $|\psi_{ext}\rangle = |\mathcal{M}_\mathcal{G}\rangle \otimes |\chi_x\rangle \otimes |\chi_y\rangle \otimes |\chi_z\rangle$ and M is the number of z-bonds present in the lattice (which is equal to half of the total lattice sites). We know that the projection operator P commutes with all spin operators. Let $\hat{O}$ be any operator made out of the product of the spins at different sites. We wish to evaluate,

$$\begin{aligned} \langle \hat{O} \rangle &= \langle \psi_w | \hat{O} | \psi_w \rangle \\ &= \langle \psi_{ext} | P \hat{O} P | \psi_{ext} \rangle 2^{2(M-1)} \\ &= \langle \psi_{ext} | \hat{O} P | \psi_{ext} \rangle 2^{2(M-1)} \end{aligned} \tag{C.5}$$

Let us simplify the expression $P|\psi_{ext}\rangle$. We can write P as,

$$P = \frac{1}{2^{2N}} \sum_{i \neq j} (\prod D_i + \prod D_j) \tag{C.6}$$

A careful observation tells that the each terms in the parenthesis of the above equation has identical effects on the gauge sector of the wave function $|\psi_{ext}\rangle$. The simplest example is, $(1+\prod_i D_i)$. The next pair is $(D_i + \prod_{j\neq i} D_j)$ and so on. The action of the first term is to yield $2|\psi_{ext}\rangle$. The second pair changes the $|\psi_G\rangle$ and also annihilates one χ fermion from each adjacent links of the site $R^a_{m,n}$. The other operators in the expansion of P change $|\psi_G\rangle$ in a different way and all of them have certain number of χ fermion absent on various links. But they all have at least four or more χ fermions absent in them. But in all this resultant terms, the value of B_p for each plaquette remains one. We represent $P|\psi_{ext}\rangle$ in the following way,

$$P|\psi_{ext}\rangle = |\psi_{ext}\rangle + \sum_{[i,j,k]} N_{ijk} |\mathcal{M}_\mathcal{G}\rangle_{ijk} \otimes |\chi_{x,i}\rangle \otimes |\chi_{y,j}\rangle \otimes |\chi_{z,k}\rangle \tag{C.7}$$

Here '$[i, j, k]$' denotes a definite number of χ fermion occupation number. Now whenever we would be calculating spin-spin correlations with respect to any $|\psi_{ext}\rangle$, it must preserve the fermion occupation number $[i, j, k]$. Otherwise there will be no non-zero overlap with the original state and hence all

the spin-spin correlation function would be zero. From this consideration it is completely clear that only non-zero correlations are those which preserve the flux configurations because fermion occupation number determines the flux configurations. Again from Eq. (C.7) it is clear from the orthogonality of different gauge copies created by the operation of projection operator that $\langle\psi_{ext}|\hat{O}\hat{P}|\psi_{ext}\rangle$ is same as $\langle\psi_{ext}|\hat{O}|\psi_{ext}\rangle$.

C.2 Exact solvability of the Kitaev model

Now we can easily comment on the exact solvability of Kitaev model. If we take the operator $\hat{0}$ to be 'H', the Hamiltonian for Kitaev model then the expression, $\langle\psi_{ext}|HP|\psi_{ext}\rangle 2^{2(M-1)}$ measures whether there is a non-zeo projection of the ground state obtained in the extended Hilbert space to the physical subspace. And from the discussions made in this appendix we observe that there really exists a nonzero projection.

Appendix D

Spectrum Analysis for 3D KM

In this appendix we present some detail analysis of the spectrum obtained for 3D Kitaev Model.

D.1 Spectrum Analysis

We have seen that the spectrum for 3D Kitaev Model is given by,

$$E = \frac{\pm 1}{2\sqrt{2}} \left(\Delta_k \pm \Delta_{3k}\right)^{\frac{1}{2}} \tag{D.1}$$

where various parameters are given by

$$\begin{aligned}
\delta_{1k} &= (J_x + J_y e^{ik_1}), \;\; \delta_{2k} = (J_x + J_y e^{ik_2}) && \text{(D.2)}\\
\Delta_k &= |\delta_{1k}|^2 + |\delta_{2k}|^2 + 2J_z^2 && \text{(D.3)}\\
\Delta_{12} &= |\delta_1|^2 - |\delta_2|^2 && \text{(D.4)}\\
\Delta_{3k} &= \sqrt{(\Delta_{12}^2 + 4J_z^2(|\delta_1^2| + |\delta_1^2| + (\delta_1\delta_2 e^{-i(k_3)} + c.c))} && \text{(D.5)}
\end{aligned}$$

The condition for minimum of E can be obtained by maximising Δ_{3k}. We differentiate Δ_{3k} with respect to k_3 and get the following condition,

$$\delta_{1k}\delta_{2k} e^{-i(k_3)} = \delta_1^* \delta_2^* e^{i(k_3)} \tag{D.6}$$

This shows that $\delta_{1k}\delta_{k2} e^{-i(k_3)}$ is purely real, imaginary part is zero and its value is,

$$\delta_{1k}\delta_{2k} e^{-i(k_3)} = |\delta_{1k}||\delta_{2k}| \tag{D.7}$$

Real part of the above identity is given by,

$$\begin{aligned} R_p &= \cos k_3(J_x^2 + J_y J_x(\cos k_1 + \cos k_2) + J_y^2 \cos(k_2 + k_1)) \\ &\quad + \sin k_3(J_y J_x(\sin k_1 + \sin k_2) + J_y^2 \sin(k_2 + k_3)) \end{aligned} \tag{D.8}$$

and imaginary part is given by,

$$\begin{aligned} I_p &= i(-\sin k_3(J_x^2 + J_y J_x(\cos k_1 + \cos k_2) + J_y^2 \cos(k_1 + k_2)) \\ &\quad + \cos k_3(J_y J_x(\sin k_1 + \sin k_2) + J_y^2 \sin(k_1 + k_2))) \end{aligned} \tag{D.9}$$

From the above equation we get,

$$\tan k_z = \frac{J_y J_x(\sin k_2 + \sin k_1) + J_y^2 \sin(k_1 + k_2)}{J_x^2 + J_y J_x(\cos k_1 + \cos k_2) + J_y^2 \cos(k_1 + k_2)} \tag{D.10}$$

The Eq.(D.10) gives the condition for which the spectrum is gapless. It is clear from this above identity that for 3D Kitaev model spectrum is gapless on a contour in k-space determined by Eq. (D.10).

D.2 Some analysis

Here we derive the condition for gapless spectrum in detail. Let us call, $F = E^2 = \frac{1}{8}(\Delta_k - \Delta_{3k})$. We have also the relation for gaplessness of the spectrum, $\delta_{1k}\delta_{2k}e^{-ik_3} = |\delta_{1k}||\delta_{2k}| = \delta_{1k}^*\delta_{2k}^* e^{ik_3}$. We substitute it in the expression of Δ_{3k} and obtain,

$$\Delta_{3k} = (|\delta_{1k}| + |\delta_{2k}|)\sqrt{4J_z^2 + (|\delta_{1k}| - |\delta_{2k}|)^2} \tag{D.11}$$

Then we get for F,

$$F = |\delta_{1k}|^2 + |\delta_{2k}|^2 + J_z^2 - (|\delta_{1k}| + |\delta_{2k}|)\sqrt{4J_z^2 + (|\delta_{1k}| - |\delta_{2k}|)^2} \tag{D.12}$$

We search for the minimum of F and equate its partial differentiations w.r.t. k_1 and k_2 to zero. Doing this get the following equations,

$$\frac{\partial|\delta_{1k}|}{\partial k_1}\left(2|\delta_{1k}| - \sqrt{4J_z^2 + (|\delta_{1k}| - |\delta_{2k}|)^2} - \frac{|\delta_{1k}|^2 - |\delta_{2k}|^2}{\sqrt{4J_z^2 + (|\delta_{1k}| - |\delta_{2k}|)^2}}\right) = 0. \tag{D.13}$$

And

$$\frac{\partial|\delta_{2k}|}{\partial k_2}\left(2|\delta_{2k}| - \sqrt{4J_z^2 + (|\delta_{1k}| - |\delta_{2k}|)^2} + \frac{|\delta_{1k}|^2 - |\delta_{2k}|^2}{\sqrt{4J_z^2 + (|\delta_{1k}| - |\delta_{2k}|)^2}}\right) = 0. \tag{D.14}$$

We do not demand $\frac{\partial|\delta_{1k}|}{\partial k_1} = 0$ and $\frac{\partial|\delta_{2k}|}{\partial k_2} = 0$. They will turn out to be solutions for the gapped phase. For the moment we demand,

$$2|\delta_{1k}| - \sqrt{4J_z^2 + (|\delta_{1k}| - |\delta_{2k}|)^2} - \frac{|\delta_{1k}|^2 - |\delta_{2k}|^2}{\sqrt{4J_z^2 + (|\delta_{1k}| - |\delta_{2k}|)^2}} = 0 \qquad \text{(D.15)}$$

and

$$2|\delta_{2k}| - \sqrt{4J_z^2 + (|\delta_{1k}| - |\delta_{2k}|)^2} + \frac{|\delta_{1k}|^2 - |\delta_{2k}|^2}{\sqrt{4J_z^2 + (|\delta_{1k}| - |\delta_{2k}|)^2}} = 0 \qquad \text{(D.16)}$$

We solve for $|\delta_{2k}|$ and $|\delta_{1k}|$ for the gapless phase. Subtracting Eq. (D.15) from Eq. (D.16) we get ,

$$(|\delta_{1k}| - |\delta_{2k}|)\left(1 - \frac{|\delta_{1k}| + |\delta_{2k}|}{\sqrt{4J_z^2 + (|\delta_{1k}| - |\delta_{2k}|)^2}}\right) = 0 \qquad \text{(D.17)}$$

Then adding equation (D.15) and (D.16) we get,

$$|\delta_{1k}| + |\delta_{2k}| - \sqrt{4J_z^2 + (|\delta_{1k}| - |\delta_{2k}|)^2} = 0 \qquad \text{(D.18)}$$

Again we do not demand $|\delta_{1k}| = |\delta_{2k}|$, equating the term inside the bigger parenthesis we find the following condition,

$$|\delta_{1k}||\delta_{2k}| = J_z^2 \qquad \text{(D.19)}$$

Thus we recover the earlier solutions for the gapless phase.

D.2.1 Minimum in the gapped region

We have the following expression for 'F' in the gapped phase,

$$F = |\delta_{1k}|^2 + |\delta_{2k}|^2 + J_z^2 - (|\delta_{1k}| + |\delta_{2k}|)\sqrt{4J_z^2 + (|\delta_{1k}| - |\delta_{2k}|)^2} \qquad \text{(D.20)}$$

For finding the extrema of a given function 'F', we need to calculate the following object 'M' where 'M ' is given by,

$$M = F_{xx}(a,b)F_{yy}(a,b) - (F_{xy}(a,b))^2 \qquad \text{(D.21)}$$

If $M > 0$ and $F_{xx}(a,b) > 0$ then $F(a,b)$ is a local minimum.
If $M > 0$ and $F_{xx}(a,b) < 0$ then $F(a,b)$ is a local maximum.
If $M < 0$ then $F(a,b)$ is a saddle point.
If $M = 0$ then the second derivative test is indecisive. We only take values

for which $F_x = 0 = F_y$. Now let us look at equation (D.12). At minimum the square of spectrum is given by,

$$F = |\delta_{1k}|^2 + |\delta_{2k}|^2 + J_z^2 - (|\delta_{1k}| + |\delta_{2k}|)\sqrt{4J_z^2 + (|\delta_{1k}| - |\delta_{2k}|)^2} \quad \text{(D.22)}$$

Evaluating 'M' as directed by equation (D.21) we find that for the region $J_z \geq J_x + J_y$, $k_x = 0, k_y = 0$ is the condition for minimum. $k_x = \pi, k_y = \pi$ is the condition for extrema.

Similarly for the region, $J_y \geq J_x + J_z and J_x \geq J_y + J_z$, $k_x = \pi, k_y = \pi$ is the condition for a minimum. $k_x = 0, k_y = 0$ is the condition for an extrema.

In all cases $k_x = 0, k_y = \pi$ and $k_x = \pi, k_y = 0$ satisfy the conditions for saddle point.

Appendix E

Effective Hamiltonian in toric code limit of the Kitaev model

In this Appendix we derive the effective Hamiltonian of the 2D and 3D Kitaev model in large J_z limit, i.e, $J_z >> J_x, J_y$. This particular limit, in 2D, is often referred to as the toric code limit. We derive the effective Hamiltonian at lowest nontrivial order of perturbation. The Hamiltonian we study is given by (as given by Eq. (6.1) and Eq. (9.1)),

$$\begin{aligned} &H = H_0 + V \\ &H_0 = -J_z \sum_{z-\text{link}} \sigma_j^z \sigma_k^z, V = -J_x \sum_{x-\text{link}} \sigma_j^x \sigma_k^x - J_y \sum_{y-\text{link}} \sigma_j^y \sigma_k^y \end{aligned} \quad \text{(E.1)}$$

Here we take H_0 as the unperturbed Hamiltonian and treat V as perturbation. For a given z-bond we can have four states but among them only $|\uparrow\uparrow\rangle$ and $|\downarrow\downarrow\rangle$ contribute to the ground state subspace of the Hamiltonian H_0. If there are N_z number of z-bonds, we have 2^{N_z} number of degenerate ground state of the Hamiltonian H_0. Details of perturbation theory leading to effective Hamiltonian for 2D and 3D Kitaev model is derived in the AppendixF. Here we mention the results. The perturbation theory yields a non-trivial effective Hamiltonian only in the 4th and 6th order for 2D and 3D Kitaev model respectively. For 2D Kitaev model effective Hamiltonian is obtained by evaluating the identity,

$$\langle b|H_{eff}|a\rangle = \sum_{j_i} \frac{\langle b|V|j_1 \times j_1|V|j_2 \times j_2|V|j_3 \times j_3|V|a\rangle}{\prod_{j_i, i=1,3}(E^0 - E^0_{j_i})} \quad \text{(E.2)}$$

The corresponding formula for 3D Kitaev model is given by,

$$\langle b|H_{eff}|a\rangle = \sum_{j_i} \frac{\langle b|V|j_1 \times j_1|V|j_2 \times j_2|V|j_3 \times j_3|V|j_4 \times j_4|V|j_5 \times j_5|V|a\rangle}{\prod_{j_i, i=1,5}(E^0 - E^0_{j_i})} \tag{E.3}$$

In the above formula $i, j..$ refers only the excited states. Kitaev has shown that for 2D Kitaev model, the first non-identity corrections comes at 4th order. For 3D Kitaev model, first non-identity corrections comes in 6th order. First we re-derive the effective Hamiltonian for 2D Kitaev model and then derive the effective Hamiltonian for 3D Kitaev model. Here by 'effective Hamiltonian' we mean first non-identity corrections.

E.1 2D Kitaev model

It can be seen very easily that at first order H^1_{eff} is zero. In the 2nd order we get a non vanishing matrix element which connects every state of the ground state subspace to itself and yields a constant term which can be represented by the identity operator. The 3rd order terms vanishes identically as in this order every matrix element in Eq. (E.2) is zero. In the fourth order we get three different type of terms which give non-vanishing contributions. Let us look at the part of V which includes Hamiltonian terms of a single hexagon as shown in Fig. (E.1). Then we can write,

$$V = v_1 + v_2 + v_3 + v_4 \tag{E.4}$$

$$v_1 = -\sigma^x_1\sigma^x_2\,; v_2 = -\sigma^y_3\sigma^y_3\,; v_3 = -\sigma^x_4\sigma^x_5\,;\, v_4 = -\sigma^y_5\sigma^y_6 \tag{E.5}$$

The fourth order term in the perturbation is given by,

$$\sum_{j_1,j_2,j_3} \frac{\langle a|V|j_1\rangle\langle j_1|V|j_2\rangle\langle j_2|V|j_3\rangle\langle j_3|V|b\rangle}{(E_0 - E_{j_1})(E_0 - E_{j_2})(E_0 - E_{j_3})} \tag{E.6}$$

After inserting equation (E.4) and (E.5), we observe that following three types of terms yielding non vanishing contributions.

1. Terms in which any v_i appears four times. It yields a constant and can be represented by identity operator.
2. Terms in which any pair of v_i's appear twice. This can also be represented by a constant multiplied by identity operator.
3. Terms in which all v_i appear only once without repetition. There are 24 terms of this type. They connect different states of the ground state subspace. Below we find effective operator representing these terms.

We know that for a given z-bond the low energy subspace is given by the state, $|\uparrow\uparrow\rangle$ and $|\downarrow\downarrow\rangle$. Let us write down for a given pair of spin in a z-bond (for exmp. for spin at site 3 and 4), the effective operators in the low energy subspace can be written as,

$$\begin{aligned} \sigma_3^x \otimes \sigma_4^x &= \tau_k^x, \quad \sigma_3^y \otimes \sigma_4^y = -\tau_k^x, \quad \sigma_3^x \otimes \sigma_4^y = \sigma_3^y \otimes \sigma_4^x = \tau_k^y \\ \sigma_3^z &= \sigma_4^z = \tau_k^z, \quad \sigma_3^z \otimes \sigma_4^z = I \end{aligned} \tag{E.7}$$

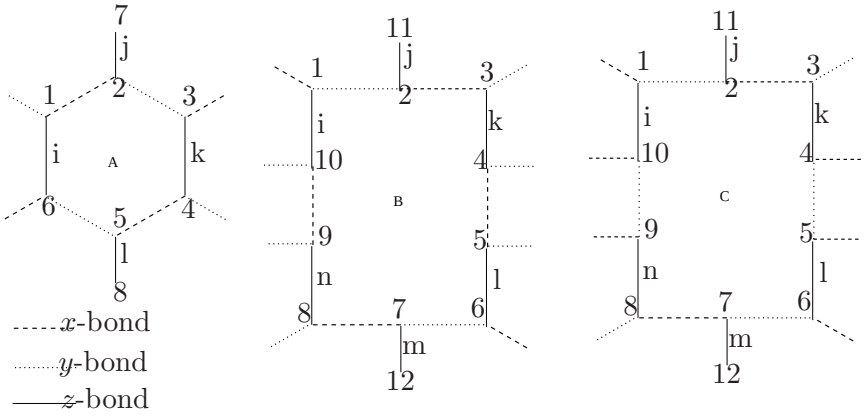

Figure E.1: In this figure we have shown the elementary plaquettes of 2D and 3D Kitaev model.

The part of the degenerate ground state subspace which is effected by V is given by the 8-site as shown in Fig. (E.1,A). There are 4 dimers involved which means we are dealing with $2^4 = 16$ states. Now we derive the H_{eff}^4 in conformity with Eq. (E.2). The fourth order term is given by,

$$\sum_p \sum_{j_1,j_2,j_3} \frac{\langle a|v_1|j_1\rangle\langle j_1|v_2|j_2\rangle\langle j_2|v_3|j_3\rangle\langle j_3|v_4|b\rangle}{(E_0 - E_{j_1})(E_0 - E_{j_2})(E_0 - E_{j_3})} \tag{E.8}$$

Here the summation is performed over the excited states and the sum over 'p' denotes a sum over other combinations of v_i obtained by permutations. Let us take any one of these terms and select $|a\rangle$ and $|b\rangle$ such that it yields a non-vanishing contribution. It is easy to see that if any one of the 24 terms yields a non vanishing contribution for a given $|a\rangle$ and $|b\rangle$, the other remaining 23 terms will be giving non vanishing contribution as well. And finally they just add up. We take, $|b\rangle = |\uparrow_1\uparrow_6\uparrow_2\uparrow_7\uparrow_3\uparrow_4\uparrow_5\uparrow_8\rangle$. Let us calculate the following term,

$$\sum_{j_1,j_2,j_3} \frac{\langle a|v_1|j_1\rangle\langle j_1|v_2|j_2\rangle\langle j_2|v_3|j_3\rangle\langle j_3|v_4|b\rangle}{(E_0-E_{j_1})(E_0-E_{j_2})(E_0-E_{j_3})} = -\frac{J_x^2J_y^2}{64J_z^3}$$
$$|b\rangle = |\uparrow_1\uparrow_6\uparrow_2\uparrow_7\uparrow_3\uparrow_4\uparrow_5\uparrow_8\rangle$$
$$|j_3\rangle = |\uparrow_1\downarrow_6\uparrow_2\uparrow_7\uparrow_3\uparrow_4\downarrow_5\uparrow_8\rangle;\ E_0-E_{j_3}=-4J_z$$
$$|j_2\rangle = |\uparrow_1\downarrow_6\uparrow_2\uparrow_7\uparrow_3\downarrow_4\uparrow_5\uparrow_8\rangle;\ E_0-E_{j_2}=-4J_z$$
$$|j_1\rangle = |\uparrow_1\downarrow_6\downarrow_2\uparrow_7\downarrow_3\downarrow_4\uparrow_5\uparrow_8\rangle;\ E_0-E_{j_1}=-4J_z$$
$$|a\rangle = |\downarrow_1\downarrow_6\uparrow_2\uparrow_7\downarrow_3\downarrow_4\uparrow_5\uparrow_8\rangle \tag{E.9}$$

In the above equation we have written in detail the various intermediate state connecting the state $|a\rangle$ and the state $|b\rangle$. Now if we look at the spin states of each dimer we see that they have changed from $|\uparrow\uparrow\rangle$ to $|\downarrow\downarrow\rangle$ or itself. Let us take the pair $|\uparrow_1\uparrow_6\rangle$. It has been connected to state $|\downarrow_1\downarrow_6\rangle$. Definitely some operator equivalent to τ_x or τ_y can only connect these two states. Similarly for the pair $|\uparrow_2\uparrow_7\rangle$, we can say τ_z or identity operator has acted on. Below we write the combination of original spin operators(denoted by σ) and their effective spin representation in the ground state subspace(represented by τ).

$$\sigma_1^x\sigma_6^y \sim \tau_i^y;\ \ \sigma_3^y\sigma_4^x \sim \tau_k^y$$
$$\sigma_2^x\sigma_2^y \sim i\tau_j^z;\ \ \sigma_5^x\sigma_5^y \sim i\tau_l^z \tag{E.10}$$

Looking at the above expression we can say that Eq. (E.7) can be written as

$$\sum_{j_1,j_2,j_3} \frac{\langle a|v_1|j_1\rangle\langle j_1|v_2|j_2\rangle\langle j_2|v_3|j_3\rangle\langle j_3|v_4|b\rangle}{(E_0-E_{j_1})(E_0-E_{j_2})(E_0-E_{j_3})} \equiv \frac{J_x^2J_y^2}{64J_z^3}\langle a|\tau_i^y\tau_j^z\tau_k^y\tau_l^z|b\rangle \tag{E.11}$$

Now summing the contributions from the remaining 23 terms we get $\frac{J_x^2J_y^2}{16J_z^3}$ which means that the effective operator representation at fourth order is given by,

$$H_{eff}^4 = -\frac{J_x^2J_y^2}{16J_z^3}\tau_i^y\tau_j^z\tau_k^y\tau_l^z \tag{E.12}$$

The above representation for effective Hamiltonian would yield right matrix element for the state $|a\rangle$ and $|b\rangle$ used in equation (E.9). Now we would show that the effective Hamiltonian representation given by equation (E.9) is true for any pair of states in the ground state subspace. Let us, for example, take $|b'\rangle = |\downarrow_1\downarrow_6\uparrow_2\uparrow_7\uparrow_3\uparrow_4\uparrow_5\uparrow_8\rangle$, then $|a'\rangle$ must be $|\uparrow_1\uparrow_6\uparrow_2\uparrow_7\downarrow_3\downarrow_4\uparrow_5\uparrow_8\rangle$. Let us write the result we got,

$$\sum_p \sum_{j_1,j_2,j_3} \frac{\langle a|v_1|j_1\rangle\langle j_1|v_2|j_2\rangle\langle j_2|v_3|j_3\rangle\langle j_3|v_4|b\rangle}{(E_0-E_{j_1})(E_0-E_{j_2})(E_0-E_{j_3})} \equiv \langle a| - \frac{J_x^2J_y^2}{16J_z^3}\tau_i^y\tau_j^z\tau_k^y\tau_l^z|b\rangle \tag{E.13}$$

Here $|a\rangle$ and $|b\rangle$ are as used in equation (E.9). Now we will show that the above equation imply the correct matrix element (H^4_{eff}) between any two given pair. For example we take $|a'\rangle$ and $|b'\rangle$. And if we replace $|a\rangle$ and $|b\rangle$ by $|a'\rangle$ and $|b'\rangle$ respectively, then we should obtain $-\frac{J_x^2J_y^2}{16J_z^3}$ instead of $\frac{J_x^2J_y^2}{16J_z^3}$. Let us define a unitary operator, $u = \sigma_1^x\sigma_6^x$, it is clear that $uu^\dagger = 1$. Now we see that,

$$\begin{aligned}
&\sum_p \sum_{j_1,j_2,j_3} \frac{\langle a'|v_1|j_1\rangle\langle j_1|v_2|j_2\rangle\langle j_2|v_3uu^\dagger|j_3\rangle\langle j_3|v_4|b'\rangle}{(E_0-E_{j_1})(E_0-E_{j_2})(E_0-E_{j_3})} \\
&= \sum_p \sum_{j_1,j_2,j_3} \frac{\langle a'|uu^\dagger v_1uu^\dagger|j_1\rangle\langle j_1|uu^\dagger v_2uu^\dagger|j_2\rangle\langle j_2|uu^\dagger v_3uu^\dagger|j_3\rangle\langle j_3|uu^\dagger v_4uu^\dagger|b'\rangle}{(E_0-E_{j_1})(E_0-E_{j_2})(E_0-E_{j_3})} \\
&= (-)\sum_p \sum_{j_1',j_2',j_3'} \frac{\langle a|v_1|j_1'\rangle\langle j_1'|v_2|j_2'\rangle\langle j_2'|v_3|j_3'\rangle\langle j_3'|v_4|b\rangle}{(E_0-E_{j_1})(E_0-E_{j_2})(E_0-E_{j_3})} \\
&= (-)\frac{J_x^2J_y^2}{16J_z^3} \qquad \text{by Eq. (E.13)}
\end{aligned} \tag{E.14}$$

Here we have used the fact $u^\dagger v_4 u = -v_4$ and all other v remain unchanged under the unitary transformation $u^\dagger v_i u$. The summation over prime and unprimed states are equivalent as they are dummy indices.

E.2 3D Kitaev model

We proceed exactly the same way as in 2d Kitaev model. We see that in second and fourth order we get non-vanishing contribution which is constant and can be represented by identity operator. Only in sixth order we get a nontrivial contribution having non-vanishing matrix element between two

different degenerate eigenstate of the H_0. Very similar to 2d Kitaev model, we need to sum a total of $6! = 720$ terms in the expansion of sixth order perturbation(we have wriiten a computer code to perform this sum). In the Fig. (E.1), we have drawn two different kind of elementary loops present in the 3d Kitaev model. In the Figure (E.1), we represent these two loop by B and C. For both the loop, we get 7/256 after summing all the 720 terms. It is to be noted that the differences in the distribution of x and y bond in the elementary plaquettes B and C in Fig. (E.1) does not make any differences in the final result. Thus we can write for the effective operator for plaquette B in Fig. (E.1)as follows,

$$H^6_{eff} = -\frac{7}{256}\frac{J_x^4 J_y^2}{J_z^5}\tau_i^x\tau_j^z\tau_k^y\tau_l^x\tau_m^z\tau_n^y \tag{E.15}$$

For plaquette C in Figure (E.1), we have the effective operator as given by,

$$H^6_{eff} = -\frac{7}{256}\frac{J_y^4 J_x^2}{J_z^5}\tau_i^y\tau_j^z\tau_k^x\tau_l^y\tau_m^z\tau_n^x \tag{E.16}$$

Now we would like to prove that the Eq. (E.15) would imply Eq. (E.16). Let us take,

$$\begin{aligned} |a\rangle &= |\uparrow_1\uparrow_{10}\uparrow_2\uparrow_{11}\uparrow_3\uparrow_4\uparrow_5\uparrow_6\uparrow_7\uparrow_{12}\uparrow_8\uparrow_9\rangle \\ &= |\Uparrow_i\Uparrow_j\Uparrow_k\Uparrow_l\Uparrow_m\Uparrow_n\rangle \qquad \text{(E.17)} \\ |b\rangle &= |\downarrow_1\downarrow_{10}\uparrow_2\uparrow_{11}\downarrow_3\downarrow_4\downarrow_5\downarrow_6\uparrow_7\uparrow_{12}\downarrow_8\downarrow_9\rangle \\ &= |\Downarrow_i\Uparrow_j\Downarrow_k\Downarrow_l\Uparrow_m\Downarrow_n\rangle \qquad \text{(E.18)} \end{aligned}$$

Fort the state $|a\rangle$ and $|b\rangle$, we have a non-vanishing matrix element at sixth order of perturbation. Let us write the equation for the sixth order perturbations for the plaquette B in the figure (E.1),

$$\begin{aligned} &\sum_{p,j}\frac{\langle b|v_1|j_1\rangle\langle j_1|v_2|j_2\rangle\langle j_2|v_3|j_3\rangle\langle j_3|v_4|j_4\rangle\langle j_4|v_5|j_5\rangle\langle j_5|v_6|a\rangle}{(E_0-E_{j_1})(E_0-E_{j_2})(E_0-E_{j_3})(E_0-E_{j_4})(E_0-E_{j_5})} \\ &= \frac{7}{256}\frac{J_y^4 J_x^2}{J_z^5} \end{aligned} \tag{E.19}$$

Here the expressions for v_i's are given by,

$$v_1 = \sigma_1^x\sigma_2^x, v_2 = \sigma_2^y\sigma_3^y, v_3 = \sigma_4^x\sigma_5^x, v_4 = \sigma_6^x\sigma_7^x, v_5 = \sigma_7^y\sigma_8^y, v_6 = \sigma_9^x\sigma_{10}^x \tag{E.20}$$

To get the expression for effective Hamiltonian for the plaquette C in Fig(E.1), we must have following v_i's in Eq. (E.19),

$$v_1 = \sigma_1^x\sigma_2^x, v_2 = \sigma_2^y\sigma_3^y, v_3 = \sigma_4^y\sigma_5^y, v_4 = \sigma_6^x\sigma_7^x, v_5 = \sigma_7^y\sigma_8^y, v_6 = \sigma_9^y\sigma_{10}^y \quad \text{(E.21)}$$

Let us define an unitary transformation U given by,

$$U = e^{i\pi(\sigma_4^z+\sigma_5^z+\sigma_9^z+\sigma_{10}^z)/4} \quad \text{(E.22)}$$

We notice that v_3 and v_6 undergoes following transformation under the action of U.

$$v_3 = \sigma_4^x\sigma_5^x \rightarrow U\sigma_4^x\sigma_5^xU^\dagger = \sigma_4^y\sigma_5^y, \quad \text{same is true for } v_6 \quad \text{(E.23)}$$

The all other v_i's in Eq. (E.20) remain unchanged under the action of 'U'. Now inserting $UU^\dagger$ into the l.h.s of Eq. (E.19) at appropriate places, we find that one must have,

$$\sum_{p,j} \frac{\langle b|v_1|j_1\rangle\langle j_1|v_2|j_2\rangle\langle j_2|v_3|j_3\rangle\langle j_3|v_4|j_4\rangle\langle j_4|v_5|j_5\rangle\langle j_5|v_6|a\rangle}{(E_0-E_{j_1})(E_0-E_{j_2})(E_0-E_{j_3})(E_0-E_{j_4})(E_0-E_{j_5})}$$
$$= \frac{7}{256}\frac{J_y^4J_x^2}{J_z^5} \quad \text{(E.24)}$$

where various v_i's are given in Eq. (E.21).

Appendix F

Perturbation theory for the Kitaev model

In this Appendix we develop perturbation theory leading to the effective Hamiltonian of the 2D and 3D Kitaev model in large J_z limit, i.e, $J_z >> J_x, J_y$. The Hamiltonian we discuss is given by,

$$H = H_0 + \lambda V \tag{F.1}$$

$$H_0 = -J_z \sum_{\langle ij \rangle_{z-bond}} \sigma_i^z \sigma_j^z \tag{F.2}$$

$$V = -J_x \sum_{\langle ij \rangle_{x-bond}} \sigma_i^x \sigma_j^x - J_y \sum_{\langle ij \rangle_{y-bond}} \sigma_i^y \sigma_j^y \tag{F.3}$$

H_0 is taken as the unperturbed Hamiltonian. We discuss the limit $J_x, J_y << J_z$. λ is an arbitrary parameter introduced to develop the perturbation theory. It can be set 1 at the end. The eigenstates of H_0 are divided into two classes, one which constitute the (degenerate) ground states and the others belongs to excited states. It may be mentioned that excited states are also degenerate. We denote the ground states as $|E_a^0\rangle$ and excited states as $|E_i^0\rangle$. We calculate the effective Hamiltonian at first non-identity corrections. Though we are dealing with a degenerate perturbation theory we follow usual non-degenerate perturbation theory as it does not create any problem for our purpose of calculating effective Hamiltonian belonging to ground state sub-space at first leading order. This privilege is special to Kitaev model and is due to the following reason.

- The usual perturbation theory fails for degenerate states as we encounter a term $\frac{\langle a|V|b\rangle}{E_a^0 - E_b^0}$ which is diverging for $E_a^0 = E_b^0$. However as

far as we have $\langle a|V|b\rangle = 0,\ a \neq b$ we are safe to use non-degenerate perturbation theory

- It happens that this is exactly the case for 2D and 3D Kitaev model where the effective Hamiltonian at lower order do not have any off diagonal matrix element in ground state subspace. Thus if we intend to calculate the leading order corrections in the ground state subspace we can use non-degenerate perturbation theory in sub-leading order.

Now we develop the perturbation theory for Kitaev model. As usual we write the expected normalized eigenvectors as,

$$|E_a\rangle = |E_a^0\rangle + \lambda|E_a^1\rangle + \lambda^2|E_a^2\rangle + \lambda^3|E_a^3\rangle + ... \tag{F.4}$$
$$E_a = E_a^0 + \lambda E_a^1 + \lambda^2 E_a^2 + \lambda^3 E_a^3 + ... \tag{F.5}$$

In the above equation $|E_a^i\rangle$ and E_a^i denote the i'th order corrections to perturbed eigenstate $|E_a\rangle$ and perturbed energy E_a. We expand $|E_a^i\rangle$ in the following way,

$$|E_a^i\rangle = \sum A_{a\gamma}|E_\gamma^0\rangle \tag{F.6}$$

Below we write down the set of equations we need to solve at various orders,

$$(H_0 - E_a^0)|E_a^1\rangle + (V - E_a^1)|E_a^0\rangle = 0 \tag{F.7}$$
$$(H_0 - E_a^0)|E_a^2\rangle + (V - E_a^1)|E_a^1\rangle - E_a^2|E_a^0\rangle = 0 \tag{F.8}$$
$$(H_0 - E_a^0)|E_a^n\rangle + (V - E_a^1)|E_a^{n-1}\rangle - \sum_{i=0}^{n-2} E^{n-i}|E_a^i\rangle \tag{F.9}$$

We also know that for calculating the n-th order corrections to energy we need to calculate the perturbed eigenvectors upto (n-1)th order. The energy correction to n-th order then obtained by calculating $\langle E_a^0 V|E_a^{n-1}\rangle$. It turns out that for calculating the effective Hamiltonian upto first non-identity corrections we need to carry the calculations upto 5th order for 3D Kitaev model. Below we write down the expressions for E_a^n and E_a^n at various order. *We continue to explain why the non-degenerate perturbation theory does not create any problems.* We define the effective Hamiltonian obtained at n-th order by the existence of following matrix element,

$$H_{eff} \equiv \tilde{E}_{ab} = P\langle E_b^0|V|E_a^{n-1}\rangle P \tag{F.10}$$

In the above equation P is the projection operator which project out any matrix element between an initial ground state and final excited state.

F.1 1st order

First order corrections to energy and eigenfunctions are given by,

$$E_a^1 = \langle E_a^0 | V | E_a^0 \rangle = 0 \tag{F.11}$$

$$|E_a\rangle = |E_a^0\rangle + \sum_{a \neq i} \frac{V_{ia}}{E_a^0 - E_i^0} |E_i^0\rangle \tag{F.12}$$

It is to be noted that the summation is over only the excited states.

F.2 2nd order

Results of the 2nd order corrections are the following,

$$E_a^2 = \sum_i \frac{|\langle E_i^0 | V | E_a^0 \rangle|^2}{E_a^0 - E_i^0} \tag{F.13}$$

$$H_{eff} = P \langle E_b^0 | V | E_a^2 \rangle P = Constant \tag{F.14}$$

$$\begin{aligned} |E_a\rangle = & \left(1 - \frac{\lambda^2}{2} \sum_{\gamma \neq a} \frac{|V_{a\gamma}|^2}{(E_a^0 - E_\gamma^0)^2} \right) |E_a^0\rangle + \lambda \sum_{\gamma \neq a} \frac{V_{\gamma a}}{E_a^0 - E_\gamma^0} |E_\gamma^0\rangle \\ & + \lambda^2 \sum_{\gamma \neq a} \frac{1}{E_a^0 - E_\gamma^0} \left(\sum_{\delta \neq a} \frac{V_{\delta a} V_{\gamma \delta}}{E_a^0 - E_\delta^0} \right) |E_\gamma^0\rangle \end{aligned} \tag{F.15}$$

It may be noted that though we have written the summation over all states, contribution in the summation comes only from the excited states.

F.3 3rd Order

Proceeding to the third order we get the following expressions for energy corrections

$$\begin{aligned}
|E_a\rangle \quad &= |E_a^0\rangle + \lambda \sum_{\gamma_1 \neq a} \frac{V_{\gamma_1 a}}{E_a^0 - E_{\gamma_1}^0} |E_{\gamma_1}^0\rangle - \frac{\lambda^2}{2} \sum_{\gamma_2 \neq a} \frac{|V_{\gamma_2 a}|^2}{(E_a^0 - E_{\gamma_2}^0)^2} |E_a^0\rangle \\
&+\lambda^2 \sum_{\gamma_2 \neq a} \sum_{\delta_2 \neq a} \frac{V_{\delta_2 a} V_{\gamma_2 \delta_2}}{(E_a^0 - E_{\gamma_2}^0)(E_a^0 - E_{\delta_2}^0)} |E_{\gamma_2}^0\rangle + \lambda^3 A_{aa}^3 |E_a^0\rangle \\
&+\lambda^3 \sum_{\gamma_3 \neq a} \left(\frac{1}{2} \sum_{\gamma_2 \neq a} \frac{|V_{\gamma_2 a}|^2 V_{\gamma_3 a}}{(E_a^0 - E_{\gamma_2}^0)^2 (E_a^0 - E_{\gamma_3})} \right) |E_{\gamma_3}^0\rangle \\
&+\lambda^3 \sum_{\gamma_3 \neq a} \left(\sum_{\gamma_2 \neq a} \sum_{\delta_2 \neq a} \frac{V_{\delta_2 a} V_{\gamma_2 \delta_2} V_{\gamma_3 \gamma_2}}{(E_a^0 - E_{\gamma_2}^0)(E_a^0 - E_{\delta_2}^0)(E_a^0 - E_{\gamma_3}^0)} \right) |E_{\gamma_3}^0\rangle \\
&+\lambda^3 \sum_{\gamma_3 \neq a} \left(E_a^2 \frac{V_{\gamma_3 a}}{(E_a^0 - E_{\gamma_3}^0)} \right) |E_{\gamma_3}^0\rangle \qquad \text{(F.16)}
\end{aligned}$$

We need to solve for A_{aa}^3 by using normalization condition. Inequalities and various matrix elements are such that the r.h.s of the above expressions are finite. The expressions for A_{aa}^3 is given by,

$$A_{aa}^3 = -\sum_{\gamma_2 \neq a} \sum_{\delta_2 \neq a} \frac{V_{\delta_2 a} V_{\gamma_2 \delta_2} V_{\gamma_2 a}}{(E_a^0 - E_{\gamma_2}^0)^2 (E_a^0 - E_{\delta_2}^0)} \qquad \text{(F.17)}$$

$$\begin{aligned}
E_a^3 \quad &= \langle E_a^0 | V | E_a^2 \rangle = \lambda \sum_{\gamma \neq a} \frac{|V_{\gamma a}|^2}{E_a^0 - E_\gamma^0} \\
&+\lambda^2 \sum_{\gamma \neq a} \sum_{\delta \neq a} \frac{V_{\delta a} V_{\gamma \delta} V_{\gamma a}}{(E_a^0 - E_\gamma^0)(E_a^0 - E_\delta^0)} \qquad \text{(F.18)} \\
H_{eff} \quad &= P \langle E_b^0 | V | E_a^2 \rangle P = 0 \qquad \text{(F.19)}
\end{aligned}$$

F.4 4TH ORDER

4th order corrections to the energies are given by,

$$
\begin{aligned}
E_a^4 &= \langle E_a^0|V|E_a^3\rangle = \lambda \sum_{\gamma_1\neq a} \frac{|V_{\gamma_1 a}|^2}{E_a^0 - E_{\gamma_1}^0} \\
&+\lambda^2 \sum_{\gamma_2\neq a}\sum_{\delta_2\neq a} \frac{V_{\gamma_2 a}V_{\delta_2 a}V_{\gamma_2\delta_2}}{(E_a^0 - E_{\gamma_2}^0)(E_a^0 - E_{\delta_2}^0)} \\
&+\lambda^3 \sum_{\gamma_3\neq a} \frac{1}{2} \sum_{\gamma_2\neq a} \frac{|V_{\gamma_2 a}|^2|V_{\gamma_3 a}|^2}{(E_a^0 - E_{\gamma_2}^0)^2(E_a^0 - E_{\gamma_3})} \\
&+\lambda^3 \sum_{\gamma_3\neq a}\sum_{\gamma_2\neq a}\sum_{\delta_2\neq a} \frac{V_{\delta_2 a}V_{\gamma_2\delta_2}V_{\gamma_3\gamma_2}V_{\gamma_3 a}}{(E_a^0 - E_{\gamma_2}^0)(E_a^0 - E_{\delta_2}^0)(E_a^0 - E_{\gamma_3}^0)} \\
&+\lambda^3 \sum_{\gamma_3\neq a} E_a^2 \frac{|V_{\gamma_3 a}|^2}{(E_a^0 - E_{\gamma_3}^0)}
\end{aligned}
\tag{F.20}
$$

At this point, for 2D Kitaev model, we get a non-vanishing matrix element for the matrix element $\langle E_b^0|V|E_a\rangle$ where $|E_a^0\rangle$ and $|E_b^0\rangle$ both belong to ground state subspace. Thus we encounter the first contribution to effective Hamiltonian. The second last term of the Eq. F.16 yields a non-vanishing matrix element with $\langle E_b^0|V$. The effective Hamiltonian for 2D Kitaev model can be written as,

$$
H_{eff} = \sum_{a,b}\sum_{\gamma_3\neq a}\sum_{\gamma_2\neq a}\sum_{\delta_2\neq a} \frac{V_{\delta_2 a}V_{\gamma_2\delta_2}V_{\gamma_3\gamma_2}V_{\gamma_3 b}}{(E_a^0 - E_{\gamma_2}^0)(E_a^0 - E_{\delta_2}^0)(E_a^0 - E_{\gamma_3}^0)} \tag{F.21}
$$

The expressions for fourth order corrections to eigenfunction is given by,

$$
|E_a^4\rangle = A_{aa}^4|E_a^0\rangle + \sum_{\gamma_4\neq a} A_{a\gamma_4}^4|E_{\gamma_4}^0\rangle \tag{F.22}
$$

$$
\begin{aligned}
A_{a\gamma_4}^4 &= -\sum_{\gamma_3\neq a}\sum_{\gamma_2\neq a} \frac{1}{2} \frac{|V_{\gamma_2 a}|^2 V_{\gamma_3 a}V_{\gamma_4 a}}{(E_a^0 - E_{\gamma_2}^0)^2(E_a^0 - E_{\gamma_3}^0)(E_a^0 - E_{\gamma_4}^0)} \\
&+\sum_{\gamma_3\neq a}\sum_{\gamma_2\neq a}\sum_{\delta_2\neq a} \frac{V_{\delta_2 a}V_{\gamma_2\delta_2}V_{\gamma_3\gamma_2}V_{\gamma_4\gamma_3}}{(E_a^0 - E_{\gamma_2}^0)(E_a^0 - E_{\gamma_3}^0)(E_a^0 - E_{\gamma_4}^0)(E_a^0 - E_{\delta_2}^0)} \\
&-E_a^2 \frac{1}{2} \sum_{\gamma_2\neq a} \frac{|V_{\gamma_2 a}|^2 V_{\gamma_4 a}}{(E_a^0 - E_{\gamma_2}^0)^2(E_a^0 - E_{\gamma_4}^0)} - E_a^2 \sum_{\delta_2\neq a}\sum_{\gamma_2\neq a} \frac{V_{\delta_2 a}V_{\gamma_2\delta_2}V_{\gamma_4\gamma_2}}{(E_a^0 - E_{\gamma_2}^0)(E_a^0 - E_{\delta_2}^0)(E_a^0 - E_{\gamma_4}^0)} \\
&-\sum_{\gamma_1\neq a} \frac{E_a^3 V_{\gamma_1 a}V_{\gamma_4\gamma_1}}{(E_a^0 - E_{\gamma_1}^0)(E_a^0 - E_{\gamma_4}^0)}
\end{aligned}
\tag{F.23}
$$

The expressions for A^4_{aa} is obtained by normalization condition and is given by,

$$\begin{aligned}
A^4_{aa} = & \frac{1}{4}\left(\sum_{\gamma_2\neq a}\frac{|V_{\gamma_2 a}|^2}{(E^0_a-E^0_{\gamma_2})^2}\right)^2+\left(\sum_{\gamma_2\neq a}\sum_{\delta_2\neq a}\frac{V_{\delta_2 a}V_{\gamma_2\delta_2}}{(E^0_a-E^0_{\gamma_2})(E^0_a-E^0_{\delta_2})}\right)^2 \\
& -\left(\sum_{\gamma_2\neq a}\frac{|V_{\gamma_2 a}|^2}{(E^0_a-E^0_{\gamma_2})^2}\right)\times\left(\sum_{\gamma_2\neq a}\sum_{\delta_2\neq a}\frac{V_{\delta_2 a}V_{\gamma_2\delta_2}}{(E^0_a-E^0_{\gamma_2})(E^0_a-E^0_{\delta_2})}\right) \\
& +\sum_{\gamma_3\neq a}\left(\frac{1}{2}\sum_{\gamma_2\neq a}\frac{|V_{\gamma_2 a}|^2|V_{\gamma_3 a}|^2}{(E^0_a-E^0_{\gamma_2})^2(E^0_a-E_{\gamma_3})^2}\right) \\
& +\sum_{\gamma_3\neq a}\left(\sum_{\gamma_2\neq a}\sum_{\delta_2\neq a}\frac{V_{\delta_2 a}V_{\gamma_2\delta_2}V_{\gamma_3\gamma_2}V_{\gamma_3 a}}{(E^0_a-E^0_{\gamma_2})(E^0_a-E^0_{\delta_2})(E^0_a-E^0_{\gamma_3})^2}\right) \\
& +\sum_{\gamma_3\neq a}\left(E^2_a\frac{|V_{\gamma_3 a}|^2}{(E^0_a-E^0_{\gamma_3})^2}\right)
\end{aligned} \tag{F.24}$$

F.5 5th order

In a similar way we can proceed to 5th order and we find that $H_{eff}=0$ for 3D Kitaev model. We do not write down the expressions for energy corrections for this order but write down the expressions for the perturbed eigenfunctions which is needed to calculate the effective Hamiltonian at next order. As usual the the perturbed eigenfunctions is obtained by calculating,

$$|E^5_a\rangle = A^5_{aa}|E^0_a\rangle+\sum_{\gamma_5\neq a}A^5_{a\gamma_5}|E^0_{\gamma_5}\rangle \tag{F.25}$$

where $A^5_{a\gamma_5}$ and A^5_{aa} are given by,

$$\begin{aligned}
A^5_{a\gamma_5} &= -\frac{E^4_a}{E^0_{\gamma_5}-E^0_a}\langle E^0_{\gamma_5}|E^1_a\rangle-\frac{E^3_a}{E^0_{\gamma_5}-E^0_a}\langle E^0_{\gamma_5}|E^2_a\rangle-\frac{E^2_a}{E^0_{\gamma_5}-E^0_a}\langle E^0_{\gamma_5}|E^3_a\rangle \\
&\quad -\frac{E^1_a}{E^0_{\gamma_5}-E^0_a}\langle E^0_{\gamma_5}|E^4_a\rangle+\frac{\langle E^0_{\gamma_5}|V|E^4_a\rangle}{E^0_a-E^0_{\gamma_5}},\quad (\mathrm{a}\neq\gamma_5)
\end{aligned} \tag{F.26}$$

Expression for A^5_{aa} is,

$$A^5_{aa} = -\frac{1}{2}(\langle E^1_a|E^4_a\rangle+\langle E^2_a|E^3_a\rangle+\langle E^4_a|E^1_a\rangle+\langle E^3_a|E^2_a\rangle) \tag{F.27}$$

Expressions for various E^i_as have already found in preceding sections.

F.6 Effective Hamiltonian for 3D Kitaev model

We are in a position to derive the effective Hamiltonian at first leading order. Before we write down it we discuss why the calculation done so far does not make any problem though we are dealing with degenerate ground states. We calculated the perturbed eigenstate $|E_a\rangle$ which reduces to $|E_a^0\rangle$ at zeroth order. $|E_a^0\rangle$ is a representative ground state eigenvector. Upto the 5th order corrections to eigenstate $|E_a^0\rangle$ and eigenvalue E_a^0 we do not encounter any term which diverges due to vanishing denominator. This can be verified easily and is due to the reason that starting from a given eigenvector belonging to ground state subspace we need a minimum six consecutive applications of perturbed Hamiltonian to reach for another degenerate ground state. However at even order of perturbations one has a possibility to return back to original state E_a^0 which corresponds to trivial corrections. We notice from the equations (F.25) and (F.26) that $|E_a^5\rangle$ contains contribution from all the preceding orders however only the last term (containing $|E_a^4\rangle$) in the Eq. F.26 yields the first non-trivial corrections to the energy. Again we see from the expressions of $|E_a^4\rangle$ that it is the fourth order term which is responsible for this non-trivial corrections. For this reason we write down the expressions for this terms explicitly,

$$
\begin{aligned}
&|\tilde{E}_a^5\rangle = \\
&\sum_{\gamma_5\neq a}\sum_{\gamma_4\neq a}\sum_{\gamma_3\neq a}\sum_{\gamma_2\neq a}\sum_{\delta_2\neq a}\frac{V_{\delta_2 a}V_{\gamma_2\delta_2}V_{\gamma_3\gamma_2}V_{\gamma_4\gamma_3}}{(E_a^0-E_{\gamma_2}^0)(E_a^0-E_{\gamma_3}^0)(E_a^0-E_{\gamma_4}^0)(E_a^0-E_{\delta_2}^0)}\times \\
&\frac{\langle E_{\gamma_5}|V|E_{\gamma_4}\rangle}{(E_a^0-E_{\gamma_5}^0)}|E_{\gamma_5}\rangle \\
&=\sum_{\gamma_5\neq a}\sum_{\gamma_4\neq a}\sum_{\gamma_3\neq a}\sum_{\gamma_2\neq a}\sum_{\delta_2\neq a}\frac{V_{\delta_2 a}V_{\gamma_2\delta_2}V_{\gamma_3\gamma_2}V_{\gamma_4\gamma_3}}{(E_a^0-E_{\gamma_2}^0)(E_a^0-E_{\gamma_3}^0)(E_a^0-E_{\gamma_4}^0)(E_a^0-E_{\delta_2}^0)}\times \\
&\frac{V_{\gamma_4\gamma_5}}{(E_a^0-E_{\gamma_5}^0)}|E_{\gamma_5}\rangle
\end{aligned}
\tag{F.28}
$$

All the variables used in the above summation are excited states only. E_{γ_5} can be such that it yields a non-vanishing matrix element of V with a ground state $|E_b^0\rangle$. This means we have $\langle E_b^0|V|E_{\gamma_5}\rangle \neq 0$ for some $|E_{\gamma_5}^0\rangle$. Here $|E_b^0\rangle$ is another degenerate ground state. Thus only at this order we find off-diagonal matrix element in the ground state subspace and it constitute the effective Hamiltonian in the ground state subspace. The H_{eff} can be

written as,

$$H_{eff}^{ba} = \sum_{\gamma_5 \neq a} \sum_{\gamma_4 \neq a} \sum_{\gamma_3 \neq a} \sum_{\gamma_2 \neq a} \sum_{\delta_2 \neq a} \frac{V_{\delta_2 a} V_{\gamma_2 \delta_2} V_{\gamma_3 \gamma_2} V_{\gamma_4 \gamma_3}}{(E_a^0 - E_{\gamma_2}^0)(E_a^0 - E_{\gamma_3}^0)(E_a^0 - E_{\gamma_4}^0)} \times$$
$$\frac{V_{\gamma_4 \gamma_5} V_{\gamma_5 b}}{(E_a^0 - E_{\delta_2}^0)(E_a^0 - E_{\gamma_5}^0)}$$
$$\equiv \langle b|H_{eff}|a\rangle$$
$$= \sum_{j_i} \frac{\langle b|V|j_1 \times j_1|V|j_2 \times j_2|V|j_3 \times j_3|V|j_4 \times j_4|V|j_5 \times j_5|V|a\rangle}{\prod_{j_i, i=1,5}(E^0 - E_{j_i}^0)} \quad \text{(F.29)}$$

In the above equation we have substituted $j_1 = \gamma_5, j_2 = \gamma_4, j_3 = \gamma_3, j_4 = \gamma_2, j_5 = \delta_2$. Similarly the effective Hamiltonian for 2D Kitaev model is obtained by evaluating,

$$H_{eff}^{ba} = \langle b|H_{eff}|a\rangle = \sum_{j_i} \frac{\langle b|V|j_1 \times j_1|V|j_2 \times j_2|V|j_3 \times j_3|V|a\rangle}{\prod_{j_i, i=1,3}(E^0 - E_{j_i}^0)} \quad \text{(F.30)}$$

The perturbation theory developed here can be applied to non-degenerate perturbation problem upto 6th order. It can also be applied to degenerate perturbation theory if it happens that perturbation does no have any off-diagonal matrix element between any two degenerate ground states upto 5th order.

Bibliography

[1] See e.g D. Pines and Ph. Nozieres, *The Theory of Quantum Liquids*, Vol 1., Benjamin, New York(1966).

[2] L. D. Landau and E. M. Lifshitz, *Statistical Physics*, Pergamon, New York(1980) 3rd ed.

[3] For a review see e.g S. Das Sarma and A. Pinczuk(ed.), *Perspectives in Quantum Hall Effects,* Wiley, New York(1996).

[4] X.-G Wen and Q. Niu, "Ground-state degeneracy of the fractional quantum Hall states in the presence of a random potential and on high-genus Riemann surfaces", Phys. Rev. B **41**, 9377(1980).

[5] B.Block, X.-G. Wen, "Effective theories of the fractional quantum Hall effect: Hierarchy construction", Phys. Rev. B **42**, 8145(1990).

[6] N.Read, "Excitation structure of the hierarchy scheme in the fractional quantum Hall effect", Phys. Rev. Lett. **65**, 1502(1990).

[7] J. Froohlich and T. Kerler, "Universality in quantum Hall systems", Nucl. Phys. B **354**, 369(1991).

[8] G. Moore and N. Read, "Nonabelions in the fractional quantum hall effect", Nucl. Phys. B **360**, 362 (1991).

[9] For a recent review see e.g. M.R. Norman and C. Pepin, "The electronic nature of high temperature cuprate superconductors", Rep. Prog. Phys. **66**, 1547(2003).

[10] See e.g. G. R. Stewart, "Non-Fermi-liquid behavior in d and f-electron metals", Rev. Mod. Phys. **73**, 797 (2001).

[11] P. Coleman *et. al.* , "How do Fermi liquids get heavy and die?", J. Phys. Cond. Mat. **13**, R723(2001).

[12] See e.g. S. Maekawa *et al.*, "Physics of Transition Metal Oxides", Springer, Berlin(2004).

[13] M. B. Hastings, "Lieb-Schultz-Mattis in higher dimensions", Phys. Rev. B **69**, 104431(2004).

[14] X.-G. Wen, "Topological orders in rigid states", Int. J. Mod. Phys. B **4**, 239(1990).

[15] X.-G. Wen, "Topolgical orders and chern-simons theory in strongly correlated quantum liquid", Int. J. Mod. Phys. B **5**, 1641(1991).

[16] E. Ardonne, P. Fendley and E. Fradkin, "Topological order and conformal quantum critical points", Annals of Phys. **310**, 493(2004).

[17] X.-W. Wen, "Mean-field theory of spin-liquid states with finite energy gap and topological orders", Phys. Rev. B **44**, 2664(1991).

[18] X.-W. Wen, "Quantum orders and symmetric spin liquids", Phys. Rev. B **65**, 165113(2001).

[19] H. Bombin and M.A. Martin-Delgado, " Exact topological quantum order in D=3 and beyond: Branyons and brane-net condensates", Phys. Rev. B **75**, 075103(2007).

[20] W. Thruston."Three-dimensional geometry and topology", Vol 1. Edited by Silvio Levy. Princeton Mathematical Series **35**. Princeton University Press, Princeton, NJ, 1997.

[21] M. Levin and X.-G. Wen, " String-net condensation: A physical mechanism for topological phases", Phys. Rev. B **71**, 045110 (2005)

[22] A. Hamma, P. Zanardi, X.-G. Wen, " String and membrane condensation on three-dimensional lattices", Phys. Rev. B **72**, 035307 (2005).

[23] R. W. Ogburn and H. Preskill,"Topological quantum computation", Lect. Notes in Comp. Sci **1509**, 341-356(1991).

[24] J. Preskill, "Fult-tolerant Quantum computation", arXiv: quant-ph/9712048 .

[25] C . Mochon, "Anyons from nonsolvable finite groups are sufficient for universal quantum computation", Phys. Rev. A **67**, 022315 (2003).

[26] E. Dennis, A. Kitaev, A. Landahl, J. Preskill, "Topological quantum memory", J. Math. Phys. **43**, 4452-4405 (2002).

[27] S. B. Bravyi, A. Yu. Kitaev, "Quantum codes on a lattice with boundary", quant-ph/9811052 .

[28] M. A. Nielsen and I. L. Chuang, *Quantum Computation and Quantum Information* (Cambridge University Press, Cambridge, England 2000).

[29] C. H. Bennett and D. P. DiVincenzo, "Quantum information and computation", Nature **404** 247 (2000); J. Preskill, "BATTLING DECOHERENCE: THE FAULT-TOLERANT QUANTUM COMPUTER ", Phys. Today **52**, 24 (1999).

[30] A. Yu. Kitaev, A. H. Shen and M. N. Vyalyi, *Classical and Quantum Computation* (Americal Mathematical Society, 2002).

[31] S. Das Sarma, M. Friedman and C. Nayak, " Topological quantum computation ", Phys. Today **59**, 32(2006).

[32] A. Yu. Kitaev, "Fault-tolerant quantum computation by anyons", Ann. Phys. **303**, 2-30(2003).

[33] A. Yu. Kitaev, "Anyons in an exactly solved model and beyond", Ann. Phys. **321**, 2-111 (2006).

[34] M. Freedman, M. Larsen and Z. Wang, "A Modular Functor Which is Universal for Quantum Computation", Comm. Math. Phys. **227**, 605(2002).

[35] J. Preskil, *Lecture Notes on Topological Quantum Computation,* http://www.theory.caltech.edu/preskill/ph219/topological.ps

[36] P. Shor, in: *Proceedings of the 35th Annual Symposium on Fundamentals of Computer Science.*, IEEE Press, Los Almitos, CA, 1994, pp. 124-134.

[37] C. Nayak, et. al, "Non-Abelian Anyons and Topological Quantum Computation", Rev. Mod. Phys. **80**, 10831159 (2008).

[38] S. Das Sarma, M. Freedman, C. Nayak,"Topologically-Protected Qubits from a Possible Non-Abelian Fractional Quantum Hall State", Phys. Rev. Lett. **94**, 166802/1-4 (2005)

[39] B. Duocot, M. V. Feigelman, L. B. Ioffe, A. S. Ioselevich, " Protected qubits and Chern-Simons theories in Josephson junction arrays", Phys. Rev. B **71**, 024505(2005).

[40] X. G. Wen, *Quantum Field Theory of Many-body Systems*, Oxford University Press, 2004.

[41] Avinash Khare, Fractional Statistics And Quantum Theory, World Scientific Publishing Company; Second edition.

[42] F. Wilczek, Fractional Statistics and anyon superconductivity, (Word Scientific, Singapore, 1990).

[43] E. H. Lieb, T. D. Shultz and D. C. Mattis, "Two soluble models of an antiferromagnetic chain", Ann. Phys. (N. Y.) **16**, 407(1961).

[44] See, for example, V. Emery, in " Highly Conducting One Dimensional Solids", edited by J. Devreese, R. Evrard, and V. Van Doren (Plenum Press, New York, 1979), p. 247; M.P.A. Fisher and L. Glazman in "Mesoscopic Electron Transport", edited by L.P. Kouwenhoven, L.L. Sohn and G. Schon (Kluwer Academic, Boston,1997), and references therein.

[45] J. Vidal, R. Thomale, K. P. Schmidt, S. Dusuel, "Self-duality and bound states of the toric code model in a transverse field", Phys. Rev. B **80**, 081104 (2009).

[46] J. Vidal, S. Dusuel, K. P. Schmidt, "Low-energy effective theory of the toric code model in a parallel field", Phys. Rev. B **79** 033109(2009).

[47] S. Dusuel, K. P. Schmidt, J. Vidal, R. L. Zaffino, "Perturbative study of the Kitaev model with spontaneous time-reversal symmetry breaking", Phys. Rev. B **78**, 125102 (2008).

[48] J. Vidal, K. P. Schmidt, S. Dusuel, "Perturbative approach to an exactly solved problem: the Kitaev honeycomb model", Phys. Rev. B **78**, 245121 (2008).

[49] I.S. Tupitsyn, A. Kitaev, N.V. Prokof'ev, P. C. E. Stamp, "Topological multicritical point in the Toric Code and 3D gauge Higgs Models", Phys. Rev. B **82**, 085114 (2010).

[50] D. S. Rokshar and S. A. Kivelson, "Superconductivity and the Quantum Hard-Core Dimer Gas", Phys. Rev. Lett. **61**, 2376(1988).

[51] N. Read and B. Chakraborty, "Statistics of the excitations of the resonating-valence-bond state", Phys. Rev. B, **40**, 7133 (1989).

[52] R. Moessner and S. L. Sondhi,"Resonating Valence Bond Phase in the Triangular Lattice Quantum Dimer Model", Phys Rev. Lett **86**, 1881(2001).

[53] V. Kalmeyer and R. B. Laughin, "Equivalence of the resonating-valence-bond and fractional quantum Hall states", Phys. Rev. Lett. **59**, 2095(1987).

[54] P. W. Anderson,"The Resonating Valence Bond State in La_2CuO_4 and Superconductivity", Science **235**, 1196(1987).

[55] G. Baskaran, Z. Zou and P. W. Anderson, "The resonating valence bond state and high-Tc superconductivity – A mean field theory", Solid State Commn. **63**, 973(1987).

[56] X. G. Wen, F. wilczek, and A. Zee, "Chiral spin states and superconductivity", Phys. Rev. B **39**, 11413(1989).

[57] N. Read and S. Sachdev, "Large-N expansion for frustrated quantum antiferromagnets", Phys. Rev. Lett. **66**, 1773(1991).

[58] S. Sachdev and K. Park, "Ground States of Quantum Antiferromagnets in Two Dimensions", Annals of Phys. **298**, 58(2002).

[59] L. Balents, M. P. A. Fisher, and S. M. Girvin, "Fractionalization in an easy-axis Kagome antiferromagnet", Phys. Rev. B **65**, 224412(2002).

[60] R. Jackiw and C. Rebbi, "Solitons with fermion number 1/2", Phys. Rev. D **13**, 3398(1978).

[61] S. Kivelson, J Sethna and P. Rokshar, " Topology of the resonating valence-bond state: Solitons and high-Tc superconductivity", Phys. Rev. B **35**, 8865(1987).

[62] W. P Su, J. R. Schrieffer and A. J. Heeger, "Solitons in Polyacetylene", Phys. Rev. Lett.**42**, 1698 (1979).

[63] L. D. Faddeev and L. A Takhtajan, "What is the spin of a spin wave?", Phys. Lett. A **85**, 375(1981).

[64] R. B. Laughlin, "Anomalous Quantum Hall Effect: An Incompressible Quantum Fluid with Fractionally Charged Excitations", Phys. Rev. Lett. **50**, 1395(1983).

[65] G. Baskaran and R. Shankar, "ON THE GAUGE THEORY OF THE RESONATING VALENCE BOND STATES", Mod. Phys. Lett B **2**, 1211(1988).

[66] V. Kalmayer and R. B. Laughlin, "Equivalence of the resonating-valence-bond and fractional quantum Hall states", Phys. Rev. Lett, **59**, 2095(1987).

[67] Senthil. T, Fisher. M. P. A, "Z_2 gauge theory of electron fractionalization in strongly correlated systems", Phys. Rev. B **62**, 7850-7881(2000).

[68] B. S. Shastry, "Exact solution of a S=1/2 Heisenberg antiferromagnetic chain with long-ranged interactions", Phys. Rev. Lett **60**, 639(1988).

[69] R. Laughlin, "Anomalous Quantum Hall Effect: An Incompressible Quantum Fluid with Fractionally Charged Excitations", Phys. Rev. Lett. **50**, 1395(1983).

[70] R. B. Laughlin, "Anomalous Quantum Hall Effect: An Incompressible Quantum Fluid with Fractionally Charged Excitations", Phys. Rev. Lett. **50**, 1395-1398(1983)

[71] L. Saminadayar, D. C. Glattli, Y.Jin, B.Etienne, "Observation of the e/3 Fractionally Charged Laughlin Quasiparticle", Phys. Rev. Lett. **79**, 2526-2529(1997)

[72] C. Nayak and F. Wilczek, "2n Quasihole States Realize 2^{n-1}-Dimensional Spinor Braiding Statistics in Paired Quantum Hall States", Nucl. Phys. B **479**, 529-553(1996).

[73] R. de-Picciotto, M. Reznikov, M. Heiblum, V. Umansky, G. Bunin, D. Mahalu, "Direct observation of a fractional charge", Nature **389**, 162-164 (1997).

[74] K.P. Schmidt, S Dusuel, and J. Vidal, " Emergent Fermions and Anyons in the Kitaev Model", Phys. Rev. Lett. **100**, 057208 (2008).

[75] Michael Levin and Xiao-Gang Wen, "Fermions, strings, and gauge fields in lattice spin models", Phys. Rev. B **67**, 245316 (2003).

[76] G. Baskaran, S. Mandal, and R. Shankar, " Exact Results for Spin Dynamics and Fractionalization in the Kitaev Model", Phys. Rev. Lett, **98**, 247201 (2007).

[77] Saptarshi Mandal, R Shankar, G Baskaran. "Jordan-Wigner Transformation and Novel Spin Correlations in Kitaev MOdel", Poster 14, International Conference on Mott Insulator, IISc Bangalore, July,2006.

[78] H. D. Chen and Z. Nussinov, "Exact results of the Kitaev model on a hexagonal lattice: spin states, string and brane correlators, and anyonic excitations", J. Phys. A: Math. Theor. **41**, 075001(2008).

[79] Xiao-Yong Feng, Guang-Ming Zhang, Tao Xiang, "Topological characterization of quantum phase transitions in a S=1/2 spin model", Phys. Rev. Lett. **98**, 087204 (2007).

[80] G. Baskaran, Saptarshi Mandal, R Shankar. "RVB Physics, Gauge fixing and Jordan-Wigner Transformations in Kitaev Model", To be published.

[81] Shuo Yang, Shi-Jian Gu, Chang-Pu Sun, Hai-Qing Lin, "Fidelity susceptibility and long-range correlation in the Kitaev honeycomb model", Phys. Rev. A **78**, 012304 (2008).

[82] K. Sengupta, D. Sen, and S. Mondal, " Exact Results for Quench Dynamics and Defect Production in a Two-Dimensional Model", Phys. Rev. Lett. **100**, 077204(2008).

[83] G. Baskaran , Diptiman Sen and R. Shankar, "Spin-S Kitaev model: Classical Ground States, Order by Disorder and Exact Correlation Functions", Phys. Rev. B **78**, 115116 (2008)

[84] Samarth Chandra, Kabir Ramola, Deepak Dhar, " Classical Heisenberg spins on a hexagonal lattice with Kitaev couplings ", arXiv:1004.4627.

[85] S. Yang, D. L. Zhou, and C. P. Sun, " Mosaic spin models with topological order", Phys. Rev. B **76**, 180404(R)(2007).

[86] H. Yao and S.A. Kivelson, " Exact Chiral Spin Liquid with Non-Abelian Anyons", Phys. Rev. Lett. **99**, 247203 (2007).

[87] Saptarshi Mandal, Naveen Surendran, "An exactly solvable Kitaev model in three dimensions", arXiv:0801:0229, Phys. Rev. B **79**, 024426 (2009).

[88] T. Si and Y. Yu, "Anyonic Loops in Three Dimensional Spin liquid and Chiral Spin Liquid", Nucl. Phys. B 803, 428 (2008).

[89] Shinsei Ryu, "Three-dimensional topological phase on the diamond lattice", Phys. Rev. B **79**, 075124 (2009).

[90] I.S. Tupitsyn, A. Kitaev, N.V. Prokof'ev, P.C.E. Stamp, " Topological multicritical point in the Toric Code and 3D gauge Higgs Models ", Phys. Rev. B **82**, 085114 (2010).

[91] G. Kells, A. T. Bolukbasi, V. Lahtinen, J. K. Slingerland, J. K. Pachos and J. Vala, "Topological degeneracy and vortex dynamics in the Kitaev honeycomb model", Phys. Rev. Lett. **101**, 240404,2008.

[92] Shastry, B. S, Jha, S.S, Singh, V. Exactly solvable problem on condensed matter and relativistic field theory, Proceedings, Panchagani, January 30-February 12, 1985, Berlin, Springer-Verlag.

[93] Baxter, Rodney J, Exactly solved models in statistical mechanics, Academic press.

[94] Sutherland, Bill. Beautiful models: 70 years of exactly solved quantum many-body problems, Chennai, World Scientific

[95] Vladimir E. Korepin, Fabian H. L. Ebler, Exactly solvable models of strongly correlated electrons, Singapore, World Scientific.

[96] L. M. Duan, E. Demler and M. D. Lukin, "Controlling Spin Exchange Interactions of Ultracold Atoms in Optical Lattices", Phys. Rev. Lett. **91**, 090402(2003).

[97] A. Micheli, G. K. Brennen, and P. Zoller, "A toolbox for lattice-spin models with polar molecules", Nature Phys. **2**, 341(2006).

[98] A. O. Sboychakov, Sergey Savel'ev, A. L. Rakhmanov, Franco Nori, "Asymmetric long Josephson junction acting as a ratchet for a quantum field ", Phys. Rev. Lett. **104**, 190602(2010).

[99] G Jackeli, G Khaliullin, "Mott Insulators in the Strong Spin-Orbit Coupling Limit: From Heisenberg to a Quantum Compass and Kitaev Models", Phys. Rev. Lett **102** 017205 (2009).

[100] Jir Chaloupka, George Jackeli, Giniyat Khaliullin, " Kitaev-Heisenberg Model on Honeycomb Lattice: Possible Exotic Phases in Iridium Oxides A_2IrO_3", Phys. Rev. Lett. **105**, 027204 (2010).

[101] S. Mandal, S. Bhattacharjee, K. Sengupta, R. Shankar, "Confinement-deconfinement transition in a generalized Kitaev model", arXiv:0903.3785.

[102] S. Sachdev, *Quantum Phase Transition*, (Cambridge University Press, Cambridge, 1999).

[103] A. Polkovnikov, " Universal adiabatic dynamics in the vicinity of a quantum critical point", Phys. Rev. B **72**, 161201(R)(2005).

[104] S. Dusuel, K. P. Schmidt, J. Vidal, "Creation and Manipulation of Anyons in the Kitaev Model", Phys. Rev. Lett. **100**, 177204 (2008).

[105] G. Kells, A. T. Bolukbasi, V. Lahtinen, J. K. Slingerland, J. K. Pachos, J. Vala, "Topological degeneracy and vortex manipulation in Kitaev's honeycomb model", Phys. Rev. Lett. **101**, 240404(2008).

[106] M. Aguado, G. K. Brennen, F. Verstraete, J. I. Cirac, "Creation, manipulation, and detection of Abelian and non-Abelian anyons in optical lattices", Phys. Rev. Lett. **101**, 260501 (2008).

[107] Liang Jiang, Gavin K. Brennen, Alexey V. Gorshkov, Klemens Hammerer, Mohammad Hafezi, Eugene Demler, Mikhail D. Lukin, Peter Zoller, " Anyonic interferometry and protected memories in atomic spin lattices", Nature Physics **4**, 482 - 488 (01 Jun 2008).

[108] C. Zhang et. al., "Anyonic braiding in optical lattices", Proc. natl. Acad. Sci. U.S.A. **104**, 18415(2007).

[109] H. Bombin, and M.A. Martin-Delgado, " Topological Computation without Braiding", Phys. Rev. Lett. **98**, 160502(2007).

[110] E. Lieb, "Flux Phase of the Half-Filled Band", Phys. Rev. Lett. **73**, 2158(1994).

[111] A. Osterloh, L. Amico, G. Falci, and R. Fazio, "Scaling of entanglement close to a quantum phase transition", Nature (London) **416**, 608(2002).

[112] T. J. Osborne and M. A. Nielsen, "Entanglement in a simple quantum phase transition", Phys. Rev. A **66**, 032110 (2002).

[113] J. I. Latorre, E. Rico, and G. Vidal, "Ground state entanglement in quantum spin chains", Quantum Inf. Comput. **4**, 48(2004), arXiv:quant-ph/0304098.

[114] G. Vidal, J. I. Latorre, E. Rico, and A. Kitaev, "Entanglement in Quantum Critical Phenomena", Phys. Rev. Lett. **90**, 227902 (2003).

[115] G. Vidal and R. F. Werner, "Computable measure of entanglement", Phys. Rev. A **65**, 032314(2002).

[116] W. K. Wootters, "Entanglement of Formation of an Arbitrary State of Two Qubits", Phys. Rev. Lett. **80**, 2245(1998).

[117] Jose I. Latorre, Roman Orus, Enridue Rico, Julien Vidal, "Entanglement entropy in the Lipkin-Meshkov-Glick model", Phys. Rev. A, **71**, 064101, 2005.

[118] L. -A. Wu, M.S. Sarandy, and D. A. Lidar, "Quantum Phase Transitions and Bipartite Entanglement", Phys. Rev. Lett. **93**, 250404(2004).

[119] , C. H. Bennett, H. J. Bernstein, S. Popescu, and B. Schumacher, Concentrating partial entanglement by local operations, Phys. Rev. A, **53**, 2046 (1996).

[120] Julien Vidal, Concurrence in collective models, Phys. Rev. A **73**, 062318 (2006).

[121] Julien Vidal, Sebastien Dusuel, and Thomas Barthel, "Entanglement entropy in collective models", J. Stat. Mech. **0701**, P015(2007).

[122] Florian Mintert, Ana Maria Rey, Indubala I. Satija,and Charles W. Clark, "Phase transitions, entanglement and quantum noise interferometry in cold atoms" EPL **86**, 17003(2009).

[123] Thomas Barthel, Sebastien Dusuel, and Julien Vidal, "Entanglement entropy beyond the free case", Phys. Rev. Lett, **97**, 220402(2006).

[124] T. Barthel, M.-C. Chung, and U. Schollwck, " Entanglement scaling in critical two-dimensional fermionic and bosonic systems", Phys. Rev. A **74**, 022329(2006).

[125] S. A. Cheong and C. L. Henley. "Many-body density matrices for free fermions", Phys. Rev. B **69**, 075111(2004).

[126] Michael M. Wolf, " Violation of the Entropic Area Law for Fermions", Phys. Rev. Lett. **96**, 010404(2006).

[127] Dimitri Gioev and Israel Klich, " Entanglement Entropy of Fermions in Any Dimension and the Widom Conjecture", Phys. Rev. Lett **96**, 100503(2006).

[128] A. Peres, "Separability Criterion for Density Matrices", Phys. Rev. Lett. **77**, 1413 (1996).

[129] Alioscia Hamma, Radu Ionicioiu, and Paolo Zanardi, "Ground state entanglement and geometric entropy in the Kitaev model", Phys.Lett. A **337**, 22 (2005) .

[130] Alexei Kitaev, John Preskill, "Topological Entanglement Entropy", Phys. Rev. Lett. **96**, 110404(2006).

[131] Michael Levin and Xiao-Gang Wen, "Detecting Topological Order in a Ground StateWave Function", Phys. Rev. Lett. **96**, 110405(2006).

[132] Jian-Hui Zhao and Huan-Qiang Zhou, "Singularities in ground state fidelity and quantum phase transitions for the Kitaev model", Phys. Rev. B **80**, 014403 (2009).

[133] Shi-Jian Gu and Hai-Qing Lin, "Scaling dimension of fidelity susceptibility in quantum phase transitions", EPL **87**, 10003(2009).

[134] Miguel Aguado and Guifre Vidal, "Entanglement renormalization and topological order", Phys. Rev. Lett. **100**, 070404 (2008).

[135] A Svelik, Quantum Field Theory of Condensed Matter Physics, Cambridge University Press.

[136] E Fradkin, Field Theories of Condensed Matter Physics, Levant Pub.

[137] Bill Sutherland, 70 Years of Exactly Solved Quantum Many-Body Problems, World Scientific Publishing Company.

[138] R J Baxter, Exactly Solved Models in Statistical Mechanics, Academic Press.

[139] Giuseppe Mussardo, Statistical Field Theory: An Introduction to Exactly Solved Models in Statistical Physics, Oxford University Press, USA.